THREE-DIMENSIONAL MORPHOLOGY OF DIPLOCRATERION AND OPHIOMORPHA AND THEIR IMPACT ON RESERVOIR PROPERTIES

MARY KATHRYNE LEAMAN

Three-Dimensional Morphology of *Diplocraterion* and *Ophiomorpha* and Their Impact on Reservoir Properties

by
© Mary Kathryne Leaman, B.Sc., Geol.I.T.

A thesis submitted to the
School of Graduate Studies
in partial fulfillment of the requirements for the degree of

Master of Science
Department of Earth Sciences
Memorial University of Newfoundland

April, 2013

St. John's Newfoundland

Abstract

The morphology of *Ophiomorpha irregulaire* and *Diplocraterion* is poorly understood in three dimensions, and their effects on reservoir quality are under-appreciated. This Master's thesis focuses on morphological characteristics to aid in the identification of the trace fossils in cross section, and to form models of the trace-makers' behaviour, which is now understood to affect permeability. Understanding of the trace-makers' behaviour has led to a predictive understanding of sediment distribution within burrows and explains some morphological features. Based on the morphology and behaviour of modern day trace makers, *Neotrypaea californiensis* is an analogue trace-maker of *O. irregulaire* and *Diplocraterion*. Permeability measurements indicate that *O. irregulaire* reduces on average horizontal permeability (k_h) by 28% and k_v by 14%. *Diplocraterion* show an increase in permeability within the shafts and around the typical 'dumbbell' morphology relative to the matrix. *Ophiomorpha* and *Diplocraterion* have the potential to dramatically alter reservoir estimations and should be incorporated into reservoir characterisation studies.

Acknowledgements

I would like to take this opportunity to thank the many people who have helped and supported me over the past two years. First, I would like to thank my supervisor Dr. Duncan McIlroy, both for taking me on as a student on good faith, and providing mentorship for the duration of the project. I have definitely learned a lot over the past two years! This project was financially supported by Petroleum Research Newfoundland and Labrador (PRAC) and a Natural Sciences and Engineering Research Council of Canada (NSERC) grant to DMc. Funding from the Department of Earth Sciences, School of Graduate Studies, Faculty of Science and the Graduate Students' Union allowed me to travel to Asturias, Spain and Long Beach, California to present parts of my thesis. Thanks to Dr. Suzanne Dufour, my supervisory committee member, for helping bridge the gap between the worlds of biology and geology. Scientific research would benefit more from inter-science relationships.

I would like to thank all my new friends in the Ichnology Research Group, especially these great people who had a direct involvement with my project (in no particular order): Dr. Nicola (Nikki) Tonkin, Dr. Liam Herringshaw, Dr. Rich Callow, Małgorzata (Czarrna) Bednarz, Chris Boyd, Dario Harazim, Dr. Michael Garton, Elisabeth (Lisi) Kahlmeyer, Colin Brisco and Edgars (Eddie) Rudzitis.

A huge thank you goes to Michael, Liam and Chris for their assistance in the UK collecting samples. Chris and I could not have collected our samples without Michael's and Liam's geological knowledge of the region. I can't forget Michael's rock saw abilities and giving us the pleasure of meeting his family and Bucket.

On a slightly unrelated note to my thesis, I would like to thank Chris again for nurturing my photography skills. To both Chris and Dario for being hilarious office mates and engaging in many thoughtful white-picket-fence-life discussions. To Megan McDonald for being my marathon training partner in the first year of my thesis. To the rest of the Ichnology Research Group and the "Fifth Floor Gang" you're all amazing, and you made my time in NL that much better!

I cannot forget to thank my family and friends near and far for their continuing support in my education endeavours. My parents, for supporting my dream since it popped into my head in Grade 6, and always just being a phone call away. To my brother Greg, it's been great having you so close these past few years, I will definitely miss it! Lastly, to Matt for supporting me in every way possible through the duration of this degree; without your continuing support I wouldn't be Magic Mary. xo

Table of Contents

List of Tables

List of Figures

List of Appendices

Co-Authorship Statement

Two manuscripts are included within this thesis (presented in Appendices A and B) that are co-authored by the candidate. The nature and extent of work contributed for each manuscript is described below.

The manuscript entitled "Precision serial grinding and volumetric 3D reconstruction of large ichnological specimens" (presented in its entirety in Appendix A) was submitted to *Ichnos* in early January 2012, and will be edited and resubmitted by the end of 2012. The author list is as follows: Małgorzata Bednarz, Liam G. Herringshaw, Christopher Boyd, **Mary Leaman**, Elisabeth Kahlmeyer, and Duncan McIlroy. As a co-author, I contributed to the manuscript by:

- Providing multiple revisions of the text and figures;
- Writing text on serial grinding and burrow selection methods; and
- Creating figures relating to *Ophiomorpha*.

The manuscript entitled "The recognition of *Ophiomorpha irregulaire* on the basis of pellet morphology: restudy of material from the type locality" (presented in its entirety in Appendix B) was submitted to *Ichnos* in January 2012, accepted in May 2012, and was published in December 2012. The author list is as follows: Christopher Boyd, Duncan McIlroy, Liam G. Herringshaw, and **Mary Leaman**. As last author, I contributed to the manuscript by:

- Providing multiple revisions of the text and figures;

- Creating the reference list, including finding all the papers that were needed in text, including formatting; and
- Finding examples in the literature of inadvertently figured *Ophiomorpha* with sand-filled pellets.

Completing this work greatly aided the background literature research portion of my own *Ophiomorpha irregulaire* manuscript, entitled "What does *Ophiomorpha irregulaire* really look like?" (Chapter 2).

CHAPTER 1

Introduction and Overview

Chapter 1 – Introduction and Overview

1.1 Introduction

The sedimentology and ecology of marine environments can be dramatically affected by burrowing organisms. Burrowing organisms transport and mix sediments, and create nutrient fluxes, new biogeochemical conditions, and new ecospace within the substrate. The geological record of these effects comes in the form of trace fossils, the study of which, ichnology, is at the interface of biology, palaeontology, and sedimentary geology.

The focus of this thesis-based Master's degree is the economic geological importance of the trace fossils *Diplocraterion* and *Ophiomorpha*. These common trace fossils are present throughout the Phanerozoic and are significant components of many bioturbated marine siliciclastic successions worldwide. Such marine facies can be major hydrocarbon reservoirs, including the Ben Nevis reservoir in offshore Newfoundland. It is pertinent to assess the degree to which *Diplocraterion* and *Ophiomorpha* burrows may influence reservoir quality. The full three-dimensional morphology of these trace fossils and their sedimentological impacts on the quality of petroleum reservoirs have not been fully characterised.

The outcomes of this research will be relevant to bioturbated reservoirs worldwide. The characterisation of the sedimentological impact of *Diplocraterion* and *Ophiomorpha* on sedimentary fabric will improve our understanding of reservoir quality, which can enhance production and recompletion in bioturbated reservoirs. Three-

dimensional reconstructions of *Diplocraterion* and *Ophiomorpha* will aid in field- and core-based identifications of the trace fossils, particularly from the two-dimensional cross sections observed in core. A better morphological understanding of *Ophiomorpha* is needed for taxonomic classification. Understanding these trace fossils in greater detail will also be of paleoecological significance, providing new information on trace-maker behaviour that can be incorporated into palaeoenvironmental analyses.

1.2 Literature Review

This study comprises three linked components, which will form the basis for three published papers. The study is unified by the need to better understand the impact of bioturbation on reservoir intervals, and centres on the Ben Nevis Formation. Previous work has shown that bioturbation is a significant control on the reservoir quality of the Ben Nevis Formation of Hebron Field (Tonkin et al., 2010). This work builds on the pre-established methodologies of those authors, but expands the work to consider the prominent ichnofabric-forming trace fossils *Diplocraterion* and *Ophiomorpha* in three dimensions.

1.2.1 Reservoir Quality in the Ben Nevis Formation

The Jeanne d'Arc Basin is situated offshore Newfoundland on the north-eastern Grand Banks, approximately 350 kilometres southeast of St. John's. Today, the basin contains three producing fields with multiple reservoirs. The Hebron-Ben Nevis field is expected to come onto production next with potential resources of the Ben Nevis field estimated at 114 million barrels of oil and 12.1 billion m^3 of gas (Tonkin et al., 2010; C-

NLOPB, 2010). The Ben Nevis Formation was deposited during the last of three rifting phases that occurred during Late Triassic to Early Cretaceous time (Tankard and Welsink, 1987; Tonkin et al., 2010).

The Ben Nevis Field was discovered in 1980, with the discovery well Mobil et al. Ben Nevis I-45. At present there is only one other well drilled, Chevron et al. Ben Nevis L-55 (1999) (Tonkin et al., 2010). The early Aptian to Albian sandstones of the Ben Nevis Formation can be divided into two units, the Gambo Member and the upward-fining sequence. The base of the Gambo Member (the basal member of the Ben Nevis Formation) defines the mid-Aptian unconformity, which has been related to uplift and erosion during continental breakup (Tankard and Welsink, 1987; Tonkin et al., 2010). The Gambo Member includes a wide range of clastic grain sizes, abundant organic-rich laminae, interbeds of carbonaceous grey shales, sporadic red and green shales. Cements are siderite and silica, but calcite cements are completely absent (Sinclair, 1993).

The upward-fining sequence is found either above the Gambo Member or directly overlying the mid-Aptian unconformity (Sinclair, 1993). The base of the sandstone is characterised by massive, fine- to medium-grained, rarely coarse-grained, quartzose, also containing fine-grained bioclastic and carbonaceous debris, along with glauconite. Weakly cemented sandstones alternate with heavily calcite-cemented sandstones, which can be associated either with shell debris beds or with round concretions (Sinclair, 1993).

The cored interval of the L-55 core includes 82 m of net porous sandstone, occurring mostly in the bioturbated interval. Bioturbation intensity in the sandstone-

dominated reservoir is strongly facies-controlled, with *Ophiomorpha* burrows being the most abundant and obvious trace fossil (Tonkin et al., 2010).

1.2.2 Diplocraterion

Diplocraterion is the U-shaped burrow of a presumed suspension-feeder with a spreite between its tubes (Fig. 1.1). The tubes of the U-burrow are vertical and perpendicular to the bedding plane and are rarely topped with large funnels (Fürsich, 1974a). Spreiten are likely formed by the trace-maker moving up and down within the burrow in order to deposit feed or in response to palaeoenvironmental change. For example, if the sedimentation rate is low, or the erosional rate is high, the trace-maker may adjust the base of the U-burrow downwards from the sediment-water interface, creating a convex-upward protrusive spreite. When sedimentation rates are high, the trace-maker may adjust the U-burrow closer to the new sediment-water interface, thereby creating a convex-down retrusive spreite (Schlirf, 2000). Scratch marks preserved inside the burrows in some *Diplocraterion* indicate that such burrows were formed in firmground conditions (Fürsich, 1975).

Five valid ichnospecies of *Diplocraterion* have been described: *Diplocraterion parallelum*, *D. helmerseni*, *D. biclavatum*, *D. habichi*, and *D. polyupsilon* (Torell, 1870; Fig. 1.2). *Diplocraterion parallelum* is characterised as having parallel burrow walls and a unidirectional spreite. Eleven ichnospecies have been synonymised with *D. parallelum*, the rationale being that morphological features previously used to characterise ichnospecies were based on accessory or preservational features (Fürsich, 1974a). Among the ichnospecies synonymised with *D. parallelum* is *D. yoyo*, an ichnospecies that

exhibits both protrusive and retrusive spreiten resulting from a yoyo-like behaviour in response to erosion and deposition (Goldring, 1962, 1964).

Of the remaining ichnospecies, *Diplocraterion helmerseni* has an expanded base, which is considered to be a distinctive accessory feature separating it from *D. parallelum*. *Diplocraterion biclavatum* is characterised by the presence of tubular extensions of the burrow shafts penetrating below the deepest U of the burrow, forming blind-ended tunnels (Fürsich, 1974a). *Diplocraterion habichi* are consistently narrow, with narrow spreiten, ranging in total width (including both vertical limbs and intervening spreite) from 0.2 to 1.6 cm. Other identifying features include discontinuous spreite and divergent arms at the top of the burrow. The latter cannot always be used for classification, since the arms are commonly eroded (Fürsich, 1974a). Lastly, *D. polyupsilon* is characterised as having a spreite formed by limbs that widen laterally and deepen through the ontogeny of the trace-maker (Fürsich, 1974a).

Although the ichnogenus *Diplocraterion* had been recognised in intertidal palaeoenvironments (MacKenzie, 1968; Ager and Wallace 1970), the first widely recognised discussion of *Diplocraterion* as an intertidal palaeoenvironmental indicator may have been made by Fürsich (1974b). The ichnospecies *D. habichi* was described as being characteristic of a tidal flat based on observations of tiny modern *Diplocraterion*-like traces made by *Corophium volutator* (Seilacher, 1967; Fürsich, 1974b). The spreiten between the *Corophium* burrow arms were only been reported from semi-consolidated mud, along tidal channels, with scratch marks on the walls (Seilacher, 1967), an observation that has not been repeated. The presence of a scratched surface (i.e., with

bioglyphs) indicates the presence of a "Glossifungites" ichnofacies, i.e., a firmground. Trace fossils similar to *Corophium* burrows have been described from intertidal facies of the Late Cretaceous of Wyoming. Based on alternating faecal pellets, *D. parallelum* is thought to represent tidal environments, but not necessarily the intertidal zone (Fürsich, 1974b).

Diplocraterion parallelum and *D. habichi* have subsequently been used as indicators of intertidal depositional environments (Fürsich, 1975). The ichnogenus *Diplocraterion* is generally considered to be indicative of high-energy environments with fluctuating currents and wave action, as are typically present in intertidal or very shallow subtidal areas (Fürsich, 1975). *Diplocraterion* is also commonly associated with hiatal surfaces, where the depositional interface remains stable over a long period due to non-deposition, often followed by cementation and commonly subsequent to erosive exposure of semi-lithified sediments (Fürsich, 1975; Lettley et al., 2007). *Diplocraterion* is thus not exclusively an intertidal trace fossil.

Palaeoenvironmental interpretations made by Fürsich (1975) have been cited at least 50 times in ichnological, sedimentological, and palaeoenvironmental studies (e.g. Frey et al., 1978; Narbonne, 1984; Frey and Howard, 1985; Bromley and Uchman, 2003). No position statement regarding the subtidal versus intertidal palaeoenvironmental distribution of the ichnogenus *Diplocraterion* is made in these papers (Fürsich, 1975, 1981) contrary to some subsequent work. A review of the literature on *Diplocraterion* and of its palaeoenvironmental use is given by Bromley and Uchman (2003). *Diplocraterion* is useful in identifying transgressive surfaces (e.g. Taylor and Gawthorpe,

1993; Taylor and Goldring, 1993; Pemberton and MacEachern, 1995) and in delineating sequence boundaries (Olóriz and Rodriguez-Tovar, 2000). *Diplocraterion parallelum* has been used to indicate colonisation events in sandy shoals in the Middle Jurassic of India (Fürsich, 1998) similar to the *Ophiomorpha* colonization windows of Goldring and Pollard (1995). The common occurrence of *Diplocraterion* in coarse-grained sandstones suggests a palaeoenvironmental association with intense hydrodynamic activity, and its association with firmground mudstones is taken to imply that the *Diplocraterion* trace-maker was primarily a suspension-feeder (Fürsich, 1974a).

While *Corophium* has been suggested as a possible modern trace-maker by some authors (Seilacher, 1967; Fürsich, 1974b), the author does not agree. It is much too small to produce the large structures of *Diplocraterion.* No appropriately-sized modern analogue trace-maker for *Diplocraterion* has been identified to date. No modern animal has been found to produce the similar U-shaped burrow with spreite, in any environment. If an analogue were found it would improve our understanding of the possible mode(s) of life of spreite-making organisms that live in U-shaped tubes.

1.2.3 Ophiomorpha

The trace fossil *Ophiomorpha* is characterised by a "distinct burrow lining that is more or less smooth walled interiorly, but which is mammillated exteriorly" (Frey et al., 1978). The thickness of the lining may vary, and it is composed of pellets. The pelletal morphology is a main diagnostic feature for ichnospecies-level classification of *Ophiomorpha.* It is conventionally considered that the trace-maker presses "pellets" that can vary in shape, size, and composition into the burrow lining which are smoothed off in

the interior (Frey et al., 1978; Fig. 1.3). *Ophiomorpha irregulaire* is characterised by irregular distribution of pellets on the roof of the burrow wall contrasting with a smooth unlined gallery floor. The roof lining is conventionally explained as providing structural reinforcement to the gallery roof in loosely consolidated sands (Frey et al., 1978).

The ichnogenus *Ophiomorpha* encompasses both galleries and shafts. The horizontal burrow, termed a gallery, is connected to the sediment-water interface by vertical or oblique shafts. The geometric shapes of the galleries can be classified as 'mazes', 'shafts' and 'boxworks' (Frey et al., 1978). A regular maze is a polygonal system of tunnels, an irregular maze has irregularly developed horizontal components, and a meander maze is a loose system of interconnected sinuous galleries. Boxwork is the non-planar version of mazes and shafts; it is subdivided into two types, regular and irregular. Regular boxwork is a three-dimensional polygonal system of vertical and horizontal components, whereas irregular boxwork lacks regularity and has burrows that may vary in diameter (Frey et al., 1978).

Ophiomorpha nodosa Lundgren, 1891 is defined by densely packed, regularly distributed, roughly hemispherical pellets on the outer surface of the burrow wall (Fig. 1.4A; Frey et al., 1978; Frey and Howard, 1990; McIlroy et al., 2009). The burrow system is highly variable in three dimensions, having sparsely branched vertical shafts and densely branched horizontal galleries (Frey and Howard, 1990).

Ophiomorpha borneensis Keij, 1965 is characterised as a system of primarily horizontal branching galleries (one to three centimeters in diameter), with rare vertical spiralling shafts. Pellets consist of two adjoined hemispherical pellets that form one large

pellet (Keij, 1965; Fig. 1.4B).

Burrow walls of *Ophiomorpha annulata* Książkiewicz, 1977 are lined with evenly spaced rows of elliptical pellets (Fig. 1.4C) arranged end to end, forming continuous horizontal rings around the wall. Pellets can be rudimentary, and some specimens may have poorly developed pelletal exteriors, but clearly lined walls. The burrow is in the form of tunnels, with long horizontal segments more abundant than the short vertical shafts. The tunnels branch in a Y-shape more sparsely than in *O. rudis*. Burrow fill is similar to that of *O. nodosa*, consisting either of structureless sediment or of chevron backfilling laminae (Frey and Howard, 1990). Morphologically, *O. annulata* exhibits similar characteristics to *O. rudis* and *O. puerilis*.

Ophiomorpha rudis Książkiewicz, 1977 has oblique shafts, with branched (Y-shaped), long horizontal galleries that are straight or slightly winding. Irregular oval to elongate granules (i.e., pellets of two to four millimeter diameter) partly cover the burrow walls, though longer segments are smooth or show scratch marks (Fig. 1.4D; Uchman, 2009). Meniscate fill has been observed in horizontal mazes in cut slabs.

Ophiomorpha irregulaire Frey, Howard and Pryor, 1978 is currently not as well characterised as other ichnospecies of *Ophiomorpha* and some debate surrounds its ichnotaxobases and palaeogeographic distribution (Bromley and Pedersen, 2008; McIlroy et al., 2009). The burrow walls are described as "consisting predominantly of sparse, irregularly distributed, ovoid to mastoid pellets or pelletal masses" (Frey et al., 1978). The distinguishing characteristics of *O. irregulaire* are its sparse, elongate or flame-like pelletal lining (Fig. 1.4E). The diagnostic characteristics include the following four

ichnotaxobases: 1) the presence of irregular, often mastoid, pellets in cross section; 2) a super abundance of galleries with lined roofs and unlined floors; 3) a rarity of vertical shafts; and 4) a tendency towards distortion of the lateral pellets into flame-like projections (McIlroy et al., 2009). From specimens at its type locality in the Blackhawk and Star Point formations of the Book Cliffs region, Utah, the burrow system is described as a horizontal "meander maze" (Frey et al., 1978; Bromley and Ekdale, 1998; McIlroy et al., 2009).

Ophiomorpha puerilis de Gibert, Netto, Tognoli and Grangeiro, 2006 has sub-cylindrical pellets and small unbranched galleries. The pellets are cylindrical with rounded ends and form a single layer around the shaft (Fig. 1.4F; de Gibert et al., 2006). *Ophiomorpha puerilis* differs from *O. nodosa* by the shape of the pellets and lack of burrow branching.

The debate around *O. irregulaire* has focused on the importance of the meander maze as an ichnotaxobase for recognition of *Ophiomorpha irregulaire*, since such morphology cannot be fully demonstrated in core (Bromley and Pedersen, 2008). A recent review of the status of *O. irregulaire* highlighted that a more clear three-dimensional morphological understanding of the ichnospecies was needed (McIlroy et al., 2009). *Ophiomorpha irregulaire* can still be identified by its distinctive characteristics, including the "presence of irregular variable pellets, a rarity of vertical shafts, galleries with lined roofs but unlined floors, and in some cases highly deformed lateral pellets" (McIlroy et al., 2009). The stratigraphical and geographical distribution of *O. irregulaire* is also under debate. Bromley and Pedersen (2008) considered *Ophiomorpha irregulaire*

to be restricted geographically and temporally to the Cretaceous Western Interior Seaway. McIlroy et al. (2009) inferred a wider distribution including Argentina, Italy, western Greenland and offshore Newfoundland and Labrador, provided that the morphology fits the taxonomic description, while conceding that the morphology remains poorly constrained. It is important to fully understand and be able to confidently identify ichnospecies of *Ophiomorpha* since it is such a prolific ichnofabric-forming trace fossil in siliciclastic reservoirs and has the potential to significantly affect reservoir quality (Tonkin et al., 2010).

1.3 Scientific Importance and Expected Outcome

The outcome of this research is relevant to bioturbated siliciclastic reservoirs worldwide. Characterisation of the sedimentological impact of *Diplocraterion* and *Ophiomorpha* on sedimentary fabrics via probe permeametry can aid in the understanding of reservoir quality, which will in time improve recovery from *Ophiomorpha*-bioturbated reservoirs. Three-dimensional reconstruction of *Diplocraterion* and *Ophiomorpha* will aid in field- and core-based identification of trace fossils, particularly from the two-dimensional cross sections seen in core. A better morphological understanding of *Ophiomorpha* is also needed for taxonomic classification since the ichnospecific diagnosis is currently insufficient (McIlroy et al., 2009). Understanding of the functional morphology of trace fossils in greater detail will also be of palaeoecological significance, providing new information on trace-maker behaviour, which is commonly incorporated into palaeoenvironmental analysis.

1.4 Methods

Outcrop samples of *Ophiomorpha* were collected prior to the study from the Book Cliffs of Utah and the Juncal Formation of California (Boyd et al., 2012). *Diplocraterion* samples were collected by Leaman from Cloughton Wyke, UK. Collected field samples were subjected to precision serial grinding, which enables the high-resolution three-dimensional morphological reconstruction of trace fossils by using Adobe Photoshop™ and VG Studio Max™. Study of additional material from the Ben Nevis Formation L-55 core, using large thin slicing, conventional thin sections and probe permeametry, provide insights into how bioturbation affects the reservoir quality, building on the work of Tonkin et al. (2010). Large thin slices were removed from the core-slab face and subsequently polished to a thickness at which they become translucent under intense transmitted light (Garton and McIlroy, 2006). This technique allows subtle sedimentary fabrics and ichnofabrics to become more readily apparent (Tonkin et al., 2010). Thin sections cut from core-slab faces and field samples, and impregnated with blue-dye to emphasize pore spaces and sorting, allow detailed study of the petrological controls on ichnology-controlled reservoir properties. Probe permeametry of outcrop and core samples allows measurement of spatial variability of the impact of the trace fossil on permeability (Tonkin et al., 2010).

For serial grinding, samples were cast in plaster and clamped into a milling machine programmed to precisely grind off increments of 0.3 (or 0.5) mm along the Z-axis. After each new surface was ground, a photograph was taken of the rock face. This process was repeated until the whole rock was documented. Photos were stacked using

Adobe Photoshop, and fossil burrows were selected and reconstructed into three-dimensional morphological models using VG Studio Max. A full explanation of the serial grinding method is presented in Appendix A.

1.5 Figures

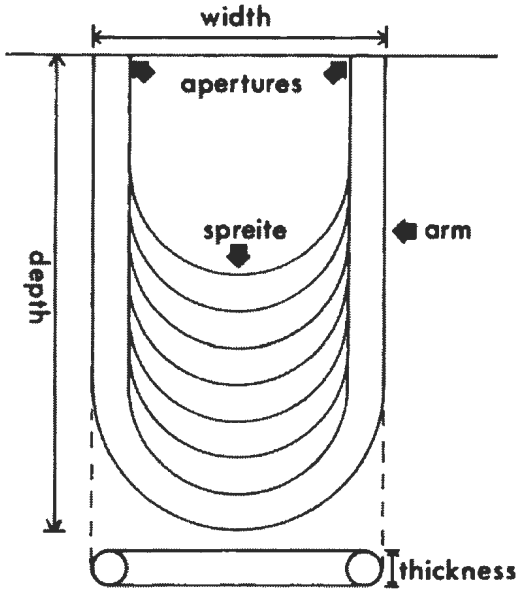

Fig. 1.1: Generalised morphology and terminology of vertical U-shaped spreite burrows (Fürsich, 1974a).

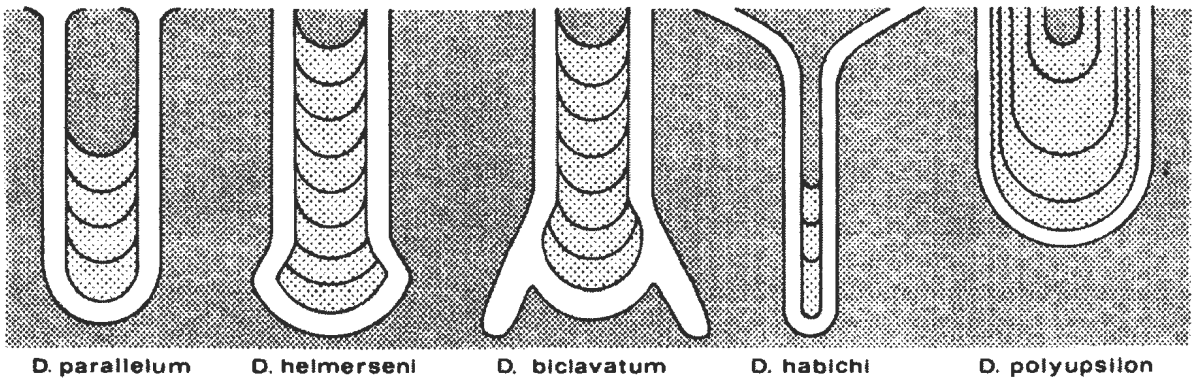

Fig. 1.2: The five ichnospecies of *Diplocraterion* described by Torell, 1870. From left to right, *Diplocraterion parallelum*, *D. helmerseni*, *D. biclavatum*, *D. habichi*, and *D. polyupsilon* (Fürsich, 1974a).

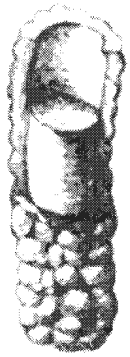

Fig. 1.3: Detail of wall lining of *Ophiomorpha* pellets on the outside, with a smooth interior (Frey et al., 1978).

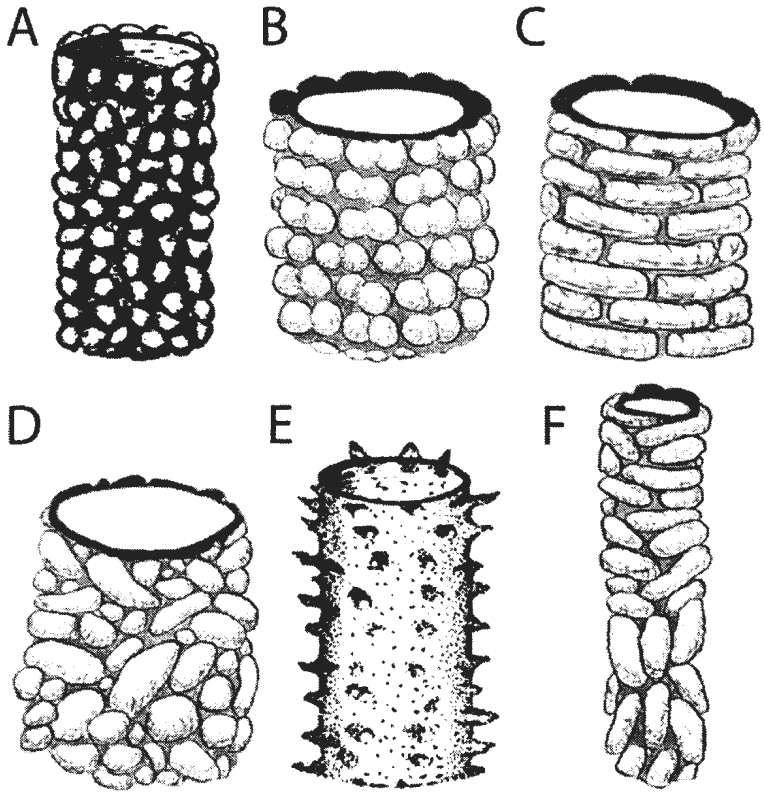

Fig. 1.4: Ichnospecies of *Ophiomorpha*, based on pellet morphology. Not to scale. A: *O. nodosa* (Frey and Howard, 1990); B: *O. borneensis*; C: *O. annulata*; D: *O. rudis*; E: *O. irregulaire* (Frey and Howard, 1990); F: *O. puerilis*. Figures B, C, D, and F were drawn according to their respective type locality descriptions.

1.6 References

Bromley, R.G., Ekdale, A.A., 1998. *Ophiomorpha irregulaire* (trace fossil): redescription from the Cretaceous of the Book Cliffs and Wasatch Plateau, Utah. Journal of Paleontology. 72, 773-778.

Bromley, R.G., Uchman, A., 2003. Trace fossils from the Lower and Middle Jurassic marginal marine deposits of the Sorthat Formation, Bornholm, Denmark. Bulletin of the Geological Society of Denmark. 52, 185-208.

Bromley, R.G., Pedersen, G.K., 2008. *Ophiomorpha irregulaire*, Mesozoic trace fossil that is either well understood but rare in outcrop or poorly understood but common in core. Palaeogeography, Palaeoclimatology, Palaeoecology. 270, 295-298.

de Gibert, J.M., Netto, R.G., Tognoli, F.M.W., Grangeiro, M.E., 2006. Commensal worm traces and possible juvenile thalassinidean burrows associated with *Ophiomorpha nodosa*, Pleistocene, southern Brazil. Palaeogeography, Palaeoclimatology, Palaeoecology. 230, 70.

Frey, R.W., Howard, J.D., Pryor, W.A., 1978. *Ophiomorpha*: its morphologic, taxonomic, and environmental significance. Palaeogeography, Palaeoclimatology, Palaeoecology. 23, 199-229.

Frey, R.W., Howard, J.D., 1985. Trace fossils from the Panther Member, Star Point Formation (Upper Cretaceous), Coal Creek Canyon, Utah. Journal of Paleontology. 59, 370-404.

Frey, R.W., Howard, J.D., 1990. Trace fossils and depositional sequences in a clastic shelf setting, Upper Cretaceous of Utah. Journal of Paleontology. 64, 803-820.

Fürsich, F., 1998. Environmental distribution of trace fossils in the Jurassic of Kachchh (Western India). Facies. 39, 243-272.

Fürsich, F.T., 1974a. On *Diplocraterion* Torell 1870 and the significance of morphological features in vertical, spreiten-bearing, U-shaped trace fossils. Journal of Paleontology. 48, 952-962.

Fürsich, F.T., 1974b. Corallian (Upper Jurassic) trace fossils from England and Normandy. Stuttgarter Beiträge zur Naturkunde. Serie B. Geologie und Paläontologie. 13, 1-51.

Fürsich, F.T., 1975. Trace fossils as environmental indicators in the Corallian of England and Normandy. Lethaia. 8, 151-172.

Fürsich, F.T., 1981. Salinity-controlled benthic associations from the Upper Jurassic of Portugal. Lethaia. 14, 203-223.

Garton, M., McIlroy, D., 2006. Large thin slicing: a new method for the study of fabrics in lithified sediments. Journal of Sedimentary Research. 76, 1252-1256.

Goldring, R., 1962. The trace fossils of the Baggy Beds (Upper Devonian) of North Devon, England. Paläontologische Zeitschrift. 36, 232-251.

Goldring, R., Pollard, J.E., 1995. A re-evaluation of *Ophiomorpha* burrows in the Wealden Group (Lower Cretaceous) of southern England. Cretaceous Research. 16, 665-680.

Keij, A., 1965. Miocene trace fossils from Borneo. Paläontologische Zeitschrift. 39, 220-228.

Książkiewicz, M., 1977. Trace fossils in the Flysch of the Polish Carpathians. Palaeontologia Polonica 36, 1–208.

Lettley, C.D., Gingras, M.K., Pearson, N.J., Pemberton, S.G. 2007. Burrowed stiffgrounds on estuarine point bars: modern and ancient examples, and criteria for their discrimination from firmgrounds developed along omission surfaces. In: MacEachern, J.A., Bann, K.L., Gingras, M.K., Pemberton, S.G. (Eds.), Applied Ichnology. Society of Economic Paleontologists and Mineralogists Short Course Notes 52, 298-306.

Lundgren, B., 1891. Studier öfver fossilforande lösa block. Geologiska Föreningens i Stockholm Förhandlingar. 13, 111-121.

MacKenzie, D.B., 1968. Studies for students. Sedimentary features of Alameda Avenue Cut, Denver, Colorado. Mountain Geologist. 5, 3-13.

McIlroy, D., Tonkin, N.S., Phillips, C., Herringshaw, L.G., 2009. Comment on "*Ophiomorpha irregulaire*, Mesozoic trace fossil that is either well understood but rare in outcrop or poorly understood but common in core" by R.G. Bromley and G.K. Pedersen: [Palaeogeography, Palaeoclimatology, Palaeoecology 270 (2008) 295-298]. Palaeogeography, Palaeoclimatology, Palaeoecology. 284, 392-395.

Narbonne, G.M., 1984. Trace fossils in Upper Silurian tidal flat to basin slope carbonates of arctic Canada. Journal of Paleontology. 58, 398-415.

Olóriz, F., Rodriguez-Tovar, F.J., 2000. *Diplocraterion*: a useful marker for sequence stratigraphy and correlation in the Kimmeridgian, Jurassic (Prebetic Zone, Betic Cordillera, southern Spain). Palaios. 15, 546-552.

Pemberton, S.G., MacEachern, J.A., 1995. The sequence stratigraphic significance of trace fossils: examples from the Cretaceous foreland basin of Alberta, Canada. In: Van Wagoner, J.A. (Ed.), Sequence stratigraphy of foreland basin deposits-outcrop and subsurface examples from the Cretaceous of North America. American Association of Petroleum Geologists Memoir. 64, 429-475.

Schlirf, M., 2000. Upper Jurassic trace fossils from the Boulonnais (northern France). Geologica et Palaeontologica. 34, 145-213.

Seilacher, A., 1967. Bathymetry of trace fossils. Marine Geology. 5, 413-428.

Sinclair, I., 1993. Tectonism: the dominant factor in mid-Cretaceous deposition in the Jeanne d'Arc Basin, Grand Banks. Marine and Petroleum Geology. 10, 530-549.

Tankard, A.J., Welsink, H.J., 1987. Extensional tectonics and stratigraphy of Hibernia oil field, Grand Banks, Newfoundland. AAPG Bulletin. 71, 1210-1232.

Taylor, A.M., Goldring, R., 1993. Description and analysis of bioturbation and ichnofabric. Journal of the Geological Society. 150, 141-148.

Tonkin, N.S., McIlroy, D., Meyer, R., Moore-Turpin, A., 2010. Bioturbation influence on reservoir quality: a case study from the Cretaceous Ben Nevis Formation, Jeanne d'Arc Basin, offshore Newfoundland, Canada. AAPG Bulletin. 94, 1059-1078.

Uchman, A., 2009. The *Ophiomorpha rudis* ichnosubfacies of the *Nereites* ichnofacies: characteristics and constraints. Palaeogeography, Palaeoclimatology, Palaeoecology. 276, 107-119.

CHAPTER 2

What does *Ophiomorpha irregulaire* really look like?

AUTHORSHIP STATEMENT

What does *Ophiomorpha irregulaire* really look like?

Authors: **Leaman, M.**, McIlroy, D., Boyd, C., Herringshaw, L.G.

This manuscript builds on McIlroy et al. (2009), and on tank experiments conducted by Liam Herringshaw. Chris Boyd started preliminary work by completing an undergraduate honours project on the type locality sample (Book Cliffs, Utah) and writing the manuscript "The recognition of *Ophiomorpha irregulaire* on the basis of pellet morphology: restudy of material from the type locality" (see Appendix B for full manuscript).

Chapter 2 – What does *Ophiomorpha irregulaire* really look like?

2.1 Abstract

Ophiomorpha irregulaire is a poorly understood and under-characterised ichnotaxon compared to other ichnospecies of *Ophiomorpha*. Debate surrounds its ichnotaxobases and palaeogeographic distribution. In core, *Ophiomorpha irregulaire* is classically characterised by its thin, "spikey" mud pellets which form the burrow lining. It is much more difficult to determine the horizontal "meander maze" that is part of the ichnospecific diagnosis of the type material.

Considering the importance of identifying *Ophiomorpha irregulaire* in ichnofabrics that commonly constitute petroleum reservoir intervals, a redescription of the type material is needed to identify the trace fossil in core and outcrop. The aims of this research are to increase the confidence in recognizing *O. irregulaire* through improved characterisation of the morphology from type locality material with regard to the meander maze, its pelletal morphology, and characteristics in cross section.

Samples were collected from the ichnospecies type locality of Book Cliffs, Utah as well as the Juncal Formation, California, to create high-resolution, three-dimensional morphological models of the trace fossil using a serial grinding method. From this model a number of previously undescribed morphological features were observed from material of the type locality.

Comparison of the morphological features from the two localities demonstrates that *O. irregulaire* exists outside the Cretaceous Western Interior Seaway, with a

stratigraphic range of at least Jurassic to Cretaceous and a palaeoenvironmental range from shallow marine to continental slope settings.

2.2 Introduction

Ophiomorpha is one of the most widely known and easily recognizable trace fossils (Frey et al., 1978), but of the currently described ichnospecies, *Ophiomorpha irregulaire* is arguably the most variable and poorly constrained. Recent debate regarding the recognition of *O. irregulaire* in core (Bromley and Pedersen, 2008; McIlroy et al., 2009) has stimulated this reconsideration of the characteristics used for ichnospecific classification, and their relative importance. *Ophiomorpha irregulaire* was originally described from the Cretaceous Blackhawk and Star Point formations of the Book Cliffs, Utah. Hitherto, the pelletal morphology of the wall lining of *O. irregulaire* has been widely used in study of *O. irregulaire* in ichnofabrics as the principle ichnotaxobase by which it can be distinguished from other ichnospecies of *Ophiomorpha*.

The ichnogenus *Ophiomorpha* is generally considered to be a useful palaeoenvironmental indicator, being common in many high-energy marine palaeoenvironments of Mesozoic and younger strata (Frey et al., 1978; McIlroy, 2004a; MacEachern et al., 2007). In addition, *Ophiomorpha* create prominent ichnofabrics seen in petroleum reservoirs, often as the dominant or elite trace fossil. Knowing the global distribution of *Ophiomorpha*, the environmental controls on its occurrence, and its detailed morphology in outcrop and core, is therefore critical to generating an understanding of the ichnogenus. Recent criticism has been made of the identification of *O. irregulaire* from core material, particularly where identification relies upon pellet

morphology (Bromley and Pedersen, 2008). A detailed characterisation of pellet morphology was not included in the original description and diagnosis of *O. irregulaire* (Bromley and Ekdale, 1998) and a careful re-examination is required using specimens from the type locality (McIlroy et al., 2009).

One of the diagnostic characteristics of *O. irregulaire* is the presence of a meander maze (Fig. 2.1; Bromley and Ekdale, 1998). Recently, Bromley and Pedersen (2008) have argued that all occurrences of *O. irregulaire* from outside the Cretaceous Western Interior Seaway (CWIS) should be rejected because of the absence of a demonstrable meander maze. This assertion excluded many records of the ichnospecies identified from core (e.g. Martin and Pollard, 1996; Pemberton et al., 2001; McIlroy, 2004b; Burns et al., 2005; Malpas et al., 2005). It is unlikely, however, that such a large, bedding-parallel feature would be recognized in core material from petroleum fields (though see McIlroy et al., 2009). The pelletal morphology of *O. irregulaire* is still inadequately described (McIlroy et al., 2009). For the practical identification of *O. irregulaire* in core, it is imperative to determine whether the pellet morphology is sufficiently distinctive to be used as a primary ichnotaxobase. If the above occurrences are to be excluded from *O. irregulaire*, it would seem that there is an additional ichnospecies of *Ophiomorpha* with a very distinctive pelletal morphology. The purpose of this paper aims to resolve these questions by characterizing *Ophiomorpha irregulaire* fully from its type locality in the Cretaceous of Utah, and by studying material with comparable pelletal morphology from Eocene turbidite facies in California.

2.3 Stratigraphical and Geographical Distribution of *Ophiomorpha irregulaire*

Twenty-two occurrences of *O. irregulaire* have been reported from twelve different countries, on all continents except Antarctica (Fig. 2.2). These range in geological age from the Early Jurassic (Pliensbachian) of Italy (Monaco and Garassino, 2001) to the mid-Quaternary of India (Kundal and Dharashivkar, 2006; see Table 1). The ichnospecies is rarely reported from strata older than Barremian, reached peak abundance in the Campanian, and was common from the Miocene to Quaternary (Table 2.2; Fig. 2.2). Where the same locality or material has been cited multiple times, only the first record is included here (e.g. Frey et al., 1978; Frey and Howard, 1982; Howard and Frey, 1984; Frey and Howard, 1985, 1990, all described *O. irregulaire* from the Book Cliffs region of Utah). We recognize that there are potential biases in the documentation of *Ophiomorpha irregulaire* due to variations in facies and the intensity at with which a region has been studied, and that the documented occurrences might not reflect the true distribution (Orr, 2001; Uchman, 2004; Löwemark and Hong, 2006).

2.4 Palaeoenvironmental Distribution of *Ophiomorpha*

Ophiomorpha has been described from a range of shallow to deep marine environments. It has also been reported from non-marine facies (e.g. Stewart, 1978; Merrill, 1984; Loope and Dingus, 1999), but most such occurrences are considered dubious (cf. Goldring and Pollard, 1995).

Ichnospecies of *Ophiomorpha* are distinguished based on the morphology of the pellets and their organisation within the burrow wall (Fig 1.4). A summary of the typical

environments in which each ichnospecies occurs is given below (see Fig. 2.3):

- *Ophiomorpha rectus* (Fischer-Ooster, 1858): deep marine environments (Uchman, 2009);
- *Ophiomorpha nodosa* Lundgren, 1891: shallow to deep marine environments, especially littoral and sublittoral settings;
- *Ophiomorpha borneensis* Keij, 1965: siliciclastic, shallow [brackish] marine (Keij, 1965), and carbonate, shallow marine environments (Pemberton and Jones, 1988);
- *Ophiomorpha annulata* Książkiewicz, 1977: siliciclastic, shallow to deep marine environments (Uchman, 1998);
- *Ophiomorpha rudis* Książkiewicz, 1977: deep marine environments (Uchman, 2009);
- *Ophiomorpha irregulaire* Frey, Howard and Pryor, 1978: siliciclastic, shallow marine environments (Frey et al., 1978). Also documented from deep marine facies herein;
- *Ophiomorpha puerilis* de Gibert, Netto, Tognoli and Grangeiro, 2006: shallow marine lagoon-barrier settings (de Gibert et al., 2006).

2.5 Neoichnology and Potential Trace-makers of *Ophiomorpha irregulaire*

It has been widely documented that modern traces equivalent to *Ophiomorpha* are produced by thalassinidean crustaceans such as the callianassid shrimp *Callichirus major* (Say, 1818) (Weimer and Hoyt, 1964; Curran, 1976; Frey et al., 1978). More than 500

thalassinidean species are known, 95% of which inhabit shallow-water (0-200 m) environments (Fig. 2.3; Dworschak, 2000, 2005). Of the callianassids, more than half (54%) inhabit very shallow water (0-2 m), and only 8.4% occur between 200 and 2000 meters (Dworschak, 2000).

The modern shrimp *Upogebia pugettensis* has been considered as a trace-maker of *Ophiomorpha*, and *Neotrypaea californiensis* as a maker of *Thalassinoides* (Swinbanks and Luternauer, 1987). *Upogebia pugettensis* creates mud-lined burrows with muddy pellets, while the latter creates unlined burrows more comparable to *Thalassinoides*. *Upogobia pugettensis* produces large, vertical, U-shaped vertical burrows with Y-shaped branching (see Fig. 19 in Swinbanks and Murray, 1981; and Fig. 2 and Fig. 5 in Swinbanks and Luternauer, 1987), uncharacteristic of *Ophiomorpha.* There is no mention of vertical shafts in the ichnospecific description of the type material for *Ophiomorpha irregulaire* (Bromley and Ekdale, 1998). Very rare, oblique, subvertical shafts were observed in *O. irregulaire* from Greenland (Pedersen and Bromley, 2006). *Upogebia pugettensis* lives in muddy substrates (e.g. tidal flats), which could cause the shrimp to line its burrow with mud for reinforcement. *Neotrypaea californiensis* typically does not line its burrows, presumably because they select environments where little to no mud occurs, though other factors may influence their location, e.g. tidal regime, salinity, eelgrass, and biointeractions (Suchanek, 1983; Swinbanks and Luternauer, 1987).

A potential trace-maker of *Ophiomorpha irregulaire* is the callianassid *Neotrypaea californiensis* Dana, 1854 (see Swinbanks and Murray, 1981; Swinbanks and Luternauer, 1987; McIlroy et al., 2009). *Neotrypaea californiensis* is a common endobenthic, deposit-

feeding crustacean in marine intertidal and nearshore environments (Hester and Pryor, 1972; Stewart, 1978; Griffis and Chavez, 1988; Gingras et al., 2000), found on the west coast of North America from Alaska to Mexico. *Neotrypaea californiensis* is preferentially recorded from clean, sand-rich to sandy mud substrates (Swinbanks and Luternauer, 1987). *Neotrypaea californiensis* can tolerate low levels of salinity to a lethal limit range of 8.75‰ to 10.5‰ (Thompson and Pritchard, 1969; Swinbanks and Luternauer, 1987) and can survive anoxic conditions for 138 ± 27 hours (Grimm and Föllmi, 1994)

2.6 Studied Material

Samples were collected from the type locality of *Ophiomorpha irregulaire*: Unit 19 of the Spring Canyon Member (Blackhawk Formation: Campanian), Coal Creek Canyon, Book Cliffs, Utah (Bromley and Ekdale, 1998). In addition, a possible specimen of *O. irregulaire* was collected from a sandy turbidite channel fill, consisting of thick bedded sandy turbidite with interbedded siltstone, in the Eocene Juncal Formation, Wagon Road Canyon, California (Van de Kamp et al., 1974).

Core material was also examined from the Lower Cretaceous Ben Nevis Formation, Jeanne d'Arc Basin, offshore Newfoundland (Ben Nevis L-55 well; cf. Tonkin et al., 2010), in order to compare the morphology of *Ophiomorpha irregulaire* obtained from type locality specimens with putative examples in core (highlighted by McIlroy et al., 2009).

Samples of *Ophiomorpha irregulaire* collected in the field were trimmed in the laboratory using a rock saw, leaving adequate matrix around the trace fossil. They were

then placed in a cardboard box and the surrounding space was filled with plaster of Paris (cf. Bednarz et al., in review). Once the plaster had set, the block was trimmed to a precise rectangular prism using a rock saw, which enabled square corners to be used for alignment during serial grinding and photography. The trace fossil block was then placed inside a HAAS VF3 VOP-C grinding machine, capable of grinding increments of rock to a precision of 0.01 mm).

The Utah and Californian samples were serially ground with 120 increments of 0.207 mm thickness, and 295 intervals of 0.305 mm thickness. After each increment had been ground, the specimen was removed and photographed. Each photograph was taken in the same position, with the corners of the block being used for alignment. Once the specimen had been ground completely, the photographs were uploaded into Adobe Photoshop. They were then processed to enhance the contrast between burrow and matrix, and cropped. The mud lining and pellets of the *Ophiomorpha* burrows were selected and separated from the sandstone host sediment in Photoshop. These burrow images were then loaded into the three-dimensional modeling program VG Studio Max, where they could be stacked and combined to produce a three-dimensional reconstruction of *Ophiomorpha irregulaire*.

2.7 Results

2.7.1 Three-Dimensional Morphology of *Ophiomorpha irregulaire*

2.7.1.1 Type Locality Specimen (Utah)

Specimens of *Ophiomorpha irregulaire* collected from the type locality show a

range of morphologies not encompassed by the original description of the type material. A full description and illustration of the morphology of *O. irregulaire* based on this material is presented below as a basis for comparison with other material. Field observations confirm that the horizontal component of the burrow consists of sinuous galleries with T- or Y-shaped junctions (the meander maze of Bromley and Ekdale, 1998). The burrow lining is generally composed of mud- or organic detritus-rich pellets that are irregularly spaced along the roofs of the burrow galleries (Fig. 2.4A; Frey et al., 1978; Bromley and Ekdale, 1998; McIlroy et al., 2009). Pellets of *O. irregulaire* are sometimes extended into flame-like structures, probably as a result of burial compaction. Some 'pointed' pellets, however, have been found to be rounded, sand-filled and mud-lined pellets with the pointed or flame-like appearance being an artefact of an incomplete, mud-rimmed, sand pellet being viewed in oblique cross section (Boyd et al., 2012; Fig. 2.4B). However, not all pellets associated with *Ophiomorpha irregulaire* are sand-filled; many of the more rounded conical pellets are completely mud-filled.

In addition to previously described features, this study also revealed a ferruginous, organic-rich, spheroidal structure in association with the burrow wall, that is considered to be a potential "fermentation chamber" (Fig. 2.4A; cf. Bromley, 1996 Figure 5.22B). In this hypothesis, the supposed crustacean trace-maker packed mud and relatively refractory plant detritus into the burrow roof and left it to undergo microbial fermentation, perhaps to be used as a future food source (Bromley, 1996).

Lastly, multiple burrow floors stacked upon one another, resembling spreiten, were identified from vertical cross section in the type locality sample (Fig. 2.4 A and C).

The burrow floor spreite is a continuous feature for the horizontal length of the burrow, captured in the hand sample.

2.7.1.2 Californian Specimen

Ophiomorpha irregulaire has hitherto been considered to be an exclusively shallow marine ichnotaxon. However, the flame-like pellets typical of *O. irregulaire* were observed in specimens of *Ophiomorpha* from a turbiditic succession in the Juncal Formation (Eocene) of California. As such, the material was examined to compare its three-dimensional morphology with that of *O. irregulaire* specimens from the type locality. The lithological contrast between burrow and host sediment is less marked in the Californian material because there is more disseminated mud in the matrix surrounding the burrow. By serially grinding the specimens, however, it was possible to determine that the burrow roof included sand-filled, mud-lined pellets with a flame-like structure similar to those of *O. irregulaire* (see Fig. 2.5), and that the coarse-scale gallery morphology was sinuous (Fig. 2.6 A-C). The material is therefore assigned to *O. irregulaire*, extending its palaeoenvironmental range to deep marine (slope) deposits.

2.7.2 *Ophiomorpha irregulaire* Ichnofabrics in Core

2.7.2.1 Ben Nevis Formation, Newfoundland

As a case study in the identification of *Ophiomorpha irregulaire* from core material, a range of *Ophiomorpha* specimens was collected from the Ben Nevis Formation in well L-55 of the Hebron Field, offshore Newfoundland (Tonkin et al., 2010). These specimens of *Ophiomorpha* display a variety of pellet types, including

flame-like (Fig. 2.7A); sand-filled and mud-lined (Fig. 2.7B and C); and conical (Fig. 2.7D). By comparison with the material from the type locality, all these pellet morphologies are accommodated within *O. irregulaire*.

The type material of *O. irregulaire* does not show a pelletal lining to the gallery floors though laminated sediment is commonly found to underlie the burrow (Fig. 2.4 A and C). Cross-sections of the horizontal gallery demonstrate a parallel lamina to the burrow floor. In transverse cross section the gallery is approximately semi-circular in outline. The laminated burrow floor is inferred to represent gallery floor adjustment to produce a retrusive spreite-like structure. Another burrow adjustment feature includes two stacked rows of pellets forming double-roofed burrows (Fig. 2.7B and D). Some examples of *O. irregulaire* formed two burrows in either close proximity to each other (Fig. 2.9A), or were slightly connected (Fig. 2.9B and C), representing turning nodes in the galleries, morphology. Lastly, many examples of collapsed sediment were observed above *Ophiomorpha irregulaire* burrows (Fig. 2.10). This study also documented *Ophiomorpha irregulaire* galleries in longitudinal section that show inclined heterolithic sandstone and mudstone laminae that resemble ripples (Fig. 2.8A and B). Such burrow fills represent forward-fill that Wanless et al. (1988) has compared to tubular tempestite, a sedimentary feature formed by storm sediment force-filling an open subsurface burrow. This unique burrow morphology could be misidentified for spreite burrows such as *Zoophycos*. An idealised sketch of *Ophiomorpha irregulaire* is presented in Fig. 2.11 with revised morphological features.

2.8 Experimental Analysis of Burrowing Behaviour

In controlled aquarium experiments, *Ophiomorpha irregulaire*-like burrows were produced by *Neotrypaea californiensis*. The shrimp were collected from the Yaquina Estuary, Oregon, US and shipped to Memorial University of Newfoundland, St. John's. The aquarium was filled with mud interlayered with sand and populated with *Neotrypaea californiensis*. Within five days oblique shafts and galleries lined with mud and mud pellets were created (Fig. 2.12).

A similar aquarium experiment using *Neotrypaea californiensis* in a sand-only tank demonstrated *N. californiensis* feeding underneath a collapsed burrow (collapse cone) (Fig. 2.13B). The sand pellets created by *N. californiensis* are likely either to reinforce their burrow lining by applying mucus to the walls (hardening the sediment), or to create mucus-rich pellets (Bromley, 1990; Fig. 2.13). Sand pellets created by *N. californiensis* have never been reported before. Sand pellets are probably created by *N. californiensis* in the field as well as in aquarium experiments, but are likely destroyed upon excavation of the burrow for observation. In this tank experiment, the shrimp created its burrow against the glass tank wall, enabling observation of pellet fabrication (Fig. 2.13).

Roof collapse has been inferred to result from poor burrow construction (Thompson and Pritchard, 1969). However, the collapse of the feeding gallery provides the shrimp with access to new sources of nutrients from the sediment-water interface (Bromley, 1990). Whilst constructing their burrows, the sediment that is excavated must be placed somewhere. *Neotrypaea* commonly mound sand on the sediment surface (Fig.

2.12A and Fig. 2.13C; Shinn, 1968; Swinbanks and Murray, 1981; Dworschak, 1983; Suchanek, 1983; Swinbanks and Luternauer, 1987). There are two types of openings to *Neotrypaea californiensis* burrows: 1) an excurrent opening (*sensu* Shinn, 1968), characterised by a large, volcano-like sediment mound; and 2) an incurrent opening that forms a funnel-shaped crater at the sediment-water interface (Shinn, 1968; Dworschak, 1983). One *N. californiensis* can extrude 18 ± 9 mL of wet sediment per day (Swinbanks and Luternauer, 1987). Previous studies have assumed that amount of sediment excavated to the surface during burrow construction is equal to the burrow volume (Griffis and Chavez, 1988). Such calculations are incorrect since *N. californiensis* are demonstrated to introduce sediment to their galleries from the overlying sediment column.

2.9 Interpretation

2.9.1 Linking Material with the Type Material

The two three-dimensional models from different localities show similar morphologies. The flame-like pelletal morphology, which is evident in both models, is interpreted to have formed by the differential compaction of mud enveloping an ellipsoidal sand pellet (Fig. 2.14; cf. Boyd et al., 2012).

The Juncal Formation sample demonstrates a meander inferred to be part of the meander maze, a diagnostic feature for *O. irregulaire,* as well as the same flame-like pellets that were observed in material from the Book Cliffs. While this small sample does not show a complete meander maze (Fig. 2.15) as described originally by Frey et al. (1978), it evidently represents a portion of a sinuous branch of the characteristic meander

maze of *Ophiomorpha irregulaire*. The presence of both the flame-like pellets and the meander maze means the specimen can confidently be identified as *Ophiomorpha irregulaire*.

Further supporting this interpretation, the *Ophiomorpha* specimens from the Ben Nevis Formation cores exhibit many morphological features similar to the modelled specimens of *O. irregulaire*. These include sand pellets and the flame-like mud pellets, and possibly the meander maze.

The burrow fill, burrow floor spreite, and double-roofed burrow could have occurred in response to a storm event hence the burrow fill is a tubular tempestite. Once the storm passed, the shrimp would have adjusted the burrow in response to deposition or erosion of sediment. Another possibility is that the crustacean adjusted the burrow due to sediment fill or collapse and then proceeded to deposit-feed from the spreite below the burrow floor after a period of time to allow for fermentation.

2.9.2 Distribution of *Ophiomorpha irregulaire*

The presence of the pellets on all samples studied, ranging in palaeogeographic distribution from offshore Newfoundland to California, including the type locality allow positive identification of *O. irregulaire* in all studied material.

By the pellets alone, it is possible to identify *O. irregulaire* in outcrop and core. The sinuous portion of the meander maze found with the same pelletal morphology increases the strength of the ichnospecific diagnosis of the Juncal Formation specimen.

While we examined none of the hand specimens of *Ophiomorpha* considered by Bromley and Pedersen (2008), the core figures from Norway, Newfoundland and Alberta

included by Bromley and Pedersen (2008; Fig. 4 A through D) as dubious examples, all exhibit the pelletal morphology described here from the type material. This lends support to the assertion of McIlroy et al. (2009) that *O. irregulaire* can be found outside the Cretaceous of the Western Interior Seaway.

With respect to the turbidite sample from California, there is enough evidence to conclude this *Ophiomorpha* does show the ichnotaxobases for *O. irregulaire*. To date there have been no reports of *O. irregulaire* from deep marine facies.

2.10 Conclusion

A re-examination of *Ophiomorpha irregulaire* from its type locality, combined with a study of specimens from other localities, allows a reappraisal of the morphology of *O. irregulaire*. By applying a serial grinding and three-dimensional reconstruction techniques (cf. Bednarz and McIlroy, 2009, in review; Appendix A), we are able to consider the morphology of *O. irregulaire*. The three-dimensional model of a type specimen allowed the following observations and interpretations to be made:

1. Flame-like mud projections were present in pellets of the specimen from the type locality. The same flame-like pellets were observed in the sample from the Eocene of California.
2. Three-dimensional analysis of the flame-like mud projections shows they are in fact related to sand-filled, mud-lined pellets (see Boyd et al., 2012, for a more detailed discussion).

3. A portion of the ichnospecifically diagnostic meander maze was present in the Californian sample: The material can therefore be confidently assigned to *O. irregulaire*.
4. Specimens showing the same pellet morphologies as *O. irregulaire* from the type locality are present in the Cretaceous of offshore Newfoundland.
5. The distribution of *O. irregulaire* is geographically widespread and distribution ranges from Triassic to recent (McIlroy et al., 2009).
6. Contrary to previous reports, *Ophiomorpha irregulaire* is not restricted to the Cretaceous of the Western Interior Seaway.
7. The Californian specimens of *O. irregulaire* are from a turbidite succession, demonstrating that *O. irregulaire* has a wider palaeoenvironmental distribution than previously described.
8. The extant callianassid crustacean *Neotrypaea californiensis* produces burrows that are morphologically similar to *Ophiomorpha irregulaire*.

Based on these characteristics, we argue that *Ophiomorpha irregulaire* can be reliably identified in core, and that it is widespread in the geological record, and not restricted to Cretaceous shallow marine settings from central-western North America. Ichnologists and sedimentologists should re-examine core samples to assess its distribution, and apply a similar approach to identifying many of the other trace fossils that are commonly found in siliciclastic successions.

2.11 Acknowledgements

This work is supported by Petroleum Research Atlantic Canada (PRAC), SLOPES, and a Natural Sciences and Engineering Research Council of Canada (NSERC) grant to DMc. M. Leaman thanks Małgorzata (Czarrna) Bednarz for her tremendous help with the three-dimensional modeling and Elisabeth Kahlmeyer for graphic design assistance. This manuscript was improved by the reviews of Andrew Rindsberg and Evan Edinger.

2.12 References

Anderson, B.G., Droser, M.L., 1998. Ichnofabrics and geometric configurations of *Ophiomorpha* within a sequence stratigraphic framework: an example from the Upper Cretaceous US Western Interior. Sedimentology. 45, 379-396.

Bednarz, M., McIlroy, D., 2009. Three-dimensional reconstruction of "phycosiphoniform" burrows: Implications for identification of trace fossils in core. Palaeontologia Electronica. 12 (3), 13A 15 p. http://palaeo-electronica.org/2009_3/195/index.html.

Bednarz, M., Herringshaw, L.G., Boyd, C., Leaman, M., Kahlmeyer, E., McIlroy, D., in review. Precision serial grinding and volumetric 3D reconstruction of large ichnological specimens. Ichnos.

Boyd, C., McIlroy, D., Herringshaw, L.G., Leaman, M., 2012. The recognition of *Ophiomorpha irregulaire* on the basis of pellet morphology: restudy of material from the type locality. Ichnos. 19, 185-189.

Bromley, R.G., 1990. Trace Fossils: Biology and taphonomy, special topics in palaeontology. Unwin Hyman, London. 280 p.

Bromley, R.G., Ekdale, A.A., 1998. *Ophiomorpha irregulaire* (trace fossil): redescription from the Cretaceous of the Book Cliffs and Wasatch Plateau, Utah. Journal of Paleontology. 72, 773-778.

Bromley, R.G., Pedersen, G.K., 2008. *Ophiomorpha irregulaire*, Mesozoic trace fossil that is either well understood but rare in outcrop or poorly understood but common in core. Palaeogeography, Palaeoclimatology, Palaeoecology. 270, 295-298.

Burns, F.E., Hooper, E., 2001. Omission colonisation surfaces within the Lower Cretaceous Mardie Greensand, Northern Carnarvon Basin, NW Shelf, Australia. American Association of Petroleum Geologists Annual Meeting. Denver, Colorado.

Burns, F.E., Burley, S.D., Gawthorpe, R.L., Pollard, J.E., 2005. Diagenetic signatures of stratal surfaces in the Upper Jurassic Fulmar Formation, Central North Sea, UKCS. Sedimentology. 52, 1155-1185.

Corbett, M.J., Fielding, C.R., Birgenheier, L.P., 2011. Stratigraphy of a Cretaceous coastal-plain fluvial succession: the Campanian Masuk Formation, Henry Mountains Syncline, Utah, U.S.A. Journal of Sedimentary Research. 81, 80-96.

Curran, H.A., 1976. A trace fossil brood structure of probable Callianassid origin. Journal of Paleontology. 50, 249-259.

Dam, G., Pedersen, G.K., Sønderholm, M., Midtgaard, H.H., Larsen, L.M., Nøhr-Hansen, H., Pedersen, A.K., 2009. Lithostratigraphy of the Cretaceous-Paleocene Nuussuaq Group, Nuussuaq Basin, West Greenland. In: Ineson, J.R. (Ed.), Geological Survey of Denmark and Greenland Bulletin. Geological Survey of Denmark and Greenland Ministry of Climate and Energy, 19, pp. 1-171.

de Gibert, J.M., Martinell, J., 1995. Sedimentary substrate and trace fossil assemblages in marine Pliocene deposits in Northeast Spain. Geobios. 28, Supplement 1, 197-206.

de Gibert, J.M., Netto, R.G., Tognoli, F.M.W., Grangeiro, M.E., 2006. Commensal worm traces and possible juvenile thalassinidean burrows associated with *Ophiomorpha nodosa*, Pleistocene, southern Brazil. Palaeogeography, Palaeoclimatology, Palaeoecology. 230, 70.

Dworschak, P.C., 1983. The biology of *Upogebia pusilla* (Petagna) (Decapoda, Thalassinidea) I. The Burrows. Marine Ecology. 4, 19-43.

Dworschak, P.C., 2000. Global diversity in the *Thalassinidea* (Decapoda). Journal of Crustacean Biology. 20, 238-245.

Dworschak, P.C., 2005. Global diversity in the *Thalassinidea* (Decapoda): an update (1998-2004). Nauplius. 13, 57-63.

Fischer-Ooster, C., 1858. Die fossilen Fucoiden der Schweizer Alpen, nebst Erörterungen über deren geologisches Alter. Huber, Bern.

Frey, R.W., Howard, J.D., Pryor, W.A., 1978. *Ophiomorpha*: its morphologic, taxonomic, and environmental significance. Palaeogeography, Palaeoclimatology, Palaeoecology. 23, 199-229.

Frey, R.W., Howard, J.D., 1982. Trace fossils from the Upper Cretaceous of the Western Interior: potential criteria for facies models. The Mountain Geologist. 19, 1-10.

Frey, R.W., Howard, J.D., 1985. Trace fossils from the Panther Member, Star Point Formation (Upper Cretaceous), Coal Creek Canyon, Utah. Journal of Paleontology. 59, 370-404.

Frey, R.W., Howard, J.D., 1990. Trace fossils and depositional sequences in a clastic shelf setting, Upper Cretaceous of Utah. Journal of Paleontology. 64, 803-820.

Gingras, M.K., Hubbard, S.M., Pemberton, S.G., Saunders, T., 2000. The significance of Pleistocene *Psilonichnus* at Willapa Bay, Washington. Palaios. 15, 142-151.

Gingras, M.K., Rasanen, M.E., Pemberton, S.G., Romero, L.P., 2002. Ichnology and sedimentology reveal depositional characteristics of bay-margin parasequences in the Miocene Amazonian Foreland Basin. Journal of Sedimentary Research. 72, 871-883.

Goldring, F., Pollard, J.E., 1995. A re-evaluation of *Ophiomorpha* burrows in the Wealden Group (Lower Cretaceous) of southern England. Cretaceous Research. 16, 665-680.

Griffis, R.B., Chavez, F.L., 1988. Effects of sediment type on burrows of *Callianassa californiensis* Dana and *C. gigas* Dana. Journal of Experimental Marine Biology and Ecology. 117, 239-253.

Grimm, K.A., Föllmi, K.B., 1994. Doomed pioneers: Allochthonous crustacean tracemakers in anaerobic basinal strata, Oligo-Miocene San Gregorio Formation, Baja California Sur, Mexico. Palaios. 9, 313-334.

Herringshaw, L.G., Sherwood, O.A., McIlroy, D., 2010. Ecosystem engineering by bioturbating polychaetes in event bed microcosms. Palaios. 25, 46-58.

Hester, N.C., Pryor, W.A., 1972. Blade-shaped crustacean burrows of Eocene age: a composite form of *Ophiomorpha*. Geological Society of America Bulletin. 83, 677-688.

Howard, J.D., Frey, R.W., 1984. Characteristic trace fossils in nearshore to offshore sequences, Upper Cretaceous of east-central Utah. Canadian Journal of Earth Sciences. 21, 200-219.

Keij, A., 1965. Miocene trace fossils from Borneo. Paläontologische Zeitschrift. 39, 220-228.

Książkiewicz, M., 1977. Trace fossils in the Flysch of the Polish Carpathians. Palaeontologia Polonica 36, 1–208.

Kundal, P., Dharashivkar, A.P., 2006. Ichnofossils from the Neogene and Quaternary deposits of Dwarka-Okha Area, Jamnagar District, Gujarat. Journal of Geological Society of India. 68, 299-315.

Kundal, P., Mude, S.N., 2008. Ichnofossils from the Neogene-Quaternary sediments of the Porbandar area, Saurashtra, Gujarat, India. Journal of the Palaeontological Society of India. 53, 207-214.

Le Roux, J.P., Puratich, J., Mourgues, F.A., Oyarzún, J.L., Otero, R.A., Torres, T., Hervé, F., 2010. Estuary deposits in the Río Baguales Formation (Chattian-Aquitanean), Magallanes Province, Chile. Andean Geology. 37, 329-344.

Loope, D.B., Dingus, L., 1999. Mud-filled *Ophiomorpha* from Upper Cretaceous continental redbeds of southern Mongolia: an ichnologic clue to the origin of detrital, grain-coating clays. Palaios. 14, 451-458.

Löwemark, L., Hong, E., 2006. *Schaubcylindrichnus formosus* isp. nov. in Miocene sandstones from northeastern Taiwan. Ichnos. 13, 267-276.

Lundgren, B., 1891. Studier öfver fossilforande lösa block. Geologiska Föreningens i Stockholm Förhandlingar. 13, 111-121.

MacEachern, J.A., Gingras, M.K., 2007. Recognition of brackish-water trace-fossil suites in the Cretaceous Western Interior Seaway of Alberta, Canada. In: Bromley, R.G., Buatois, L.A., Mángano, M.G., Genise, J.F., Melchor, R.N. (Eds.), Sediment-organism interactions: a multifaceted ichnology. SEPM Special Publication, 89, pp. 149-194.

MacEachern, J.A., Bann, K.L., Pemberton, S.G., Gingras, M.K., 2007. The ichnofacies paradigm: high resolution paleoenvironmental interpretation of the rock record. In: MacEachern, J.A., Bann, K.L., Gingras, M.K., Pemberton, S.G. (Eds.) Applied Ichnology, SEPM Short Course Notes. 52, 27-64.

MacEachern, J.A., Hobbs, T.W., 2004. The ichnological expression of marine and marginal marine conglomerates and conglomeratic intervals, Cretaceous Western Interior Seaway, Alberta and northeastern British Columbia. In: Moslow, T., Zonneveld, J.-P. (Eds.), Marine conglomerates. Bulletin of Canadian Society of Petroleum Geology, 52, pp. 77-104.

Malpas, J.A., Gawthorpe, R.L., Pollard, J.E., Sharp, I.R., 2005. Ichnofabric analysis of the shallow marine Nukhul Formation (Miocene), Suez Rift, Egypt: implications for depositional processes and sequence stratigraphic evolution. Palaeogeography, Palaeoclimatology, Palaeoecology. 215, 239-264.

Martin, M.A., Pollard, J.E., 1996. The role of trace fossil (ichnofabric) analysis in the development of depositional models for the Upper Jurassic Fulmar Formation of the Kittiwake Field (Quadrant 21 UKCS). In: Hurst, A., Johnson, H.D., Burley,

S.D., Canham, A.C., MacKertich, D.S. (Eds.), Geology of the Humber Group: Central Graben and Moray Firth, UKCS. Geological Society of London, Special Publication 114, pp. 163-183.

McIlroy, D., Tonkin, N.S., Phillips, C., Herringshaw, L.G., 2009. Comment on "*Ophiomorpha irregulaire*, Mesozoic trace fossil that is either well understood but rare in outcrop or poorly understood but common in core" by R.G. Bromley and G.K. Pedersen: [Palaeogeography, Palaeoclimatology, Palaeoecology 270 (2008) 295-298]. Palaeogeography, Palaeoclimatology, Palaeoecology. 284, 392-395.

McIlroy, D., 2004a. Some ichnological concepts, methodologies, applications and frontiers. In: McIlroy, D. (Ed.), The application of ichnology to stratigraphic and palaeoenvironmental analysis. Geological Society, London, Special Publications, 228, pp. 3-27.

McIlroy, D., 2004b. Ichnofabrics and sedimentary facies of a tide-dominated delta: Jurassic Ile Formation of Kristin Field, Haltenbanken, offshore mid-Norway. In: McIlroy, D. (Ed.), The application of ichnology to palaeoenvironmental and stratigraphic analysis. Geological Society, London, Special Publications, 228, pp. 237-272.

Merrill, R.D., 1984. *Ophiomorpha* and other nonmarine trace fossils from the Eocene Ione Formation, California. Journal of Paleontology. 58, 542-549.

Monaco, P., Garassino, A., 2001. Burrows and body fossil of decapod crustaceans in the Calcari Grigi, Lower Jurassic, Trento Platform (Italy). Geobios. 34, 291-301.

Monaco, P., Giannetti, A., 2002. Three-dimensional burrow systems and taphofacies in shallowing-upward parasequences, Lower Jurassic carbonate platform (Calcari Grigi, Southern Alps, Italy). Facies. 47, 57-82.

Orr, P., 2001. Colonization of the deep-marine environment during the early Phanerozoic: the ichnofaunal record. Geological Journal. 36, 265-278.

Pedersen, G.K., Bromley, R.G., 2006. *Ophiomorpha irregulaire*, rare trace fossil in shallow marine sandstones, Cretaceous Atane Formation, West Greenland. Cretaceous Research. 27, 964-972.

Pemberton, S.G., Jones, B., 1988. Ichnology of the Pleistocene Ironshore Formation, Grand Cayman Island, British West Indies. Journal of Paleontology. 62, 495-505.

Pemberton, S.G., Spila, M., Pulham, A.J., Saunders, T., MacEachern, J.A., Robbins, D., Sinclair, I.K., 2001. Ichnology and sedimentology of shallow to marginal marine systems: Ben Nevis & Avalon reservoirs, Jeanne d'Arc Basin. Geological Association of Canada, Short Course Notes 15. St. John's, Newfoundland. 343 p.

Say, T., 1818. An account of the crustacea of the United States. Journal of the Academy of Natural Sciences of Philadelphia. 1, 235-253.

Seilacher, A., 1967. Bathymetry of trace fossils. Marine Geology. 5, 413-428.

Shinn, E.A., 1968. Burrowing in recent lime sediments of Florida and the Bahamas. Journal of Paleontology. 42, 879-894.

Stewart, D.J., 1978. *Ophiomorpha*: a marine indicator? Proceedings of the Geologists' Association. 89, 33-41.

Suchanek, T.H., 1983. Control of seagrass communities and sediment distribution by *Callianassa* (Crustacea, Thalassinidea) bioturbation. Journal of Marine Research. 41, 281-298.

Swinbanks, D.D., Murray, J.W., 1981. Biosedimentological zonation of Boundary Bay tidal flats, Fraser River Delta, British Columbia. Sedimentology. 28, 201-237.

Swinbanks, D.D., Luternauer, J.L., 1987. Burrow distribution of thalassinidean shrimp on a Fraser Delta tidal flat, British Columbia. Journal of Paleontology. 61, 315-332.

Thompson, L.C., Pritchard, A.W., 1969. Osmoregulatory capacities of *Callianassa* and *Upogebia* (Crustacea: Thalassinidea). Biological Bulletin. 136, 114-129.

Tonkin, N.S., McIlroy, D., Meyer, R., Moore-Turpin, A., 2010. Bioturbation influence on reservoir quality: a case study from the Cretaceous Ben Nevis Formation, Jeanne d'Arc Basin, offshore Newfoundland, Canada. AAPG Bulletin. 94, 1059-1078.

Uchman, A., 1998. Taxonomy and ethology of flysch trace fossils: revision of the Marian Książkiewicz collection and studies of complementary material. Annales Societatis Geologorum Poloniae. 68, 105-218.

Uchman, A., 2004. Phanerozoic history of deep-sea trace fossils. In: McIlroy, D. (Ed.), The application of ichnology to palaeoenvironmental and stratigraphic analysis. Geological Society, London, Special Publications, 228, pp. 125-139.

Uchman, A., 2009. The *Ophiomorpha rudis* ichnosubfacies of the *Nereites* ichnofacies: characteristics and constraints. Palaeogeography, Palaeoclimatology, Palaeoecology. 276, 107-119.

Van de Kamp, P.C., Harper, J.D., Conniff, J.J., Morris, D.A., 1974. Facies relations in the Eocene-Oligocene in the Santa Ynez Mountains, California. Journal of the Geological Society. 130, 545-565.

Wanless, H., Tedesco, L., Tyrrell, K., 1988. Production of subtidal tubular and surficial tempestites by Hurricane Kate, Caicos Platform, British West Indies. Journal of Sedimentary Petrology. 58, 739-750.

Weimer, R.J., Hoyt, J.H., 1964. Burrows of *Callianassa major* Say, geologic indicators of littoral and shallow neritic environments. Journal of Paleontology. 38, 761-767.

2.13 Figures

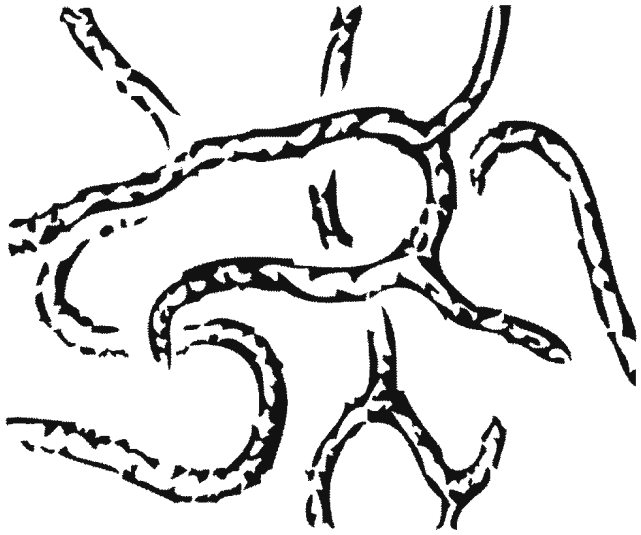

Fig. 2.1: Diagnostic meander maze of *O. irregulaire* (after Frey et al., 1978).

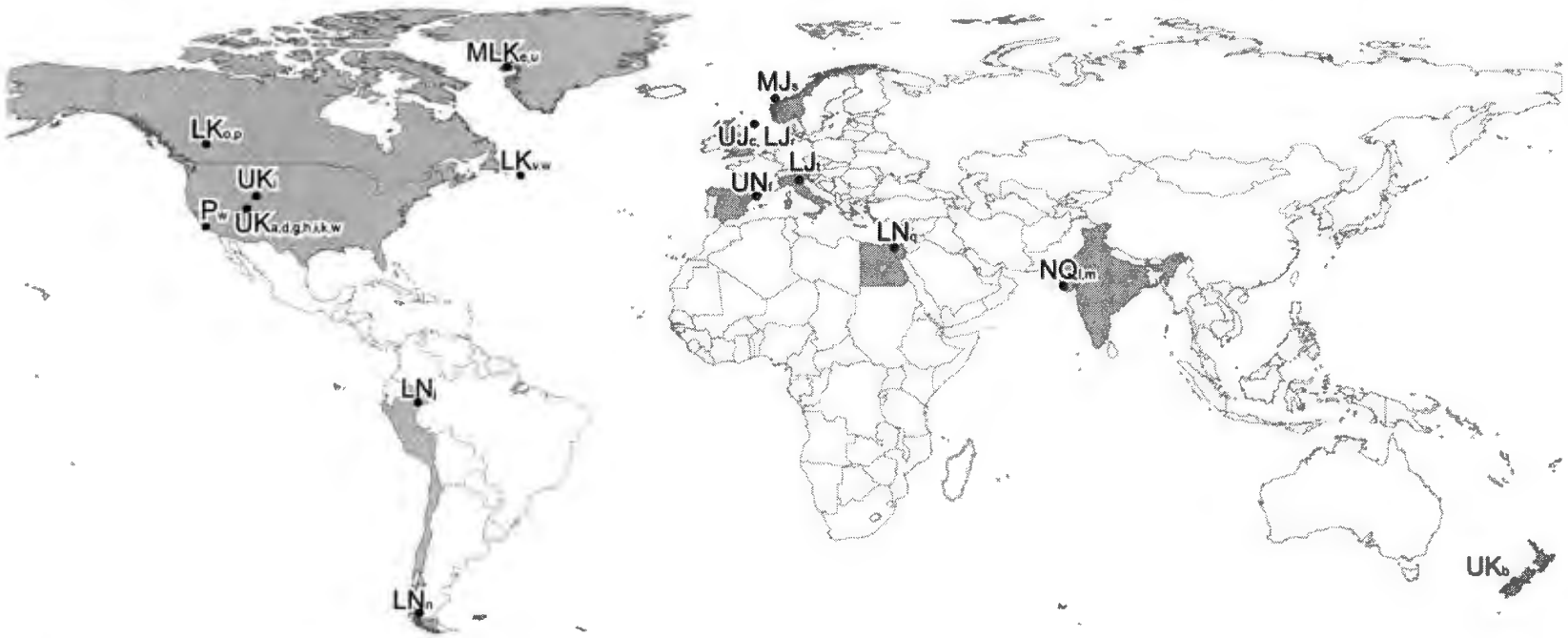

Fig. 2.2: Global distribution of *Ophiomorpha irregulaire*, which has been found on all continents except Antarctica in Jurassic to Quaternary strata (modified after Figure 1 in Löwemark and Hong, 2006). L = Late, M = Middle, U = Upper. J = Jurassic, K = Cretaceous, P = Paleogene, N = Neogene, NQ = Neogene-Quaternary. a (Bromley and Ekdale, 1998), b (Burns and Hooper, 2001), c (Burns et al., 2005), d (Corbett et al., 2011), e (Dam et al., 2009), f (de Gibert and Martinell, 1995), g (Frey and Howard, 1982), h (Frey and Howard, 1990), i (Frey et al., 1978), j (Gingras et al., 2002), k (Howard and Frey, 1984), l (Kundal and Mude, 2008), m (Kundal and Dharashivkar, 2006), n (Le Roux et al., 2010), o (MacEachern and Gingras, 2007), p (MacEachern and Hobbs, 2004), q (Malpas et al., 2005), r (Martin and Pollard, 1996), s (McIlroy, 2004), t (Monaco and Garassino, 2001), u (Pedersen and Bromley, 2006), v (Tonkin et al., 2010), w (locations mentioned within this paper).

Table 2.1: Occurrences of *Ophiomorpha irregulaire* in stratigraphic order. 'On Map' column refers to Fig. 2.2. This table only includes publications that described *O. irregulaire*, and does not include off hand mentions of the ichnospecies, nor non-English publications. General ichnospecies of *Ophiomorpha* are not included in the table. Table formatted after Uchman (2009).

	Lithostratigraphic Unit	Location	Age	References	On Map
1	Dwarka and Chaya formations	Gujarat, India	Neogene-Quaternary	Kundal and Dharashivkar (2006)	m
2	Miliolite and Dwarka formations	Gujarat, India	Neogene-Quaternary	Kundal and Mude (2008)	l
3	Sandy Clay Unit	NE Spain	Pliocene	de Gibert and Martinell (1995)	f
4	Pebas Formation	Amazon, South America	Middle Miocene	Gingras et al. (2002)	j
5	Nukhul Formation	Suez Rift, Egypt	Lower Miocene	Malpas et al. (2005)	q
6	Rio Baguales Formation	Chile	Lower Miocene	le Roux et al. (2010)	n
7	Juncal Formation	Wagon Road Canyon, California	Eocene	Herein	w
8	Blackhawk Formation	Book Cliffs, Utah	Upper Cretaceous	Bromley and Ekdale (1998)	a
9	Blackhawk Formation	Book Cliffs, Utah	Upper Cretaceous	Frey and Howard (1982)	g
10	Star Point and Blackhawk formations	Book Cliffs, Utah	Upper Cretaceous	Frey and Howard (1990)	h
11	Star Point and Blackhawk formations	Book Cliffs, Utah	Upper Cretaceous	Howard and Frey (1984)	k
12	Star Point and Blackhawk formations	Book Cliffs, Utah	Upper Cretaceous	Herein	w
13	Masuk Formation	Utah	Upper Cretaceous	Corbett et al. (2011)	d
14	Star Point, Blackhawk, and Frontier formations	Utah and Wyoming	Upper Cretaceous	Frey et al. (1978)	i
15	Qilakitsoq Member, Atane Formation	West Greenland	Middle to Upper Cretaceous	Dam et al. (2009)	e
16	Qilakitsoq Member, Atane Formation	West Greenland	Middle to Upper Cretaceous	Pedersen and Bromley (2006)	u
17	Viking and Spirit River formations	Alberta and British Columbia, Canada	Lower Cretaceous	MacEachern and Hobbs (2004)	p
18	Viking Formation	Alberta, Canada	Lower Cretaceous	MacEachern and Gingras (2007)	o
19	Ben Nevis Formation	Offshore Newfoundland, Canada	Lower Cretaceous	Tonkin et al. (2010)	v
20	Ben Nevis Formation	Offshore Newfoundland, Canada	Lower Cretaceous	Herein	w
21	Mardie Greensand Member	NW shelf, Australia	Lower Cretaceous	Burns and Hooper (2001)	b
22	Fulmar Formation	Central North Sea, UKCS	Upper Jurassic	Burns et al. (2005)	c
23	Fulmar Formation	North Central Graben, UKCS	Upper Jurassic	Martin and Pollard (1996)	r
24	Ile Formation	Norway	Middle Jurassic	McIlroy (2004b)	s
25	Rozzo Member, Calcari Grigi Formation	Valbona, Italy	Lower Jurassic	Monaco and Garassino (2001)	t

Table 2.2: Abundance of *Ophiomorpha irregulaire* based on the number of formations in which it occurs per stage (formatted after Uchman, 2009). Lithostratigraphic units are from Table 2.1.

Age, Stage	Lithostratigraphic Units	Total
Quaternary	1, 2	2
Pliocene	3	1
Miocene	4, 5, 6	3
Oligocene		
Eocene	7	1
Paleocene		
Maastrichtian		
Campanian	8, 9, 10, 11, 12, 13, 14, 15, 16	9
Santonian		
Coniacian		
Turonian	14	1
Cenomanian		
Albian	17, 18	2
Aptian	19, 20	2
Barremian	21	1
Hauterivian		
Valanginian		
Berriasian		
Tithonian		
Kimmeridgian		
Oxfordian	22, 23	2
Callovian		
Bathonian		
Bajocian		
Aalenian	24	1
Toarcian		
Pliensbachian	25	1

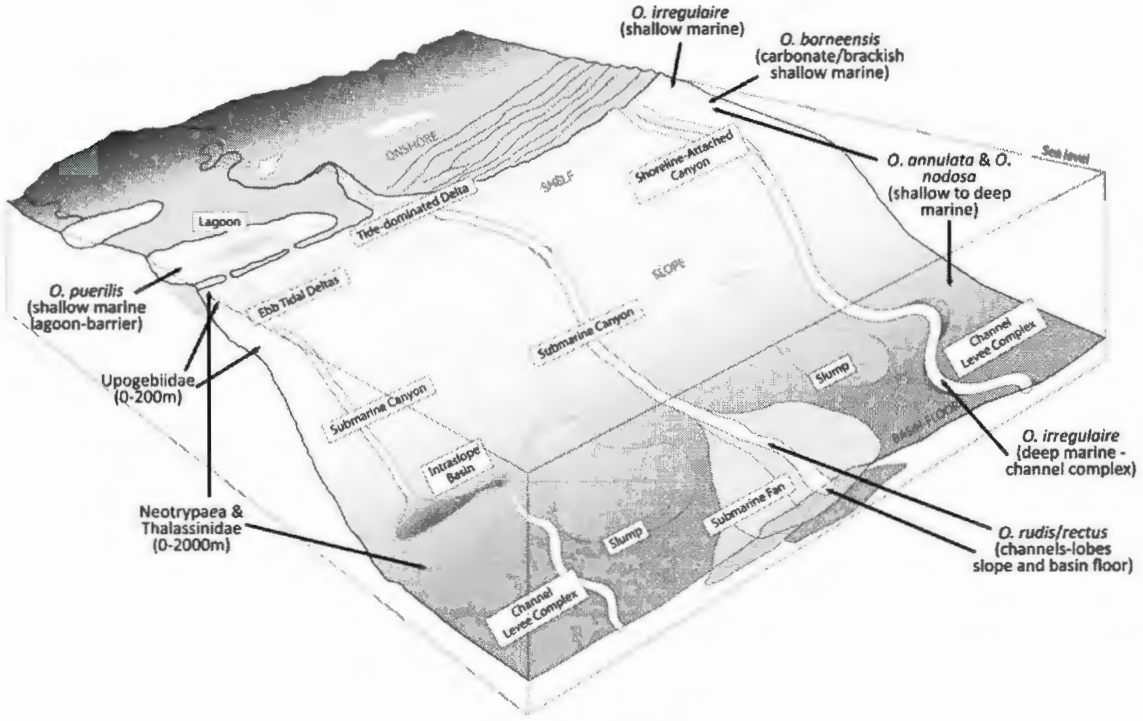

Fig. 2.3: Palaeoenvironmental distribution of all ichnospecies of *Ophiomorpha*, plotted with modern day Thalassinidean, burrowing decapod crustacean, trace-makers of *Ophiomorpha* (modified after McIlroy, 2004a).

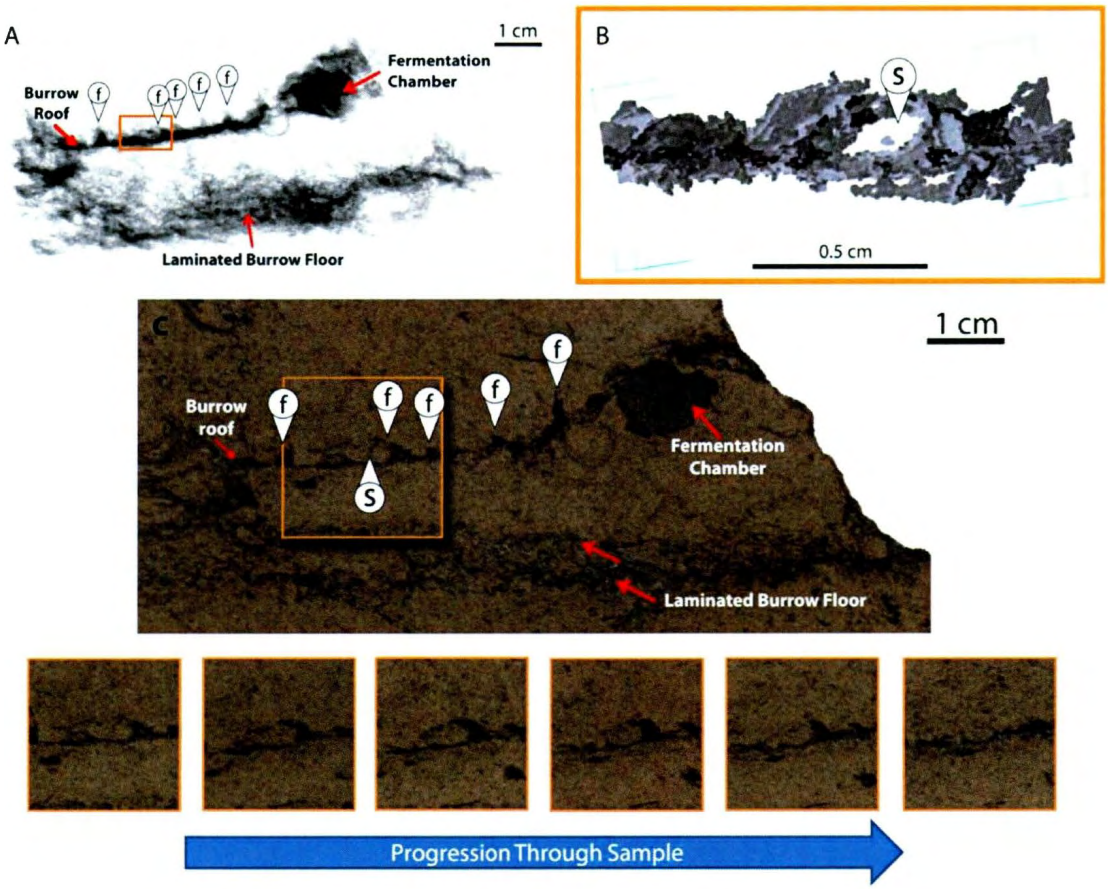

Fig. 2.4: A: Three-dimensional model of the type locality *O. irregulaire* specimen. Model rendering is similar to an X-ray; darker areas are higher densities of mud. f = irregularly-spaced flame-like mud-lined pellets, semi-perpendicular to the burrow roof. Laminated burrow floor, roof, and fermentation chamber are labeled. Orange box highlights location of Fig 2.4B. B: Close up three-dimensional model of mud-lined sand-filled pellet. This portion of the burrow roof was remodelled using a different modeling technique, illustrating the mud as solid grey. The white void in the centre of the mud lining represents a sand-filled pellet (S). C: Original rock photograph in same orientation as model in Fig. 4A, same features are also labeled. Upper half: Orange box (inset) highlights location of pellet from Fig. 2.4A and Fig. 2.4B, as well as location of pellet depicted in lower half of the figure. Lower half: shows the progression deeper into the rock by increments of 0.305 mm. Notice the morphological evolution of the flame-like mud-lined pellets. (Modified after Boyd et al., 2012)

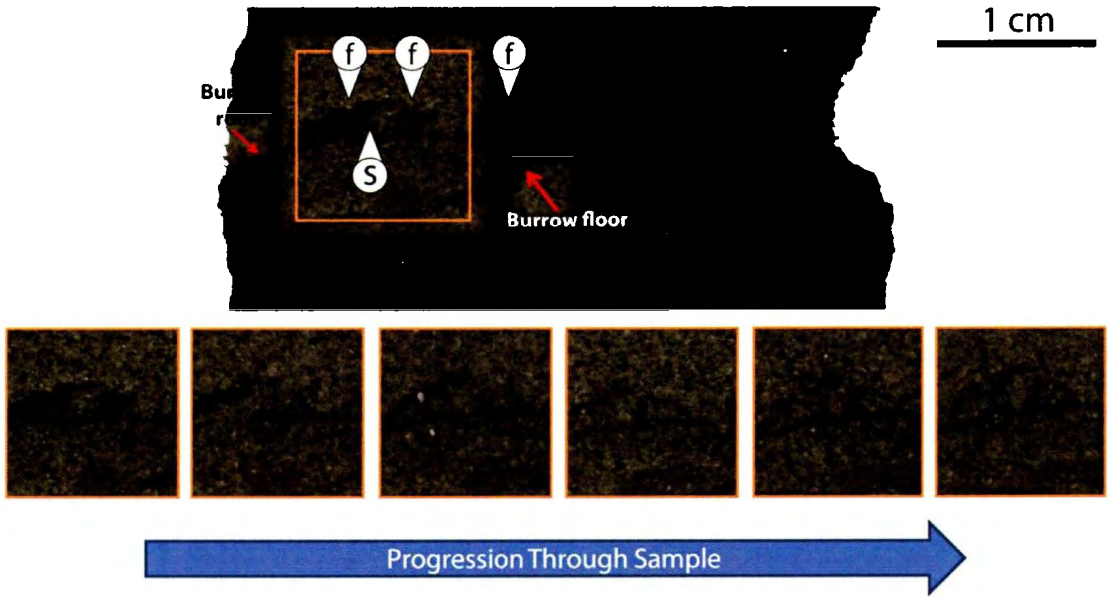

Fig. 2.5: Photograph of Juncal Formation turbidite sample. f = irregularly spaced mud-flame pellets on burrow roof; S = sand pellet. Upper Half: Orange box (inset) highlights location of pellet depicted in lower half of the figure. Lower Half: shows the progression into the rock in increments of 0.305 mm. Notice the morphological evolution of flame-like mud-lined pellets. Pellets are not as well defined compared to the type material due to a higher content of dispersed mud in the sediment; morphologically they are very similar.

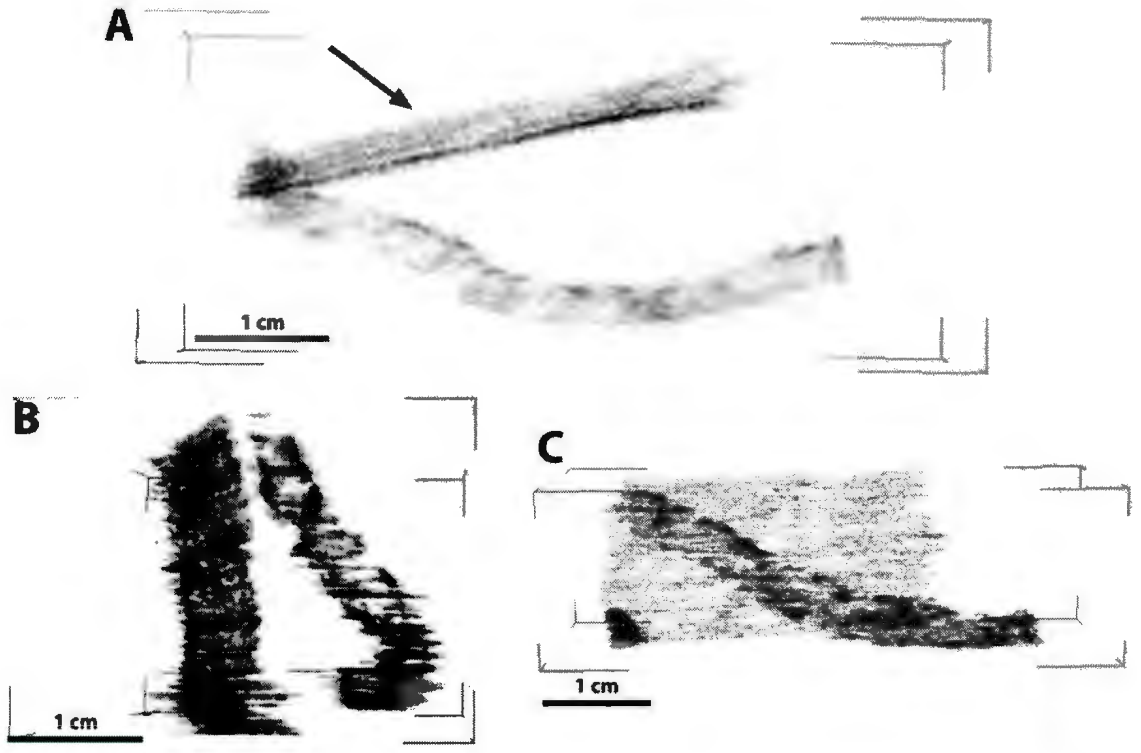

Fig. 2.6: Three-dimensional model of *Ophiomorpha irregulaire* from the Juncal Formation, California. Same modeling style as Fig. 2.4A, where the black/grey represents a higher concentration of mud. A: Cross-section with the top of the rock at the top of the photo. In the upper section of the model is a sedimentary lamina (arrow), included in the model to provide a reference position to the sinuous burrow. A portion of the meandering maze is visible. B: Longitudinal side view. Burrow can be seen either moving up or down in relation to the sedimentary laminae. C: Bottom through to top view. Laminae are stacked behind the burrow. A bend in the burrow is visible near the bottom.

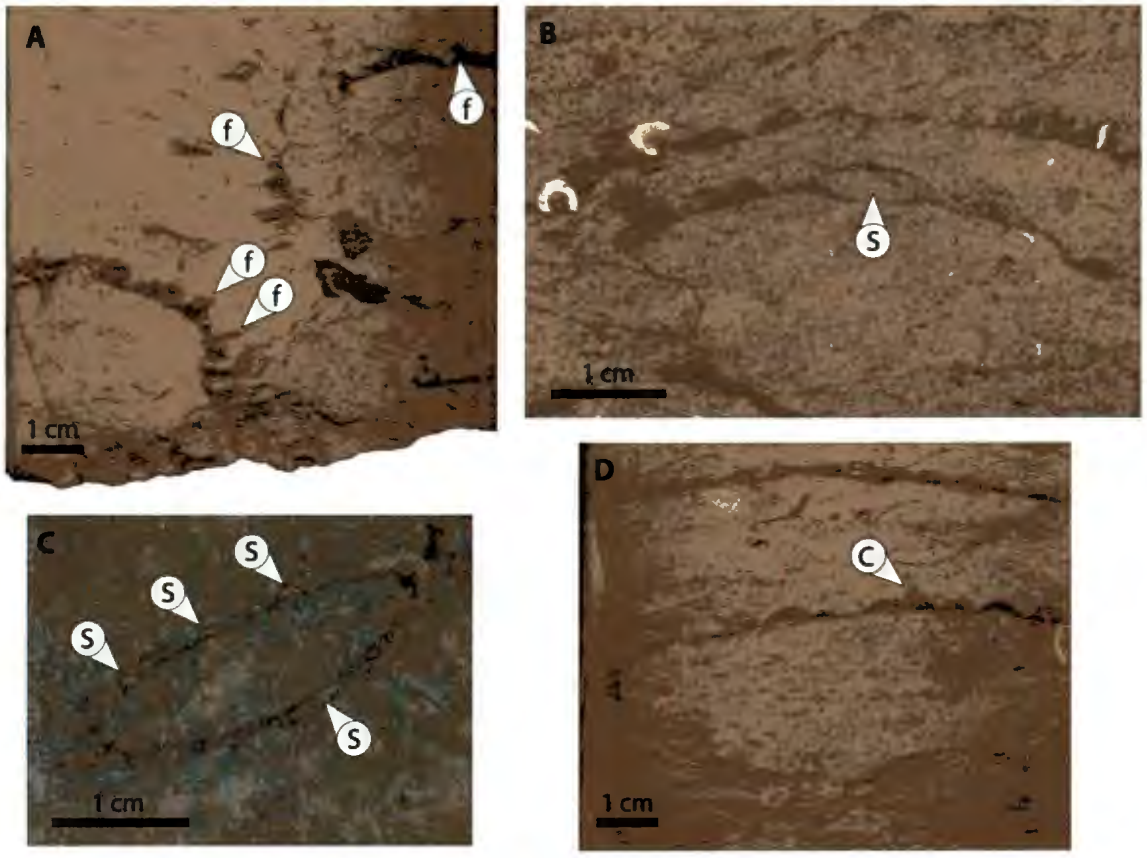

Fig. 2.7: Core photographs of *O. irregulaire*, all from Ben Nevis L-55 well. A: Flame-like mud pellets (f) in two *Ophiomorpha irregulaire*. For a large thin slice image of this core see Fig. C.2 C. B: Double-roofed *O. irregulaire*; arrow points to a sand-filled mud-lined pellet (S). For a large thin slice image of this core see Fig. C.1 A. C: *Ophiomorpha irregulaire* rimmed with sand-filled, mud-lined pellets (S) Modified from McIlroy et al., 2009. D: Double-roofed *O. irregulaire*, with conical pellets (C).

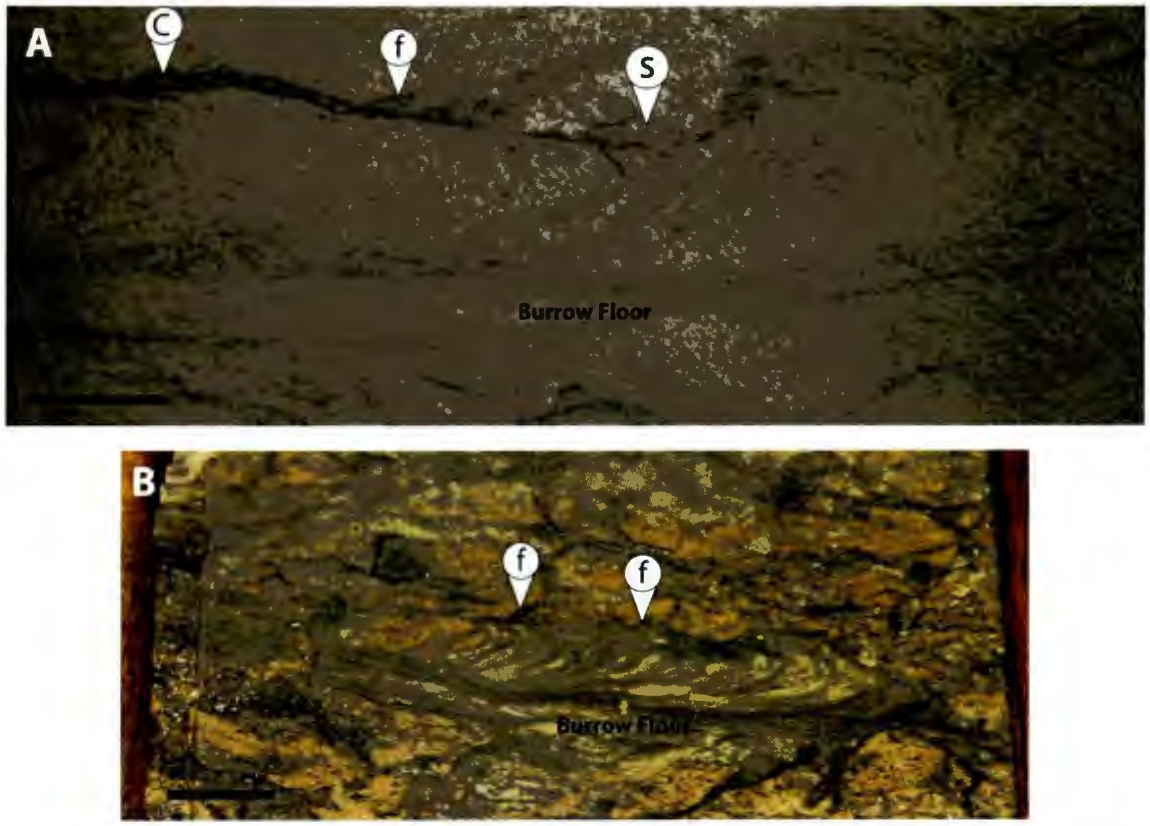

Fig. 2.8: Rippled-filled examples of *Ophiomorpha irregulaire*. Scale bars equal 1 centimeter. A: *Ophiomorpha irregulaire* from Ben Nevis L-55 well, with ripple infill and pellet-lined burrow roof; conical-shaped pellets (C), flame-like mud pellet (f), and sand-filled mud-lined pellet (S). B: *O. irregulaire* from C-13 well, offshore Newfoundland, lined with flame-like mud pellets (f).

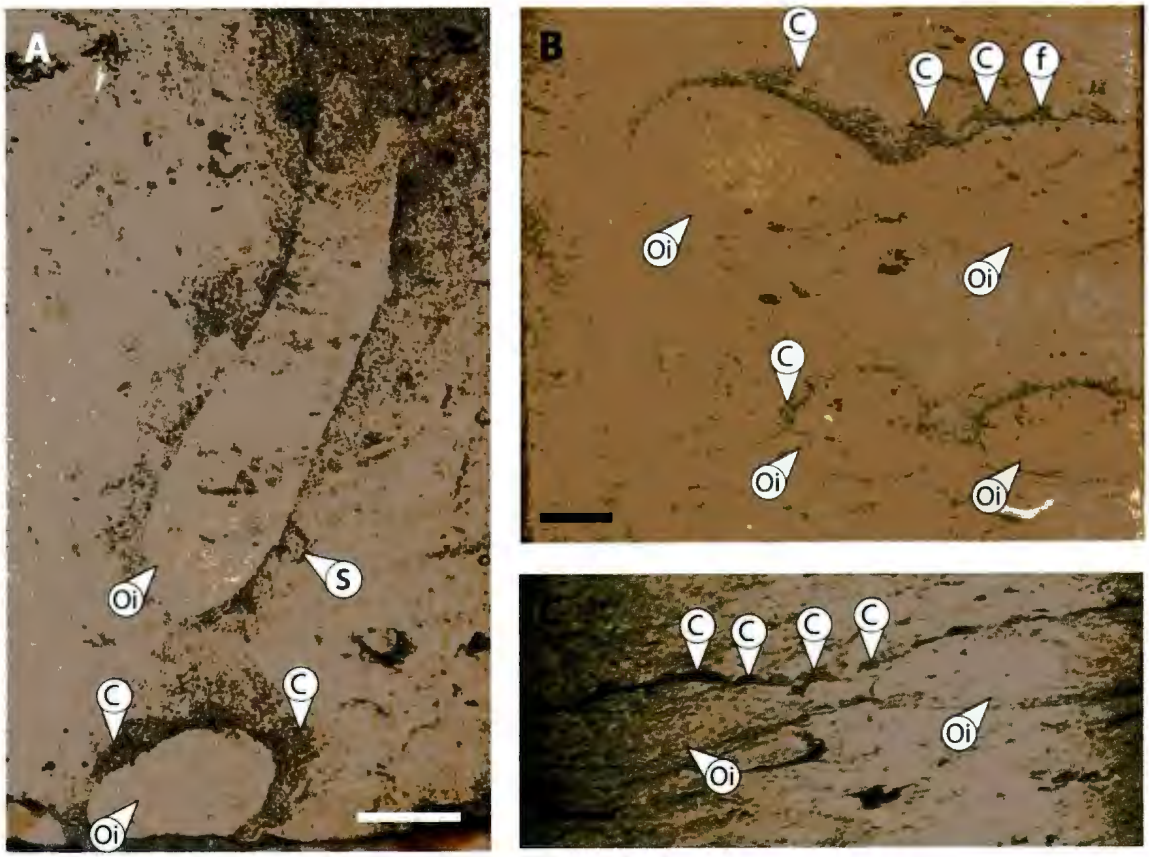

Fig. 2.9: Meandering examples of *Ophiomorpha irregulaire* in Ben Nevis L-55 core. Scale bars equal 1 centimeter. A: Two burrows in close proximity to one another that are most likely connected farther into the core. For a large thin slice image of this core see Fig. C.2. D, B and C: Two burrows that are slightly connected in the center, representing a turn-around point in the burrow morphology. Oi = *Ophiomorpha irregulaire*; C = conical pellets; f = flame-like mud pellets; and S = sand-filled mud-lined pellet.

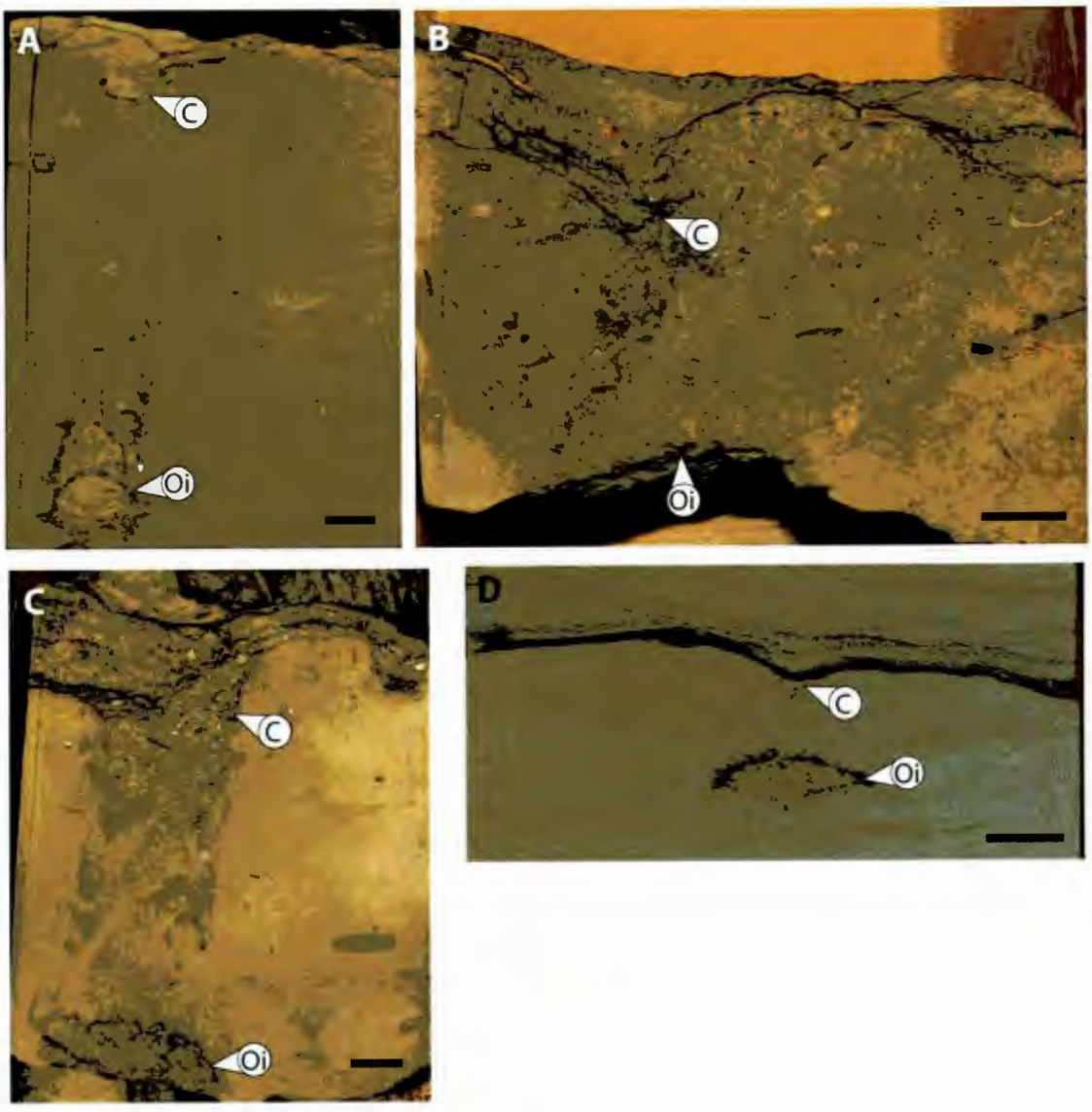

Fig. 2.10: Core examples of *O. irregulaire* showing feeding under a collapse cone of sediment. Scale bars equal 1 centimeter. C = collapse cone; Oi = *Ophiomorpha irregulaire*. A-C: from C-13 well, offshore Newfoundland. D: An example from Ile Formation Smørbukk Field, offshore Norway.

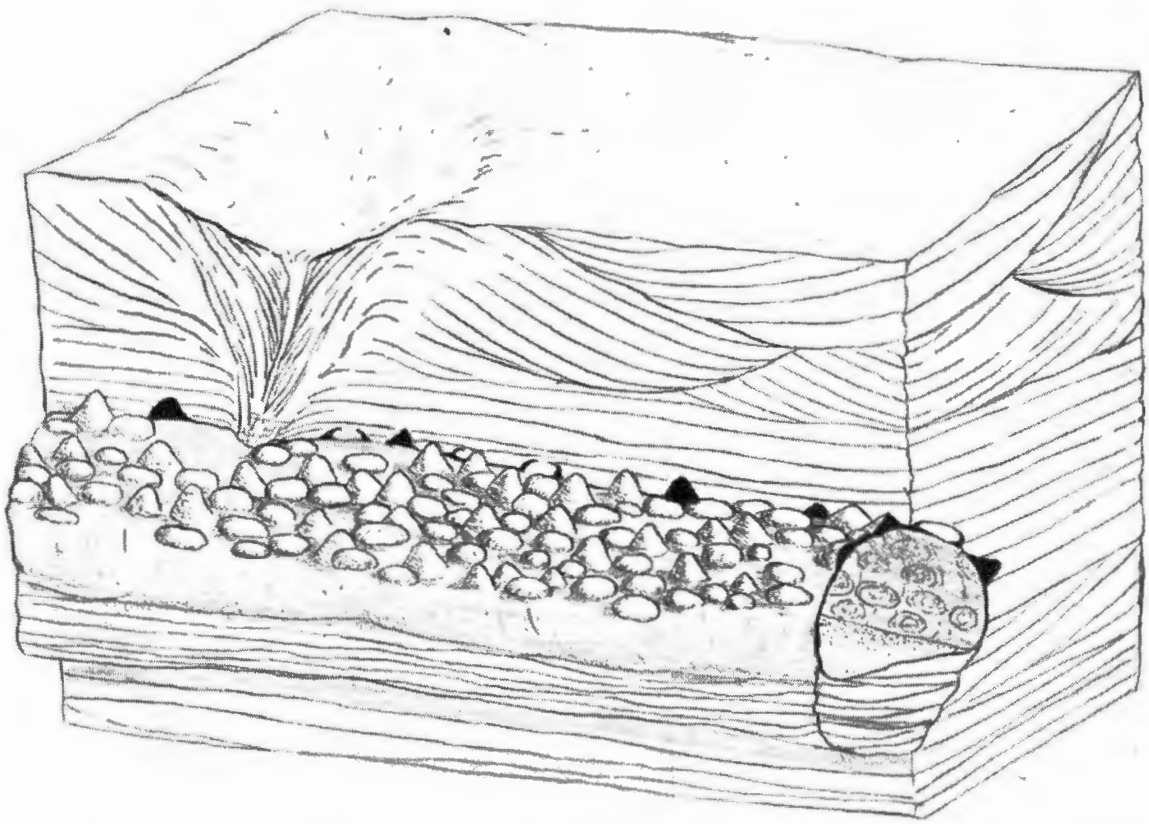

Fig. 2.11: Idealised sketch of *Ophiomorpha irregulaire* with updated morphological features, including pellet morphology and a collapse cone deposit-feeding structure.

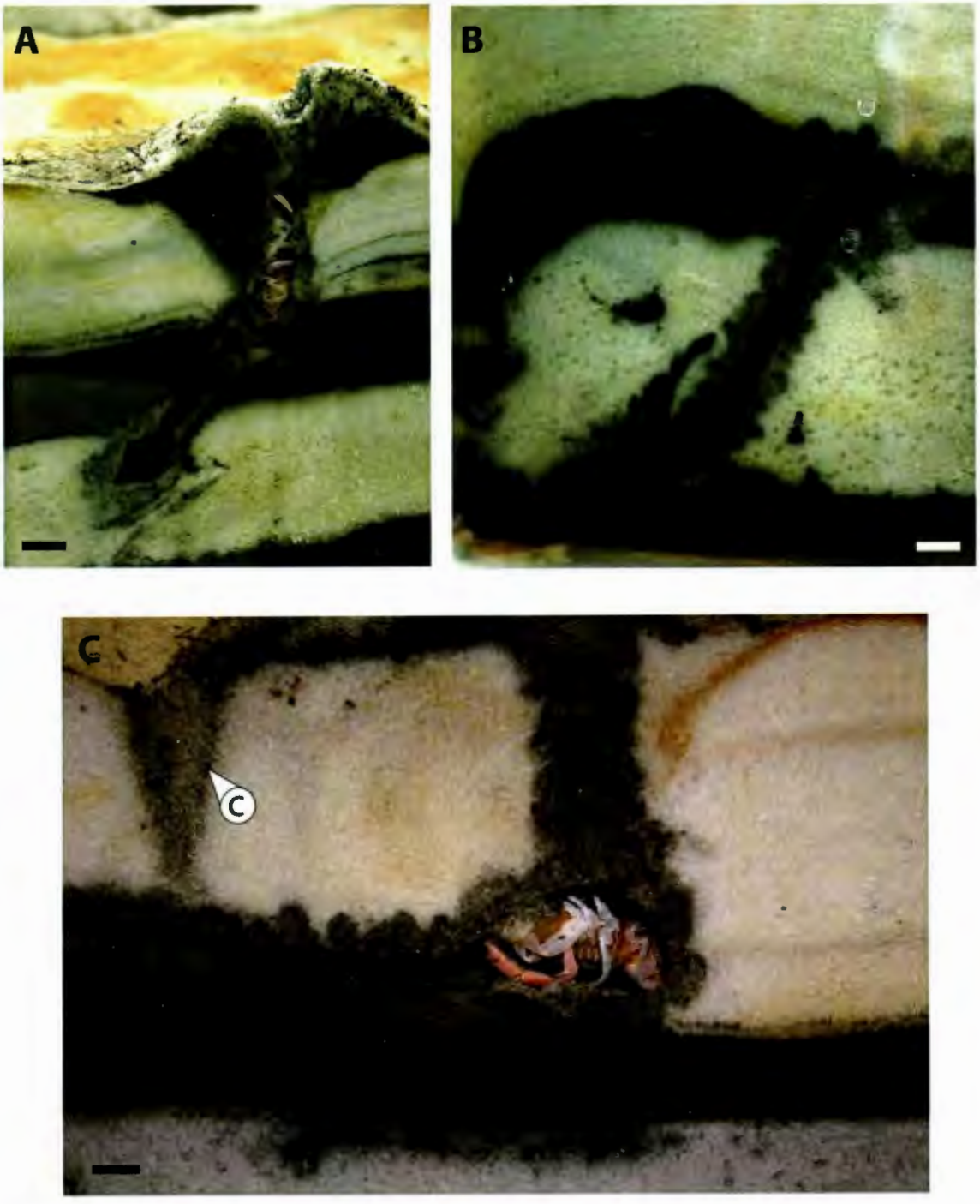

Fig. 2.12: A variety of *Neotrypaea californiensis* burrow morphologies. Scale bars equal 1 centimeter. A: An oblique burrow with resting shrimp. Bulbous end of burrow is a turning node, where the shrimp enters farther into the sediment and away from the tank glass. B: Oblique burrow lined with mud pellets. C: Gallery example of *N. californiensis* burrow; burrow roof is lined with mud pellets. Far left of photograph shows a collapse cone (C).

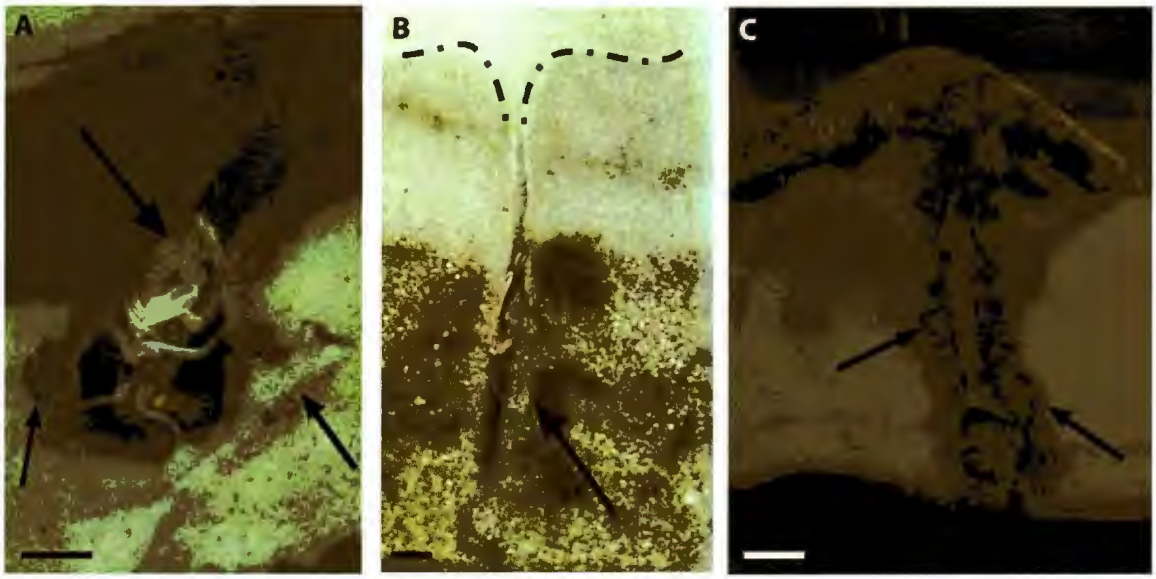

Fig. 2.13: ***Neotrypaea californiensis*** **creating sand pellets in lab aquaria. Scale bars equal 1 centimeter. A: Shrimp in the process of forming a sand pellet with claws (arrow); other two arrows indicate sandy burrow lining. B: Aquarium with clean sand. Arrow highlights the clean sand pellets lining the burrow walls; shrimp is feeding below a collapse cone (dashed lines). C: Sand-filled pellets enveloped with muddier sediment (arrows). Burrow mound at sediment-water interface.**

Fig. 2.14: A: Sketch representing the fabrication method of the mud-enveloped sand pellet, as observed in three-dimensional modeling of the Book Cliffs type locality sample (B) (modified from Boyd et al., 2012).

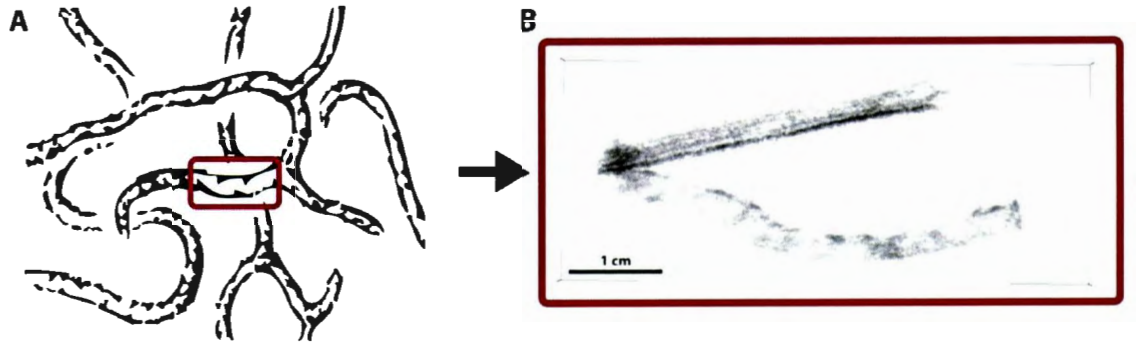

Fig. 2.15: A: Sketch by Frey et al. (1978) illustrating the "loose system of sinuous tunnels" comprising the meander maze burrow of *O. irregulaire*. Red box highlights the location of B, a similar portion of a sinuous tunnel, observed in the turbidite sample from California.

CHAPTER 3

Petrophysical Properties of *Ophiomorpha irregulaire* Ichnofabrics from BN L-55 of Hebron Field, Offshore Newfoundland

Chapter 3 – Petrophysical Properties of *Ophiomorpha irregulaire* Ichnofabrics from BN L-55 of Hebron Field, Offshore Newfoundland

3.1 Abstract

Ophiomorpha is the dominant ichnofabric-forming trace fossil in many bioturbated siliciclastic petroleum reservoirs worldwide, but its effect on reservoir permeability, especially in three dimensions, is not fully understood. Four different *Ophiomorpha*-dominated ichnofabrics in cores from the Ben Nevis Formation in the L-55 Ben Nevis well of the Jeanne d'Arc Basin, offshore Newfoundland were mapped using spot-permeametry measurements. Integration of spot-permeametry data and volumetric analysis allows us to conclude that burrows of *Ophiomorpha irregulaire* reduce k_h by an average of 28% and k_v can be decreased by 14%.

Volumetric and petrophysical study of ichnofabrics allow ichnology to become an integral part of reservoir characterisation studies. With an understanding of burrow volume and its effect on reservoir quality at the core scale, it becomes possible to make first-order interpretations and predictions of reservoir quality on a reservoir-wide scale. Study of ichnofabrics through a succession allows prediction of the intensity of bioturbation on a facies by facies basis. Variability in ichnofabrics within facies elements makes realistic first-order predictions of lateral variability, connectivity of trace fossils, and therefore reservoir properties possible. This work demonstrates that careful integration of petrophysical and ichnological analysis has the potential to greatly inform exploration for and production from bioturbated reservoir intervals.

3.2 Introduction

Ophiomorpha occurs in several prolific siliciclastic hydrocarbon reservoirs worldwide (Raychaudhuri and Pemberton, 1992; McIlroy, 2004b; Tonkin et al., 2010). The effect of bioturbation in three-dimensions within such reservoirs is not fully understood. Preliminary work in hydrocarbon reservoirs from offshore Newfoundland has demonstrated an association of *Ophiomorpha* with net-pay intervals in the Ben Nevis Formation reservoirs (Tonkin et al., 2010). This work considers *Ophiomorpha irregulaire* in three dimensions by serially grinding analogous material using the approach of Bednarz and McIlroy (2009, 2012). The integration of petrophysical and morphological data – the latter being from analogous ichnological studies in Chapter 2 – is a novel approach to both ichnology and reservoir characterisation. This new approach has the potential to transform the ways that ichnofabric data are incorporated into reservoir characterisation studies. This paper aims to develop a methodology for integrated ichnofabric and petrophysical analysis using the trace fossil *Ophiomorpha irregulaire* as a case study. Spot-permeability was conducted on cores from the Ben Nevis Formation in the L-55 Ben Nevis well, of the Jeanne d'Arc Basin, offshore Newfoundland. The storm-dominated succession is rich in *O. irregulaire* burrows including in the petroliferous part of the stratigraphic succession (Tonkin et al., 2010).

Most ichnofabric studies are based on two-dimensional slabbed core (e.g. McIlroy 2004b) or on three-dimensional datasets from X-ray computed tomography or NMR studies (Gingras et al., 2002). Study of ichnofabric in core has the obvious drawback that it is a three-dimensional phenomenon that is not completely represented in a single plane

(Chamberlain, 1978; McIlroy, 2004a). Three-dimensional studies of ichnofabrics have until recently largely relied upon non-destructive methods (e.g. X-ray computed tomography and nuclear magnetic resonance [NMR]; Gingras et al., 2002 and references within). The non-destructive methods are all limited by the fact that the data collected are not directly imaged, so some aspects of the ichnofabric cannot be studied. In contrast, the destructive serial grinding of ichnofabrics pioneered by Bednarz and McIlroy (2009, 2012) allow direct observation of subtle lithological attributes of ichnofabrics. Until now, the data collected by the serial grinding method has been purely photographic in nature, with the aim of reconstructing burrow morphology (e.g. Boyd et al., 2012). This study adds a petrophysical component to the dataset collected. Through detailed understanding of the organism-sediment interactions associated with the ichnofabric this study aims to create a generic understanding of the effects of a given trace fossil on reservoir quality. That understanding can then be integrated with a three-dimensional understanding of burrow morphology (see Chapter 2). Our study of *Ophiomorpha irregulaire* represents the first time this approach has been used.

3.3 Methods

Core-based material (four samples) from the Lower Cretaceous Ben Nevis Formation, Jeanne d'Arc Basin, offshore Newfoundland (Ben Nevis L-55 well; cf. Tonkin et al., 2010) was chosen to represent a range of morphological elements of *Ophiomorpha irregulaire* burrows. By characterizing permeability trends associated with different burrow elements it should be possible to extrapolate from this dataset to gross-scale trends associated with *O. irregulaire* burrow systems at the metre scale. Spot-

permeability was measured from each sample of core using a Temco Mini-Permeameter. The permeameter forces nitrogen gas into the rock, "reading" a one-centimeter cubed volume. Values are given in milliDarcies (mD), providing data on the connectivity of pore spaces in the studied volume of sedimentary rock. A one-centimeter spot-permeability grid was drawn on the face of the core, leaving sufficient space from the core edge to avoid the escape of nitrogen gas (resulting in a false, higher permeability reading). Three readings were conducted on each grid and averaged for a final value. Approximately two hundred spot-permeability measurements were taken on each of the four core slabs.

Four representative samples from two core samples were selected to create standard-sized thin sections to compare lithology in bioturbated and unbioturbated regions by *Ophiomorpha*. The thin sections were created from the core slab face. Prior to fabrication, samples were impregnated with a blue-dyed epoxy resin to reveal pore spaces under the microscope. Large thin slices were fabricated from the four core samples studied to enhance visibility of sedimentary structures and burrows (Garton and McIlroy, 2006).

3.4 Results

3.4.1 Lithology and Ichnofabric Descriptions

Each core sample collected represents a different *Ophiomorpha*-dominated ichnofabric assemblage from the L-55 well from the Hebron Field (Lithofacies 1 of Tonkin et al., 2010). For large thin slice images of the four ichnofabrics, refer to

Appendix C, Fig. C.2 Ichnofabric descriptions, including a description of the *Ophiomorpha* burrow appearance are described below.

3.4.1.1 *Ophiomorpha-Palaeophycus* Ichnofabric

Ophiomorpha-Palaeophycus ichnofabric samples, including a shaft of *Ophiomorpha,* consist of very fine-grained sandstone, in vertical to oblique cross-section. Directly above the burrow is a sub-vertical zone of disrupted sediment that is darker grey than the rest of the sediment. The concentric lining and lack of pellets around the burrow might invite comparison with *Psilonichnus* isp. Burrows of *Palaeophycus* isp. are visible adjacent to *Ophiomorpha*. The remaining sediment is burrow mottled. Bioturbation intensity attributed to *Ophiomorpha* is 40% and the overall bioturbation intensity is 100% (Fig. 3.1A).

Two thin sections were created from the core slab face. Approximate thin section locations are highlighted with dashed lines on Fig. 3.1A. One thin section was taken from *Ophiomorpha*-bioturbated sediment (top of core) to compare with sediment un-bioturbated by *Ophiomorpha* (bottom right of core). A comprehensive table of observations from both thin sections can be seen in Appendix C, Table C.5.

Petrology of *Ophiomorpha*-bioturbated sediment in *Ophiomorpha-Palaeophycus* ichnofabric: The coarse silty sandstone shows a patchy distribution of large 'clean' areas (with less clay content and greater porosity) and muddy areas (with higher clay content with lower porosity). The 'clean' regions show ~15% porosity, while the clay-rich areas show a clay content of ~15%. Within the patches grains are well

sorted. Pore spaces are connected (resulting in effective porosity) and intergranular (Fig. 3.3 A & B).

Petrology of unbioturbated portion of *Ophiomorpha-Palaeophycus* ichnofabric: The coarse silty sandstone is well sorted with primarily subangular grains. Porosity is again connected (effective porosity) and intergranular. Overall, this sample has less mud and higher porosity (25%) than the *Ophiomorpha*-bioturbated sample (Fig. 3.3 C & D).

3.4.1.2 *Ophiomorpha*-Burrow Mottled Ichnofabric

Ophiomorpha-burrow mottled ichnofabric consists of highly bioturbated fine-grained sandstone bioturbated by large *O. irregulaire* with flame-like "pellets" (cf. Boyd et al., 2012). The sample includes two horizontal galleries of *O. irregulaire*. Bioturbation intensity attributed to *Ophiomorpha* is 50%, while the overall bioturbation intensity is 100% (Fig. 3.1C).

3.4.1.3 *Ophiomorpha-Asterosoma* Ichnofabric

Ophiomorpha-Asterosoma ichnofabric consists of fine-grained parallel laminated sandstone with oblique *Ophiomorpha irregulaire* shafts in vertical section. Such oblique shafts are common in *O. irregulaire* whose makers colonize event beds such in this sample. Bioturbation intensity of *Ophiomorpha* is 35% and the overall bioturbation intensity is 60% (Fig. 3.2A).

3.4.1.4 *Ophiomorpha-Thalassinoides* Ichnofabric

Ophiomorpha-Thalassinoides ichnofabric is characterised by fine-grained, highly

bioturbated sandstone whose sedimentary structures have been destroyed by bioturbation. *Ophiomorpha* is present as vertical shafts and horizontal galleries, both with diffuse clay-rich zones around the tunnel. Some mud-encased sand-filled pellets line the burrow (cf. Boyd et al., 2012). Bioturbation intensity of *Ophiomorpha* is 40% and the overall bioturbation intensity is 100% (Fig. 3.2C).

Two thin sections were created from the core slab face. Approximate thin section locations are highlighted with dashed lines on Fig. 3.2C. One sample was taken above *Ophiomorpha* to investigate the burrow mottling texture. The second sample was taken from the bottom of the core, directly above the unlined horizontal oval burrow component to study the halo sediment. A comprehensive table of observations from both thin sections can be seen in Appendix C, Table C.5.

Burrow mottled sediment sample from *Ophiomorpha-Thalassinoides* ichnofabric: This sample consisted of very fine-grained, subangular to subrounded sandstone. Grains are moderately sorted, though with a patchy distribution of mud. Porosity is intergranular with some evidence for dissolution of shell debris and non-quartz grains. One fracture pore was noted through the mud-rich layer of the thin section.

The *Ophiomorpha* horizontal burrow sample was studied in three components for better comparison; 1. Passive burrow fill; 2. Near-burrow sediment; and 3. Host sediment (beyond the near-burrow sediment; Fig. 3.4). The **passive burrow fill** is very fine-grained sandstone composed mainly of quartz grains (60%) and pore spaces (35%). It is poorly sorted with subangular to rounded grains. Pore spaces are intergranular and connected (effective porosity) with some evidence for dissolution of sub-euhedral non-

quartz grains (Fig. 3.4). The **near-burrow sediment** has a higher quantity (10%) of clay-sized particles compared to the clay-free passive burrow fill, and less porosity (10%). The near-burrow sediment is moderately sorted with subangular to subrounded grains that are more tightly packed than the passive burrow fill. The clay particles are irregularly dispersed (500 μm to more than 7 mm) away from the edge of the passive burrow fill. The clay occludes most of the connected pores (Fig. 3.4). Porosity in the near-burrow sediment is intergranular with no evidence of dissolution. Porosity has been significantly reduced by the increase of clay in the pores and by the tightly packed quartz grains (Fig. 3.4). The **host sediment** composition is very similar to that of the passive burrow fill; however, it is coarse silty sandstone. It is poorly to moderately sorted with a higher presence of sub-euhedral dissolution. Overall, the pore spaces are connected and contain no mud (Fig. 3.4).

3.4.2 Permeability

Permeability measurements were determined for all four ichnofabrics, relating aspects of burrow morphology to permeability characteristics. Permeability values are represented as semi-transparent coloured blocks atop the core photographs (Figs. 3.1 and 3.2). Averaged permeability values are grouped into ranges on a core-specific basis. Cool colours (blues and greens) represent low permeability values, while hot colours (oranges and reds) signify high values.

3.4.2.1 *Ophiomorpha-Palaeophycus* Ichnofabric

Low permeability ($\leq$ 9 mD) values are recorded in the location of the burrow. To

the right of the burrow, in the host sediment, are higher values (≥ 10 mD) (Fig. 3.1B).

3.4.2.2 *Ophiomorpha*-Burrow Mottled Ichnofabric

Overall the permeability values are quite low (≤ 8 mD). Two high values (12+ and 8 to 10 mD) sit within the *Ophiomorpha* burrow fill, and on the mud pellet lining, respectively (Fig. 3.1D). The burrow mottled fabric exhibits a range of permeability from 4 to 8 mD.

3.4.2.3 *Ophiomorpha-Asterosoma* Ichnofabric

Lower permeability (≤ 30 mD) values are observed in conjunction with the original sedimentary laminae still present within the sample. Higher values (≥ 31 mD) are observed in the same horizontal plane as the oblique *O. irregulaire* (Fig. 3.2B). Permeability of *O. irregulaire* burrows is on average 0 to 10 mD with smaller portions reaching greater than 41 to 50 mD.

3.4.2.4 *Ophiomorpha-Thalassinoides* Ichnofabric

Low permeability (≤ 15 mD) values are noted in association with *Ophiomorpha* and bioturbation above the main burrow. Below *Ophiomorpha*, where there is less bioturbation, are the higher permeability (≥ 16 mD) values (Fig. 3.2D).

3.5 Interpretations

3.5.1 Permeability

The purpose of investigating the permeability of *Ophiomorpha* burrows was to quantify how bioturbation affects permeability with regard to the different fabrics within

which these burrows occur.

3.5.1.1 *Ophiomorpha-Palaeophycus* Ichnofabric

There was very strong correlation between the permeability values and bioturbation caused by *Ophiomorpha irregulaire* (Fig. 3.1B) in the studied sample. Directly above and atop the burrow where bioturbation was present are low permeability values. The sediment that was unbioturbated by *Ophiomorpha* had the highest permeability values. The vertical region of diffuse sediment above *Ophiomorpha* is most likely past of a collapse cone (see Fig. 2.10 in Chapter 2). In aquaria (see Chapter 2), *Neotrypaea californiensis* feed from such cones above the pellet-lined galleries. The shrimp disrupts the overlying sediment allowing the grains to fall downwards into the burrow. The downwards jostling movement is likely to cause the grains to become more tightly packed and more poorly sorted than the surrounding sediment. This phenomenon is clearly visible in the thin section observations (Fig. 3.3 A and B). The incorporation of mud into the pore spaces by the organism from the collapse cone and the increased packing of grains have significantly lowered the permeability.

3.5.1.2 *Ophiomorpha*-Burrow Mottled Ichnofabric

With the permeability overlain on the core photograph there was only a slight difference between the burrows and the surrounding fabric (Fig. 3.1D). Due to the high intensity of burrow mottling, mud laminae has been bioturbated and mixed into the host sediment. There were a small number of high permeability values throughout the grid, even with mud present. One must keep in mind that the spot-permeameter reads one cubic centimeter so that the photograph does not necessarily reflect the 1 cm^3 volume and

therefore behind the exposed core-face there could be no mud at all. Within the burrow cores, permeability values are slightly higher (4 to 8 mD) than in the surrounding sediment (2 to 4 mD). Thus the trace-making organism may have removed mud particles from the burrow core and placed them in the burrow roof, creating mud pellets. It is noteworthy that the *Ophiomorpha* burrow cores have been reburrowed by other indistinguishable trace fossils, which could also increase permeability.

3.5.1.3 *Ophiomorpha-Asterosoma* Ichnofabric

The lowest permeability values were found in the original sedimentary laminae below the burrow and the bioturbated sediment above the burrow (Fig. 3.2B). This is due to the presence of low permeability muddy laminae in the sandstone and also mud mixed into the sand by bioturbation. The diffuse sediment (Fig. 3.2 A, DS label) directly above the burrow is inferred to represent the margins of a collapse feeding cone. Around the burrow, and laterally adjacent, there was an increase in permeability. But within the burrow it is low. The trace-making organism is most likely to have taken mud from around the burrow to create the burrow lining pellets, as demonstrated in the *Ophiomorpha*-burrow mottled ichnofabric. Even though the burrow fill was sandy, the mini-permeameter does not have fine enough resolution to measure only the sand. The mini-permeameter therefore read a combination of the sand and mud wall lining; this is also the case with the fine muddy laminae below the burrow.

3.5.1.4 *Ophiomorpha-Thalassinoides* Ichnofabric

The *Ophiomorpha irregulaire* burrow in this ichnofabric show reduced permeability relative to surrounding sediment (Fig. 3.2D). This sample is highly

bioturbated and high permeability values correspond to 'cleaned' (clay-poor) sediment regions by burrows. Around *O. irregulaire* at the base of the core sample (where the thin section was taken) there is a lack of pellets surrounding the burrow. Instead there is a hazy irregular lining of muddy sediment, similar to the circular top-most portion of the *Ophiomorpha*. Thin section analysis revealed pore spaces that were significantly cleaner and larger within the burrow fill than in the muddy near-burrow sediment. Grain sorting, roundness and high porosity suggest that the burrow fill was passively filled, possibly after the shrimp left the burrow. Within the near-burrow sediment, the blue-stained epoxy demonstrates the presence of pore spaces, but the pores are largely filled with clay-sized sediment. The high concentration of mud within the pore spaces and pore throats would significantly reduce permeability. It has been observed in lab tank experiments that *Upogebia pugettensis* irrigate their burrows by sealing off the burrow and beating their pleopods to pump water into the blind-ended burrow (Herringshaw and McIlroy, in press). As pore waters permeate the sediment, particulate matter is transported alongwith it by the process known as "bioinfiltration" (Herringshaw and McIlroy, in press). Clay-sized material is transported into the adjacent more permeable sand by the bioirrigating currents. There is no evidence for the clays being emplaced by the appendages of *U. pugettensis*. Bioinfiltration has the potential to deliver particulate nutrients to the near-burrow environment, including organic nutrients such as flocs and colloids. The introduction of such clay materials into sandstones may also induce early diagenesis (Pemberton and Gingras, 2005; Herringshaw and McIlroy, in press).

3.5.2 Reservoir Quality

To quantify the effects of bioturbation on the host sediment, the permeability values within the grids occupying the space of the dominant *Ophiomorpha irregulaire* burrow are averaged and divided by the average of the grids unaffected by *Ophiomorpha*. For example: *Ophiomorpha* Bioturbated Value ÷ Non-*Ophiomorpha* Bioturbated Value = 'X'. 'X' is then subtracted from 1, to quantify the final reduction (negative value) or enhancement (positive value) of permeability relative to the host sediment. Figure 3.7 demonstrates this process with the core sample from *Ophiomorpha-Palaeophycus* ichnofabric. For the remaining ichnofabrics the calculations have been completed and only the final photographs and values are shown (Fig. 3.8).

Ichnofabrics are divided into whether the burrow would affect the horizontal or vertical permeability, k_h and k_v, respectively. These divisions are based on very fine-scale observations, and could vary depending on the intensity of bioturbation and the distribution of *Ophiomorpha* within a bed. While this is based only on a small dataset, reservoir calculations based on the presence and quantity of the burrows could dramatically alter reservoir quality estimates.

The *Ophiomorpha irregulaire* burrow morphology meanders in three dimensions (Chapter 2 Fig. 2.6; and Fig. 3.6). The four ichnofabrics presented herein show on average a decrease in horizontal permeability (28%). Owing to the horizontal morphology of *Ophiomorpha*, vertical permeability was decreased by 14% (Fig. 3.8). However, reduction or enhancement in the vertical component must also be considered since there are vertical components to the burrow. Whole core slab does not show the full

three-dimensional burrow morphology, and the vertical burrow component of the burrow cannot be ignored.

Recent computer modeling demonstrates that burrows of the *Skolithos* ichnofacies (*Ophiomorpha* included) become fully connected, vertically and laterally, at a bioturbation intensity of only 20% (P90; La Croix et al., 2012). At an intensity of 20% original sedimentary structures, including some burrows, are visible (Fig. 3.6). Burrow connectivity occurs at a much lower bioturbation intensity than previously thought. Therefore, with minimal bioturbation *Ophiomorpha irregulaire* are considered likely to be connected. It has been determined that *Ophiomorpha irregulaire* reduces permeability (except in the *Ophiomorpha-Asterosoma* ichnofabric), it does not matter whether the burrows are connected or not because they do not act as fluid flow conduits. At a 20% bioturbation intensity *Ophiomorpha irregulaire* decrease the original reservoir volume estimates by a minimum of 14%. 20% of the *Ophiomorpha* ichnofabric by volume have reduced permeability by at least 14%.

3.6 Conclusion

Ophiomorpha irregulaire is found to variably decrease horizontal permeability (k_h) by an average of 28% and to a maximum of 70%, but k_h can also increase by 82%. Vertical permeability can be decreased by 14%. The sedimentary fabric surrounding the burrows must also be taken into account when considering permeability increases and decreases. The overall bioturbation intensity must also be considered to determine the volume that burrows of *Ophiomorpha irregulaire* occupy within the sediment. The mechanisms by which reduce or increase in permeability are explained herein by

observations of the behaviour of the trace-making organism (*Neotrypaea californiensis*). Understanding burrow morphology and behaviour provides insight on how fluids flow through highly bioturbated reservoirs. This work suggests that *Ophiomorpha* has profound effects on reservoir volumes, and that the near-burrow environments should also be more closely studied.

3.7 Future Work

Understanding of the Ben Nevis Formation core should be extended to include unbioturbated facies. Furthermore, facies and the reservoir characteristics could be extrapolated to other wells and well logs within the region. Ideally, a robust dataset would be created to understand the effects of the burrow in each facies.

This project has emphasised the importance of studying the near-burrow environment (*Ophiomorpha-Thalassinoides* ichnofabric). A greater focus on near-burrow environments should be undertaken specifically with respect to bioinfiltration and biogenic collapse cones. These features have the potential to provide much more data relating to reservoir quality and trace-maker behaviour than is currently understood.

This work shows the need to create linked, three-dimensional petrographical and morphological datasets in siliciclastic reservoirs (see Chapter 4).

3.8 Acknowledgements

This work was supported by Petroleum Research Atlantic Canada (PRAC) and a Natural Sciences and Engineering Research Council of Canada (NSERC) grant to DMc. M. Leaman thanks Liam G. Herringshaw and Nikki Tonkin for their assistance at the

beginning of the project; Dario Harazim and Chris Boyd for helpful discussions; and Elisabeth Kahlmeyer and Edgars Rudzitis for some data collection. This manuscript was improved by the reviews of Andrew Rindsberg and Evan Edinger.

3.9 References

Bednarz, M., McIlroy, D., 2009. Three-dimensional reconstruction of "phycosiphoniform" burrows: implications for identification of trace fossils in core. Palaeontologia Electronica. 12 (3), 13A 15 p. http://palaeo-electronica.org/2009_3/195/index.html.

Bednarz, M., McIlroy, D., 2012. Effect of phycosiphoniform burrows on shale hydrocarbon reservoir quality. AAPG Bulletin. 96, 1957-1980.

Bottjer, D.J., Droser, M.L., 1991. Ichnofabric and basin analysis. Palaios. 6, 199-205.

Boyd, C., McIlroy, D., Herringshaw, L.G., Leaman, M., 2012. The recognition of *Ophiomorpha irregulaire* on the basis of pellet morphology: restudy of material from the type locality. Ichnos. 19, 185-189.

Garton, M., McIlroy, D., 2006. Large thin slicing: a new method for the study of fabrics in lithified sediments. Journal of Sedimentary Research. 76, 1252-1256.

Gingras, M.K., McMillan, B., Balcom, B.J., Saunders, T. and Pemberton, S.G., 2002. Using magnetic resonance imaging and petrographic techniques to understand the textural attributes and porosity distribution of *Macaronichnus*-burrowed sandstone. Journal of Sedimentary Research. 72, 552-558.

Herringshaw, L.G., McIlroy, D. in press. Bioinfiltration: Intra-sedimentary particulate transport by burrow-irrigating taxa. Journal of Sedimentary Research.

McIlroy, D., 2004a. Some ichnological concepts, methodologies, applications and frontiers. In: McIlroy, D. (Ed.), The application of ichnology to stratigraphic and palaeoenvironmental analysis. Geological Society, London, Special Publications, 228, pp. 3-27.

McIlroy, D., 2004b. Ichnofabrics and sedimentary facies of a tide-dominated delta: Jurassic Ile Formation of Kristin Field, Haltenbanken, Offshore Mid-Norway. In: McIlroy, D. (Ed.), The application of ichnology to palaeoenvironmental and stratigraphic analysis. Geological Society, London, Special Publications, 228, pp. 237-272.

McIlroy, D., 2008. Ichnological analysis: The common ground between ichnofacies workers and ichnofabric analysts. Palaeogeography, Palaeoclimatology, Palaeoecology. 270, 332-338.

La Croix, A., Gingras, M., Dashtgard, S., Pemberton, S.G., 2012. Computer modeling bioturbation: the creation of porous and permeable fluid-flow pathways. AAPG Bulletin. 96, 545-556.

Pemberton, S.G., Gingras, M.K., 2005. Classification and characterizations of biogenically enhanced permeability. AAPG Bulletin. 89, 1493-1517.

Raychaudhuri, I., Pemberton, S.G., 1992. Ichnologic and sedimentologic characteristics of open marine to storm dominated restricted marine settings within the Viking/Bow Island Formations, south-central Alberta. In: Pemberton, S.G. (ed.), Applications of ichnology to petroleum exploration: a core workshop: Society of Economic Paleontologists and Mineralogists, Core Workshop, 17, pp. 119-139.

Tonkin, N.S., McIlroy, D., Meyer, R., Moore-Turpin, A., 2010. Bioturbation influence on reservoir quality: a case study from the Cretaceous Ben Nevis Formation, Jeanne d'Arc Basin, offshore Newfoundland, Canada. AAPG Bulletin. 94, 1059-1078.

3.10 Figures

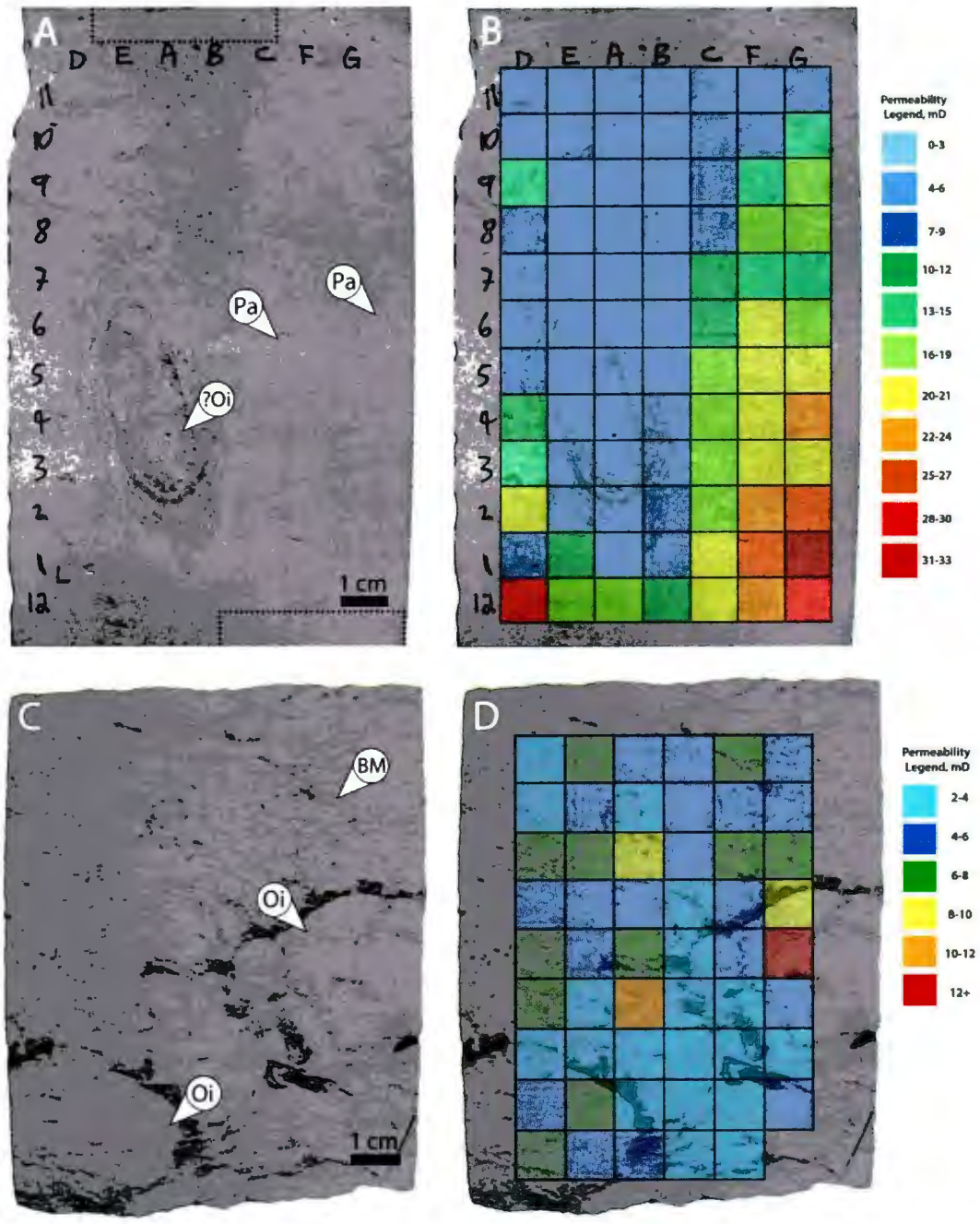

Fig. 3.1: Core samples collected from Ben Nevis L-55 well, offshore Newfoundland. A & B = *Ophiomorpha-Palaeophycus* ichnofabric; C & D = *Ophiomorpha*-burrow mottled ichnofabric. B & D: Cores are shown with semi-transparent mini-permeability range blocks overlain. Each square within the grid represents one centimeter. BM = Burrow Mottling; Oi = *Ophiomorpha irregulaire*; and Pa = *Palaeophycus*. Dashed lines on A represent locations from which thin sections were taken (Fig. 3.3).

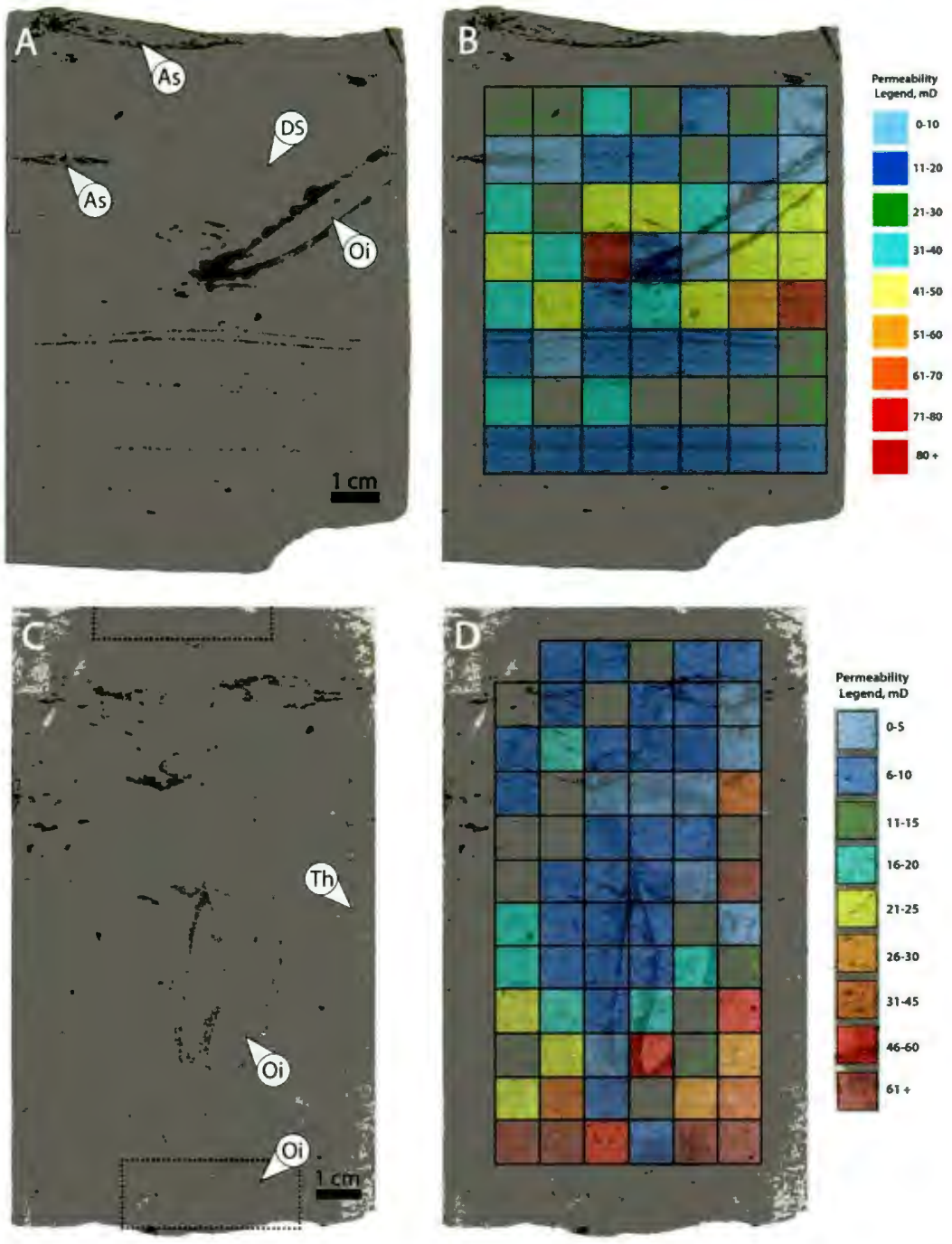

Fig. 3.2: Core samples collected from Ben Nevis L-55 well, offshore Newfoundland. A & B = *Ophiomorpha-Asterosoma* ichnofabric; C & D = *Ophiomorpha-Thalassinoides* ichnofabric. B & D: Cores are shown with semi-transparent mini-permeability range blocks overlain. Each square within the grid represents one centimeter. As = *Asterosoma*; DS = diffuse sediment; Oi = *Ophiomorpha irregulaire*; and Th = *Thalassinoides*. Dashed lines on C represent locations from which thin sections were taken (Fig. 3.4 and Fig. 3.5, bottom and top samples respectively).

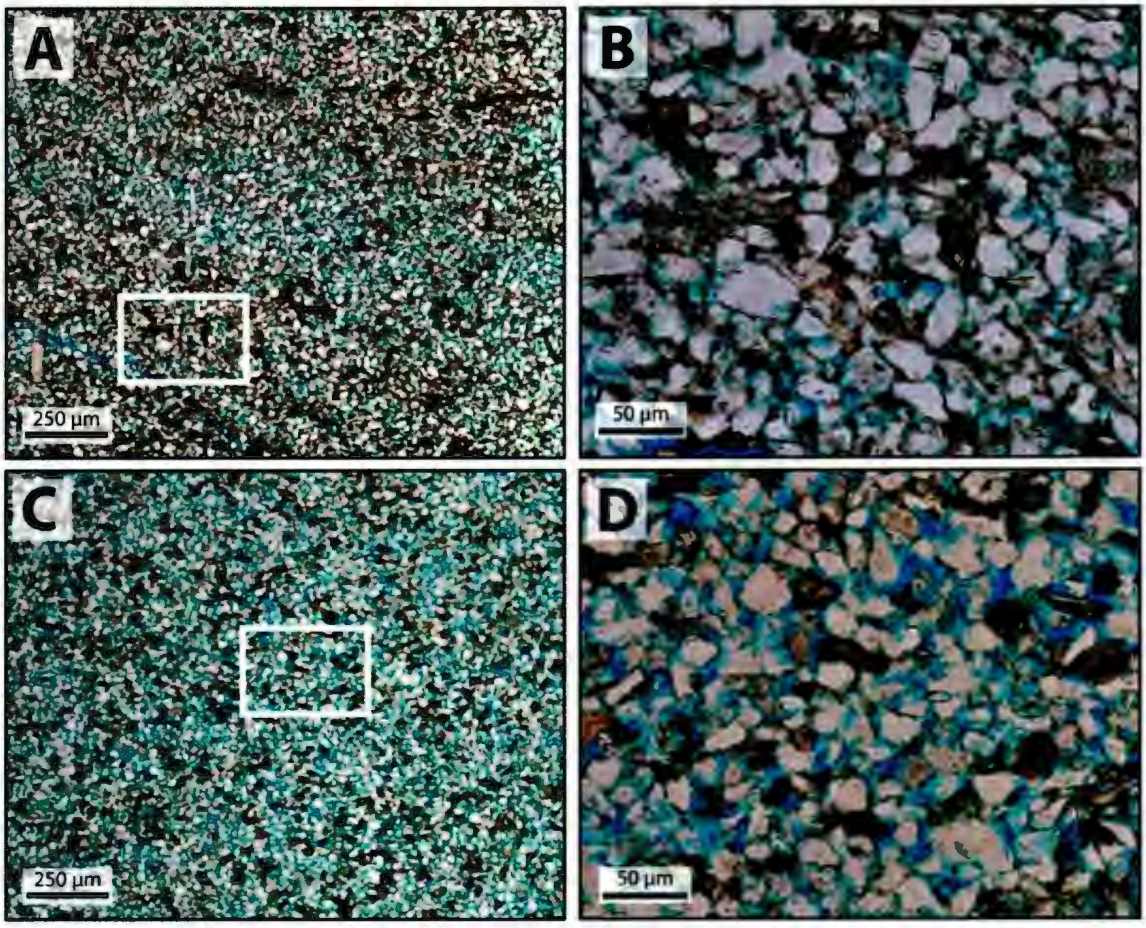

Fig. 3.3: Two thin sections created from *Ophiomorpha-Palaeophycus* ichnofabric (Fig. 3.1 A & B). A and B are bioturbated by *Ophiomorpha*, from the top of the core sample, while C and D are unbioturbated by *Ophiomorpha*, from the base of the core sample. See Fig. 3.1 A for exact thin section location. The white boxes on A and C represent the locations of where photos B and D were taken from, respectively. The *Ophiomorpha*-bioturbated sample (A and B) show an elevated quantity of clay-sized particles (15%) unevenly distributed throughout the whole section, occupying the pore spaces (15%). While the unbioturbated by *Ophiomorpha* sample (C and D) shows no mud and much cleaner pore spaces (25%). For a detailed description of the thin sections see Appendix C, Table C.5.

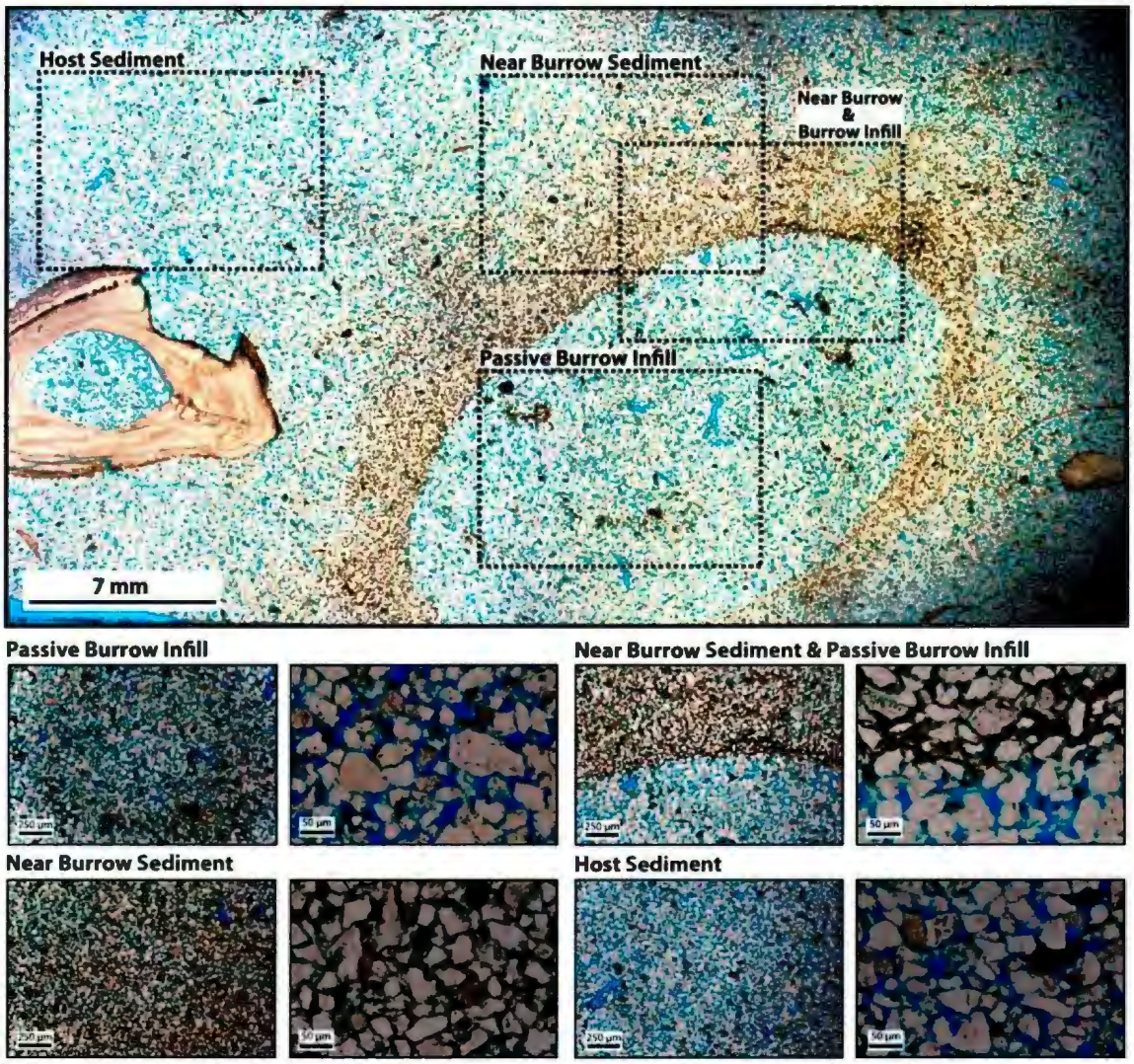

Fig. 3.4: One thin section (large top photograph) was taken from *Ophiomorpha-Thalassinoides* ichnofabric in the *Ophiomorpha*-bioturbated section. See Fig. 3.2 C for exact thin section location. The smaller eight thin section images are close ups of distinct regions of the burrow, indicated by the black dashed boxes on the thin section overview. A large shell fragment is visible above the scale bar. The core shows very poorly sorted quartz grains (60%; little to no mud or lithics) and high porosity (35%). The near-burrow sediment exhibits moderately sorted quartz and lithic grains (70% and 10%, respectively). Porosity is approximately 10%, however infilled with clay-sized sediment (10%). The near-burrow sediment shows a distinct mud-lining at the termination of the burrow core (near-burrow sediment and passive burrow infill images). The host sediment displays a very similar composition to that of the core. For a detailed description of the thin sections see Appendix C, Table C.5.

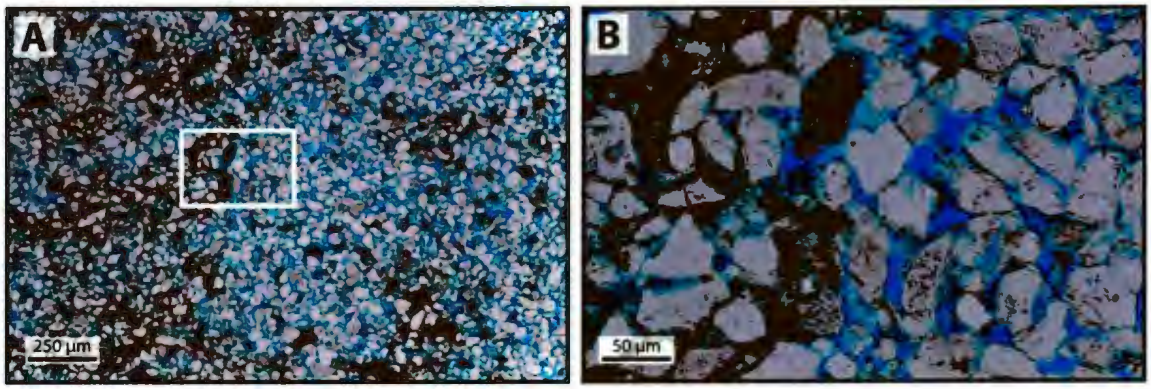

Fig. 3.5: Second thin section from the *Ophiomorpha-Thalassinoides* ichnofabric, from the burrow mottling fabric, unbioturbated by *Ophiomorpha*, taken from above the vertically inclined burrow. See Fig. 3.2 C for exact thin section location. The white box in A represents the location of where photograph B was taken from. Burrow mottling is evident by the patchy distribution of clay-sized grains (10%, A) occupying the pore spaces (20%, B). For a detailed description of the thin sections see Appendix C, Table C.5.

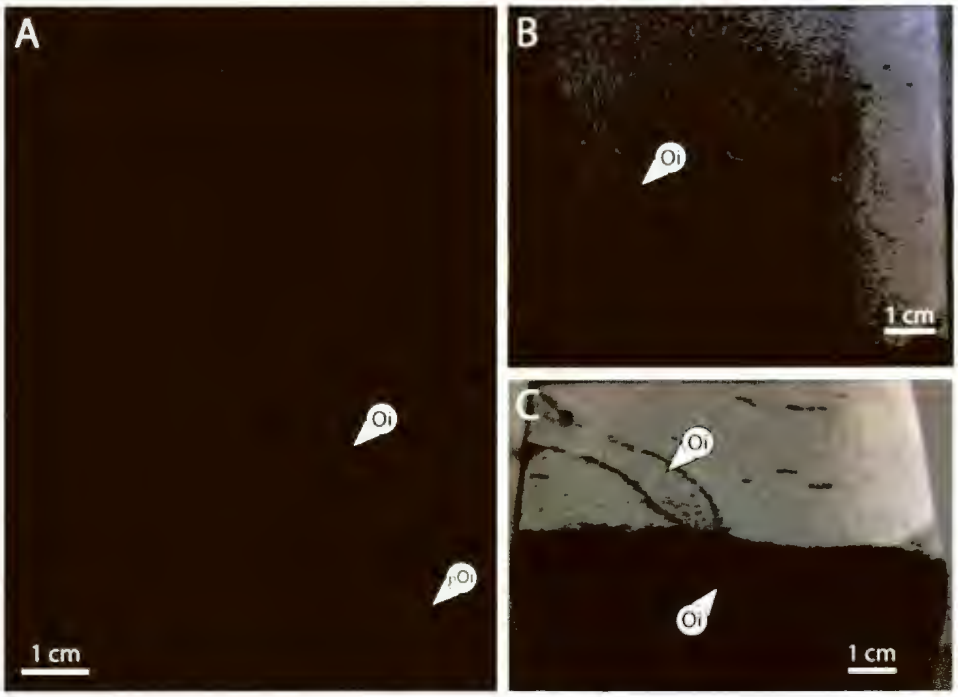

Fig. 3.6: 20% bioturbation intensities of *Ophiomorpha* ichnofabrics in vertical cross section, from offshore Newfoundland, well F-12 (A; Hibernian Formation, Lower Cretaceous) and L-55 (B and C). Oi = *Ophiomorpha irregulaire* and pOi = past *Ophiomorpha irregulaire*. A: Upward movement of *Ophiomorpha irregulaire*, illustrated by the faint shadow of its former burrow (pOi). B and C: A meandering example of *Ophiomorpha irregulaire* in the same piece of core. Burrows become laterally and vertically connected at 20% bioturbation intensities, according to La Croix et al. (2012).

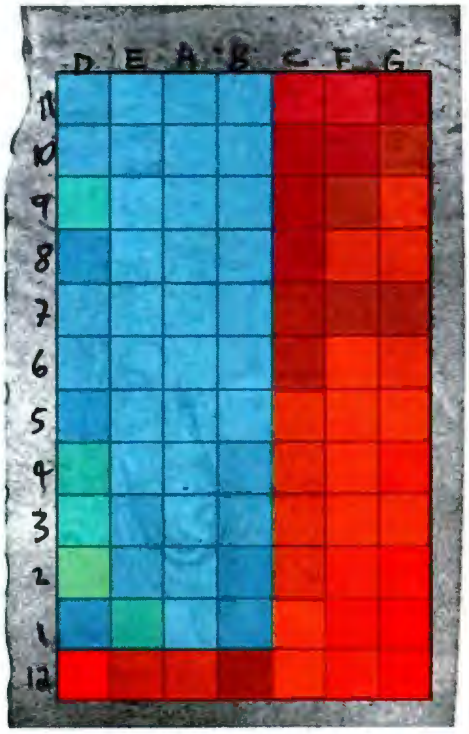

Average *Ophiomorpha* Bioturbated = 5.24 mD

Average Non-*Ophiomorpha* Bioturbated = 17.49 mD

$$\frac{\textit{Ophiomorpha}}{\text{Non-}\textit{Ophiomorpha}} = 0.30$$

$$= 0.30 - 1.0$$

$$= -70\%$$

Fig. 3.7: A pictorial explanation of the calculations into determining if the *Ophiomorpha* burrow has reduced (negative final value) or enhanced (positive final value) the permeametry compared to the host sediment. Blue grids represent low permeability values affected by the burrowing of *Ophiomorpha*, while red grids are higher permeability values, unaffected by the burrowing of *Ophiomorpha* (though the red grids still represent highly bioturbated sediment).

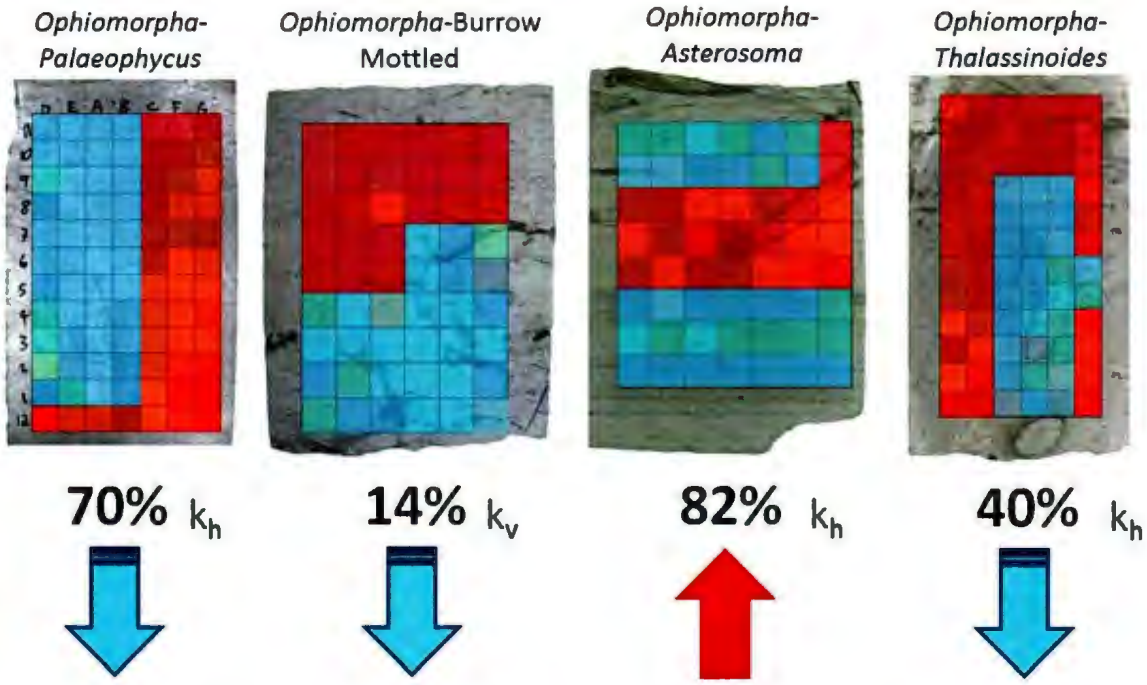

Fig. 3.8: Blue grids represent low permeability values affected by the burrowing of *Ophiomorpha*, while red grids are higher permeability values, not affected by the burrowing of *Ophiomorpha* (though the red grids are still highly bioturbated). The shades of blue and red vary due to their opacity and the underlying rock and permeability grid colours. The opposite colour combination is true for the *Ophiomorpha-Asterosoma* ichnofabric. In this example *Ophiomorpha* exhibited an increase in permeability. Based on the calculations in Fig. 3.7, either an increase or decrease of horizontal permeability (k_h) or vertical permeability (k_v) is indicated for each ichnofabric. k_h and k_v were determined by the morphology of the *Ophiomorpha* burrow.

CHAPTER 4

Three-Dimensional Morphological and Permeability Modelling of *Diplocraterion*

Chapter 4 – Three-Dimensional Morphological and Permeability Modelling of *Diplocraterion*

4.1 Abstract

Three-dimensional mini-permeametry of a *Diplocraterion* ichnofabric from the Middle Jurassic Scarborough Formation of North Yorkshire, UK, reveals some of the relationships between ichnofossils and reservoir quality in conventional siliciclastic petroleum reservoir facies. This work focuses on the effect that the various *Diplocraterion* burrowing behaviours have on the permeability characteristics of the near-burrow environment. Samples were studied using serial grinding and mini-permeametry. This is the first documented attempt at combining these techniques to create an integrated understanding of the inter relationship of trace fossil morphology and reservoir quality in three dimensions.

Palaeobiological insights arising from the three-dimensional modelling include evidence for resuspension feeding, deposit feeding, sediment cleaning and "collapse-cone feeding". Higher than expected permeability values (<150 mD) were measured from the sandy shafts of *Diplocraterion* and adjacent areas. Zones of enhanced permeability associated with the intershaft area are inferred to result from sediment cleaning, and size-selective deposit feeding. Bioturbation by *Diplocraterion* is found to improve reservoir quality by sediment cleaning and creation of highly permeable vertical conduits in a reservoir facies with otherwise low permeability.

4.2 Introduction

Diplocraterion isp. is a vertically oriented U-shaped burrow with spreite between the tubes, and is typically classified as a suspension-feeding trace or dominichnion (e.g. Fürsich, 1974). The ichnogenus is named for the twin funnel-shaped craters that characterize the openings of the U-burrow in the type material (Torell, 1870) however, these have rarely been documented, and greater taxonomic importance is now placed on the inter-tube spreite.

Spreiten are formed between the arm tubes when the trace-maker adjusts the burrow position. Convex-upward protrusive spreiten are considered to form as the trace-maker moves the bottom of the open U-burrow deeper into the sediment. Protrusive spreite therefore preserve the position of successive burrow roofs. The reasons for protrusive burrowing behaviour are typically thought to be either: 1) a response to erosion in which the U-burrow is adjusted such that the bottom of the U retains a similar distance from the sediment-water interface (Goldring, 1962; Cornish, 1986; Bromley, 1996) or 2) low rates of sedimentation or non-deposition which allow the *Diplocraterion* to develop through the ontogeny of the trace-maker, becoming longer, deeper and commonly wider with time (Cornish, 1986). If the base of the U-burrow nears the sediment-water interface, then a concave-upwards retrusive spreite is formed. A retrusive spreite therefore preserves the position of successive burrow floors. The conventional model used to explain the development of a retrusive spreiten, is that the trace-maker adjusts the base of the burrow to maintain a constant distance from the sediment-water interface during a period of slow, continuous sediment accumulation.

Diplocraterion burrows that preserve both protrusive and retrusive spreiten were classified as *Diplocraterion yoyo* (Goldring, 1962), until synonymised with *D. parallelum* by Fürsich (1974). The rationale for this is that since the burrowing activity is forced by extrinsic factors, sedimentation rate in this case, it did not reflect different behaviour to that seen in the pre-existing *D. parallelum* Torell 1870.

This study focuses on three-dimensional reconstruction of a *Diplocraterion* specimen from the Scarborough Formation (Middle Jurassic), Cloughton Wyke, UK that shows both protrusive and retrusive spreiten. The progressive exposure of the specimen, which was entirely encased in its host sediment, has the distinct advantage over most classical ichnological studies that organism-sediment interactions in the form of ichnofabric can be studied together. Many earlier analyses of *Diplocraterion* relied on exposed weathered cross sections or slabbed core-based material. This project models the morphological features of *Diplocraterion* in three dimensions to gain a better understanding of its burrowing behaviour, and to understand the effect *Diplocraterion* has on permeability. *Diplocraterion* samples were collected with the intent of studying the distribution of permeability and morphology using serial grinding and mini-permeametry techniques. This is the first documented attempt at combining these techniques, which have led to a more complete understanding of the trace fossil and of its impact on reservoir quality in three dimensions.

4.3 Methods

4.3.1 Field Collection and Preparation for Milling

Hand samples of *Diplocraterion* were collected from cliff faces and float in the Cloughton Wyke region of England (Fig. 4.1). The rocks are Middle Jurassic-aged from the Scarborough Formation, Hundale Point, North Yorkshire. Specimens were selected based on two criteria to try to ensure as complete a trace fossil as possible: 1) the presence of tubular openings at the top of the sample; and 2) absence of the base of the U at the bottom of the sample.

Samples were trimmed to 14.5 × 16.5 × 15.0 cm to fit in the C&C milling machine. The bottom, weathered rock surface was sawn off and subsequently ground flat using the C&C milling machine to ensure a smooth surface for the mini-permeameter nozzle. Measurements and photographs of the rock were taken before and after trimming, in the event that observations of the outer host sediment were needed.

Once trimmed, the block was placed upside-down in a close-fitting cardboard box and encased in plaster of Paris. The plaster was left to set for a week. The cardboard box was then removed, and the plaster was left to set for another two days. Once solid, the outer plaster surface was smoothed off using a hand sander. One surface was then was ground flat in the milling machine to form a stable base during the grinding process.

4.3.2 Permeametry

A one-centimeter grid was drawn on the top surface of the rock with a fine-point permanent marker. The grid lines from the top surface were extended down to the outer

faces of the plaster block using a plumb line. This was done to ensure that the grid could be placed at precisely the same position for each permeametrically studied surface. A one-centimeter margin was left around the outer edge of the rock to prevent any edge effects during permeability measurements. The specimen studied herein allowed creation of a 12 cm × 14 cm permeability grid.

Permeability measurements were collected using a Temco mini-permeameter machine giving a value in milliDarcies (mD). The nozzle tip chosen allows study of a one-centimeter cubed volume of the rock space at a time. Measurements were taken three times on each grid space and averaged. Once the permeability grid was documented, the surface was ground off as part of the three-dimensional tomographic study. The permeametric study was repeated at one centimeter intervals throughout the rock volume to allow study of permeametric variability throughout the rock volume in relation to elements of the burrow.

4.3.3 Serial Grinding and Photography

The serial grinding study was completed using a programmable C&C milling machine. For the *Diplocraterion* sample, a Z-axis grinding depth of 0.5 mm was used. Each new surface exposed was photographed, and after each increment one centimeter of thickness had been ground away, the permeametric approach outlined above was repeated. To enhance the contrast of the burrows and matrix, mineral oil was applied to the rock face. A Canon EOS 30D camera was used to take all photographs with settings of *f*/8, 0.4", ISO 100, AF, with mirror lock-up, and with a Canon EOS 100 mm *f*/2.8 macro lens attached. Photographs were checked for focus and sharpness on a tethered

laptop computer, prior to repeating the grinding process.

4.4 Morphological Elements of *Diplocraterion* in Three Dimensions

The three-dimensional analysis of the studied specimen shows several specimens of *Diplocraterion* isp. that show distinctive burrow morphologies not evident from study of hand specimens or cut slabs. The subsections below highlight new and incompletely understood aspects of *Diplocraterion* morphology that have implications for behavioural interpretation of trace fossils.

4.4.1 *Diplocraterion* Morphological Element #1

In plan view, the *Diplocraterion* model resembles a dumbbell (Fig. 4.2). This is the classic *Diplocraterion* morphology that many ichnologists use to identify *Diplocraterion*, particularly in the field. Of particular note is that, in the studied specimen, only one of the vertical shafts is sand-filled and mud-lined (Fig. 4.2 Shaft A). The fill of the second shaft is mud-lined, and the fill is a poorly structured sandy mudstone (Fig. 4.2 Shaft B). In vertical cross section it can be seen that Shaft B reaches higher stratigraphic levels than Shaft A, by approximately one centimeter. Shaft B shows a downward tapering in the upper circa four centimeters of the shaft. The concentric lining to the shaft is present both above and below the constriction (Fig. 4.3). The surface termination of Shaft A is neither eroded nor bioturbated.

4.4.2 *Diplocraterion* Morphological Element #2

In plan view, this *Diplocraterio*n shows a branch orientated perpendicular to the main U-burrow. *Diplocraterion* Ω is cross-cut by *Diplocraterion* Σ (Fig. 4.4).

Diplocraterion Ω shows a well-developed retrusive spreite (Fig. 4.5B black dashed lines), formed as the base of the U was shifted towards the sediment-water interface (Fig. 4.5 A and B).

The sand-rich causative tube of *Diplocraterion* Σ is preserved above a series of retrusive spreite laminae, which cross-cut an earlier set of protrusive laminae (Fig. 4.4B). The margin of *Diplocraterion* Σ that crosscuts *Diplocraterion* Ω is rich in dark organic matter (Fig. 4.4 orange arrow; and Fig. 4.5 A and C, orange arrows), such as is found above the retrusive spreite of *Diplocraterion* Ω (Fig. 4.4 red arrow; and Fig. 4.5 B and C, red arrows) of the burrow.

4.4.3 *Diplocraterion* Morphological Element #3

The third *Diplocraterion* from the serial grinding study is unusual in that in its lower portion it preserves only one J-shaped shaft (Fig. 4.6). The shaft crosscuts a series of retrusive spreite laminae that are demonstrably part of the same trace fossil (Fig. 4.7). The retrusive laminae have organic-rich layers that are clearly cut by the sand-filled shaft. The shaft penetrates deeper into the sediment than the spreite (Fig. 4.7). Direct study of the original photographs from which the model was built demonstrates that the mud-rich spreite are rich in faecal pellets (approximately 0.5 mm × 1.5 mm; Fig. 4.8).

4.5 Spatial Variability of Permeability

Permeability measurements were taken on 13 surfaces of the rock sample at one centimeter spacing in the Z-axis. Original averaged permeability values for each surface are presented in tables (D.1 to D.13) in Appendix D. Permeability measurements were

not conducted on parts of the ground surfaces of sandstone where the probe-permeameter was affected by cracks in the rock or where grid squares were too close to the rock edge. The permeability data in milliDarcies (mD) were recorded as absolute values (Appendix D Tables D.1 to D.13), and the average of three permeability readings was plotted on the colour-coded surface maps alongside the distribution of *Diplocraterion* on the same surface (Fig. 4.9). The images of burrows overlain on the colour-coded permeability grid are combined from the distribution of the burrow in the 20 image slices that comprise the 1 cm^3 rock volume sampled by the permeability measurement. These figures demonstrate the relationships between three-dimensional burrow morphology and composition with permeability. Earlier studies of the interrelationship between trace fossil morphology and permeability have taken the image of the 2D surface from which the permeability measurements were taken to be representative of the full cube sampled by permeametry (e.g. Spila et al., 2007; Tonkin et al., 2010). Burrows that lie over the edge of the permeability grid were too close to the rock edge to be measured with the permeameter, but are still shown in the figures for context. These burrows were modelled, but not incorporated into the study.

In all cases, the sand-filled shafts of *Diplocraterion* show an increase in permeability relative to the host sediment. The vertical connectivity of that permeability is not perfect; in some shafts the sandy fill is capped by a constriction above which is a concentric mud-rich (apex-down) cone.

In many cases there is an increase in permeability around the *Diplocraterion* shafts relative to the host sediment values (Fig. 4.10). It must however be kept in mind

that the surrounding fabric to the several *Diplocraterion* is also bioturbated by other organisms. As such, near-burrow permeability differences may result from the sediment cleaning effects of associated burrows other than *Diplocraterion*.

4.6 Interpretations

This study has identified several important morphological elements that are not normally described in *Diplocraterion* isp., and which are certainly not present in the type material of *D. parallelum*, the type species of *Diplocraterion*, from the Cambrian of Sweden (Jensen, 1997). Most documented *Diplocraterion* are protrusive in nature. The specimens show both protrusive and retrusive behaviour within a single trace fossil.

Diplocraterion yoyo was created to encompass trace fossils with a U-burrow showing both protrusive and retrusive spreite (Goldring, 1962; from the Devonian Baggy Beds of North Devonshire, England). Subsequently the consensus was that protrusive and retrusive behaviour (and the spreiten they create) result from the same behaviour of burrow adjustment (Fürsich, 1974; Bromley, 1996). For this reason *D. yoyo* has been synonymised with *D. parallelum*. The justification for this synonymization relies upon the premise that the factor controlling whether the burrowing organism produces protrusive or retrusive spreite, is that the base of the causative U-burrow of *Diplocraterion* needs to be kept at the optimal distance from the sediment-water interface (Fürsich, 1974). Thus it was inferred that if erosion occurred, the burrow would be adjusted deeper (producing protrusive spreite), or if deposition occurred, the U-burrow would need to become shallower (producing retrusive spreite). Similar rationales have been recently adopted by much of the ichnological community based on the work of the

working group for ichnotaxonomy which preclude sedimentologically-driven morphologies from having taxonomic importance (Bertling et al., 2006).

Below we provide evidence that protrusive and retrusive spreiten—in reconstructed *Diplocraterion* specimens that are closely comparable to *D. yoyo*—may not be solely created in response to sedimentation and erosion, but that they could reflect sophisticated feeding behaviours largely overlooked. Many of the morphological components of the three-dimensional models created herein are analogous to structures produced by modern thalassinidean shrimps, including *Neotrypaea* and *Upogebia* in aquarium experiments conducted as part of this study.

4.6.1 Morphology

4.6.1.1 Funnel-feeding in *Diplocraterion*

The concentrically lined burrow shafts described from *D. yoyo* are found in our *Diplocraterion* morphological element #1 (Fig. 4.11B). The same specimen also shows the plugged tube that is present in the type material of *D. yoyo* (Goldring, 1962; Fig. 4.11A). We also note that the upper termination of the sand-filled burrow shaft is at a lower stratigraphic level than the mud-plugged shaft (cf. Goldring, 1962). By comparing Goldring's idealised sketch with serially ground surfaces through the studied material it is clear that there are such remarkable similarities that it is difficult to consider our material to belong to *D. parallelum* rather than Goldring's *D. yoyo* (Fig. 4.11 A and B).

The ring laminae around the upper plugged and constricted shaft (highlighted in white dashes) are thicker and less organized than in the sand-filled shaft (Fig. 4.11A). The idealized model of *D. yoyo* clearly shows a conical mud-filled structure. The obvious

comparison for this structure is the feeding cone of the polychaete worm *Arenicola marina* (Bromley, 1996 and references cited therein), though *A. marina* will not generally produce a U-burrow, a J-shaped burrow being the normal morphology for the open/causative burrow.

In our aquarium experiments, however, we have documented *N. californiensis* undertaking collapse-cone deposit-feeding behaviour from the top of a shaft, as seen in *Diplocraterion* morphological element #1 (Fig. 4.11C). Prior to feeding, the *Neotrypea* were observed to pump water down the burrow shaft using their pleopods. While it is not possible to demonstrate the reason for this behaviour, the subsequent deliberate collapse of sediment through the shaft termination is analogous to the bioirrigating behaviour of *A. marina. Arenicola* bioirrigates sediment in order to increase microbial and meiofaunal productivity in the cone prior to cone-collapse and ingestion of sediment. While funnels were documented in the type material of *D. parallelum* (Torell, 1870), it is a feature seldom documented since. Indeed, most workers consider *Diplocraterion* to be a U-shaped burrow created for the purpose of suspension feeding (MacEachern and Gingras, 2007). Funnels have generally been considered to be a sedimentological phenomenon rather than a result of biological activity and are generally not considered to be of taxonomic use (Bertling et al., 2006; Schlirf and Uchman, 2005).

The three-dimensional model of *Diplocraterion* morphological element #1 does not show evidence of protrusive and retrusive behaviour, only the latter. *Diplocraterion* morphological element #1 does not therefore meet all of the taxonomic criteria for description as *Diplocraterion yoyo*, though it shows many similar characteristics, but not

the ichnospecific diagnostic morphology. The specimen does demonstrate the funnel-feeding morphology connected to the sediment-water interface on one end of the tube (Fig. 4.12A). On the other end, above the sand-filled shaft there may well have been a surface detritus mound, which is rarely preserved in the rock record (Fig. 4.12A). In modern environments, burrowing shrimps excavate their burrows by placing sediment at the sediment-water interface via the open burrow (Fig. 4.12B). This mound and depression morphology also aids the shrimp in hydrodynamic purposes, drawing stagnant water out of the tube using the Bernoulli principle (Vogel, 1989).

4.6.1.2 Collapse-Feeding in *Diplocraterion*

The bedding-parallel cross sections of burrow B reveal a thin organic feature between the shafts of this *Diplocraterion*. This morphology is the classic "dumbbell" expression of *Diplocraterion*, suggesting that it is the expression of a common *Diplocraterion* behaviour. Many authors have considered the thin bar to represent the spreite between the shafts of the causative U-burrow. Intuitively, however, the spreite cannot reasonably be narrower than the causative burrow as they are formed by it. An alternative explanation must therefore be sought.

The organic-rich mudstone layer between the shafts is planar in nature, and overlies the spreite *sensu stricto* from which it is morphologically distinct. The distribution of laminae in the near-burrow environment adjacent to the muddy planar structure makes it clear that the laminae are downwarped towards the plane. This suggests that sediment collapse occurred between the limbs of the U-burrow. Therefore, the collapse evidenced in the three-dimensional modelling study was a deliberate effect,

caused by the trace-maker to collapse the roof in order to deposit-feed on sediment originating between the limbs of the U-burrow. The net effect of such sediment collapse would be the creation of a linear depression or fissure on the seafloor between the surface expressions of the U-burrow (Fig. 4.13A). Such a depression is likely to have formed a sediment trap for fine-grained material, which through time could form the planar structure. The collapse cone of *Arenicola marina* and various thalassinid shrimp is commonly found to be rich in organic detritus and mud. We therefore propose that collapse feeding was undertaken by *Diplocraterion* in order to collect surface detritus by an organism living at depth in the sediment without exposing itself to the risks of surface deposit feeding (Fig. 4.13B).

In the process of collapse feeding, the position of the burrow floor is typically migrated towards the sediment-water interface, thereby producing a spreite. We therefore consider that retrusive spreiten may be formed as a result of collapse feeding, and as such that retrusive spreite formation has a valid palaeobiological and thus taxonomic implications. The spreiten thus formed are commonly rich in fecal pellets. The orthogonal protrusive *Diplocraterion* burrow in this specimen appears to have been reburrowed with retrusive laminae, perhaps thereby undertaking coprophagy. It should therefore be considered that protrusive spreite formation in *Diplocraterion* (as in the similar *Rhizocorallium*) might result from deposit-feeding behaviour. If protrusive spreiten are the action of a deposit-feeding organism, it is clear that protrusive spreiten are behaviourally distinct from retrusive spreiten and thus worthy of ichnotaxonomic distinction. This *Diplocraterion* shows both protrusive and retrusive behaviour in the

same burrow, indicating that it could have behavioural traits distinct from those of typical *Diplocraterion parallellum*, and is most likely *D. yoyo.*

The shifting axis of the U-burrow is a common feature of *Diplocraterion* from the Helwath Beck Member, and several other Jurassic units on the Yorkshire coast. It may well be a response to the complete utilization of the resources at one locality. The response to the drying up of food resources by collapse feeding is likely to be lateral burrow adjustment (Fig. 4.4). Such apparent branching or lateral burrow adjustment has not hitherto been considered a feature of any species of *Diplocraterion*.

4.6.1.3 Resuspension Feeding in *Diplocraterion*

Fecal pellets were observed throughout the retrusive spreite of *Diplocraterion* morphological element #3 (Fig. 4.8). As in *Diplocraterion yoyo*, the fecal pellets are dark, "compressed flat ended cylinders and between 1.0 × 0.25 mm and 2.0 × 0.5 mm in dimensions" (Goldring, 1962 pp. 240). In the muddy spreite of retrusive *D. yoyo* the fecal pellets are aligned parallel to the burrow margins (Goldring, 1962). This is also the case in our particular *Diplocraterion* morphological element #3 burrow (Fig. 4.8).

The presence of a J-shaped burrow crosscutting the retrusive spreite suggests deposit feeding. *Upogebia* in sandy aquaria create a U-shaped burrow with a vertical shaft protruding downwards from the base of the U (Fig. 4.14, modified for *Diplocraterion*). In our aquarium experiments, the trace-maker used the vertical shaft to resuspension feed (Fig. 4.15). In doing so the walls of the burrow are collapsed and the fine-grained material is put into suspension by the crustacean. The striking similarity between the morphologies preserved in *Diplocraterion* morphological element #3 and our

aquarium observations suggests that the Jurassic burrower may have also employed resuspension feeding. That the J-shaped morphology is associated with the fecal pellet-rich retrusive spreite suggests that coprophagous activity is likely, perhaps to exploit microbial productivity developed in association with the fecal pellets.

4.6.2 Permeability

On all 13 surfaces on which permeability was conducted, *Diplocraterion* showed an increase in permeability relating to the burrow. The majority showed an increase in the sand-filled shafts. Due to the vertical orientation of this trace fossil, and the great depths to which they can penetrate, *Diplocraterion* would act as an effective vertical fluid flow conduit in an otherwise completely bioturbated and relatively low permeable matrix. In fewer examples, a permeability increase was observed around the *Diplocraterion* dumbbell shafts compared to the surrounding matrix (Fig. 4.10). The surrounding sediment has been 'cleaned' removed of all organic matter, by the trace-maker. The trace-maker selected sediment in close proximity to the burrow and sorts through the grains, selectively choosing finer particles (organic matter) to become part of the burrow wall. The remaining clean sand was emplaced in the outer burrow wall, possibly as sand pellets. This process has been observed in tank experiments of *Neotrypaea californiensis* (Fig. 2.12). Bioinfiltration could be another explanation for a clean halo surrounding the burrow, though the process has not yet been observed to remove fine-grained particles from the burrow lining, creating a cleaning quality (Herringshaw and McIlroy, in press).

4.7 Conclusion

Several new behaviours of *Diplocraterion* are presented herein. The main conclusions from this research include:

- Three types of deposit feeding were identified: (1) funnel feeding, (2) collapse feeding, and (3) resuspension feeding. The trace-maker of *Diplocraterion* can suspension- or deposit-feed based on nutrient conditions. Modern polychaetes such as Arenicola exhibit these behaviours today.
- Goldring's (1962) *Diplocraterion yoyo* suspension-fed, based on the presence of both retrusive and protrusive spreiten. We propose that *D. yoyo* be retained as a valid ichnospecies.
- The presence of a funnel at the top of a tube with only retrusive spreite present is indicative of a deposit-feeding trace-maker.
- If the connecting material between the two tubes is thinner than the tubes, it is not created as a spreite. Spreite laminae are normally the same thickness as the tubes, usually seen at the base of the U. The thinner material represents the collapse feeding style outlined herein.
- A possible modern trace-maker could be a callianassid shrimp, based on analogous behaviour.

4.8 Acknowledgements

This work is supported by Petroleum Research Atlantic Canada (PRAC) and a Natural Sciences and Engineering Research Council of Canada (NSERC) grant to DMc.

M. Leaman thanks Liam G. Herringshaw and Nikki Tonkin for their initial support at the beginning of the project; Liam G. Herringshaw, Michael Garton and Chris Boyd for their assistance in the field; Chris Boyd for sample preparation and serial grinding; Małgorzata (Czarrna) Bednarz for three-dimensional modeling; and Colin Brisco for some data collection. This manuscript was improved by the reviews of Andrew Rindsberg and Evan Edinger.

4.9 References

Bertling, M., Braddy, S.J., Bromley, R.G., Demathieu, G.R., Genise, J., Mikuláš, R., Nielsen, J.K., Nielsen, K.S.S., Rindsberg, A.K., Schlirf, M., Uchman, A. 2006. Names for trace fossils: a uniform approach. Lethaia. 39, 256–286.

Bromley, R.G., 1996. Trace Fossils: Biology, Taphonomy and Applications, 2nd Edition. Chapman and Hall, London, 361 p.

Cornish, F.G., 1986. The trace-fossil *Diplocraterion*: Evidence of animal-sediment interactions in Cambrian tidal deposits. Palaios. 1, 478-491.

Goldring, R., 1962. The trace fossils of the Baggy Beds (Upper Devonian) of north Devon, England. Paläontologische Zeitschrift. 36, 232-251.

Fürsich, F.T., 1974. On *Diplocraterion* Torell 1870 and the significance of morphological Features in vertical, spreiten-bearing, U-Shaped trace fossils. Journal of Paleontology. 48, 952-962.

Herringshaw, L.G., McIlroy, D. in press. Bioinfiltration: Intra-sedimentary particulate transport by burrow-irrigating taxa. Journal of Sedimentary Research.

Jensen, S. 1997. Trace fossils from the Lower Cambrian Mickwitzia sandstone, south-central Sweden. Fossils and Strata. 42, 110 p.

MacEachern, J.A., and Gingras, M., 2007, Recognition of brackish-water trace fossil suites in the Cretaceous western interior seaway of Alberta, *in* Bromley, R., Buatois, L.A., Mángano, M.G., Genise, J., and Melchor, R., eds., Sediment-Organism Interactions; A Multifaceted Ichnology: SEPM, Special Publication 88, p. 149–194.

Schlirf, M., Uchman, A. 2005. Revision of the ichnogenus *Sabellarifex* Richter, 1921 and its relationship to *Skolithos* Haldeman, 1840 and *Polykladichnus* Fürsich, 1981. Journal of Systematic Palaeontology. 3, 115–131.

Spila, M.V., Pemberton, S.G., Rostron, B., and Gingras, M.K., 2007. Biogenic textural heterogeneity, fluid flow and hydrocarbon production: Bioturbated facies Ben Nevis Formation, Hibernia Field, offshore Newfoundland. In: MacEachern, J.A., Bann, K.L., Gingras, M.K., Pemberton, S.G. (Eds.), Applied Ichnology: SEPM Short Course Notes. 52, 354-371.

Tonkin, N.S., McIlroy, D., Meyer, R., Moore-Turpin, A., 2010. Bioturbation influence on reservoir quality: A case study from the Cretaceous Ben Nevis Formation, Jeanne d'Arc Basin, offshore Newfoundland, Canada. AAPG Bulletin. 94, 1059-1078.

Torell, O. 1870. Petrificata Suecana Formationis Cambricae. Lunds University Ärsskrift. 6, 1-14.

Vogel, S. 1989. Life in Moving Fluids: the Physical Biology of Flow. Princeton University Press, New Jersey, 352 p.

4.10 Figures

Fig. 4.1: Sample location of *Diplocraterion*. A: Collected from Cloughton Wyke, England (red A balloon in A and B). B: North is to the top of the photo. White arrow shows approximate collection location from the coastline of Cloughton. UK grid reference number: TA 02087 95031.

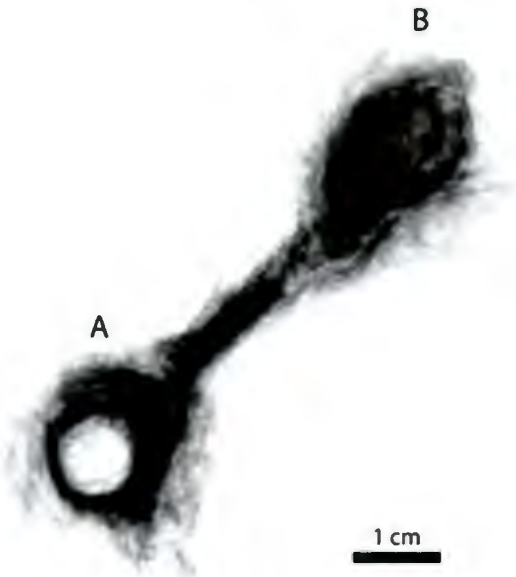

Fig. 4.2: *Diplocraterion* Morphological Element #1: Plan view of *Diplocraterion* model, representing the typical dumbbell shape. Gray and black in this modeling technique represents the mud components of the burrow. The darker black regions indicate high densities of mud. The centre of tube A appears white in this model indicating it is sand-filled, while tube B contains higher concentrations of mud.

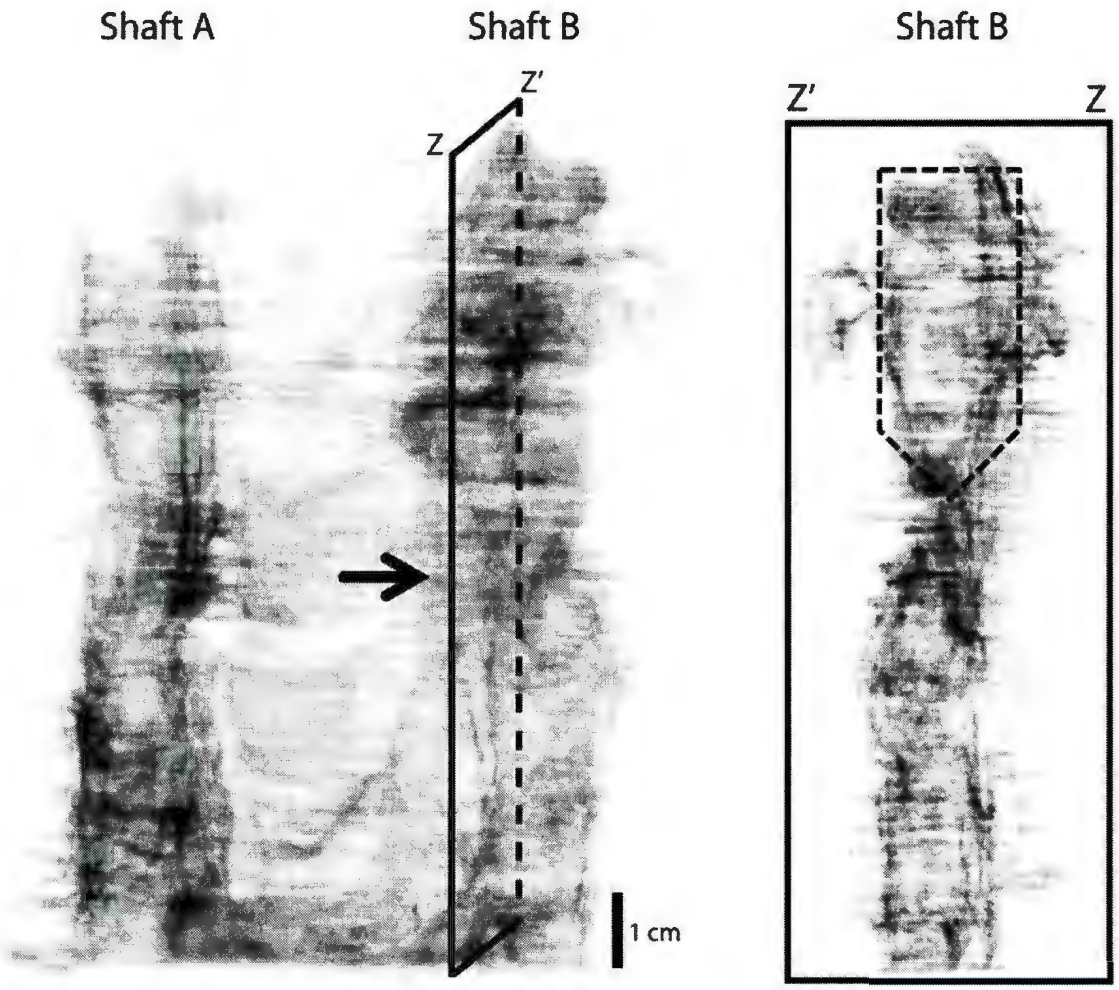

Fig. 4.3: *Diplocraterion* morphological element #1: (Left) Vertical cross section of same *Diplocraterion* as in Fig. 4.2, with a plane drawn on shaft B indicating the position of the Right figure. (Right) Vertical cross section of the inner left-hand side of shaft B. The black dashed line highlights the top most portion of the tube tapering downwards. This upper portion is muddier than the lower half.

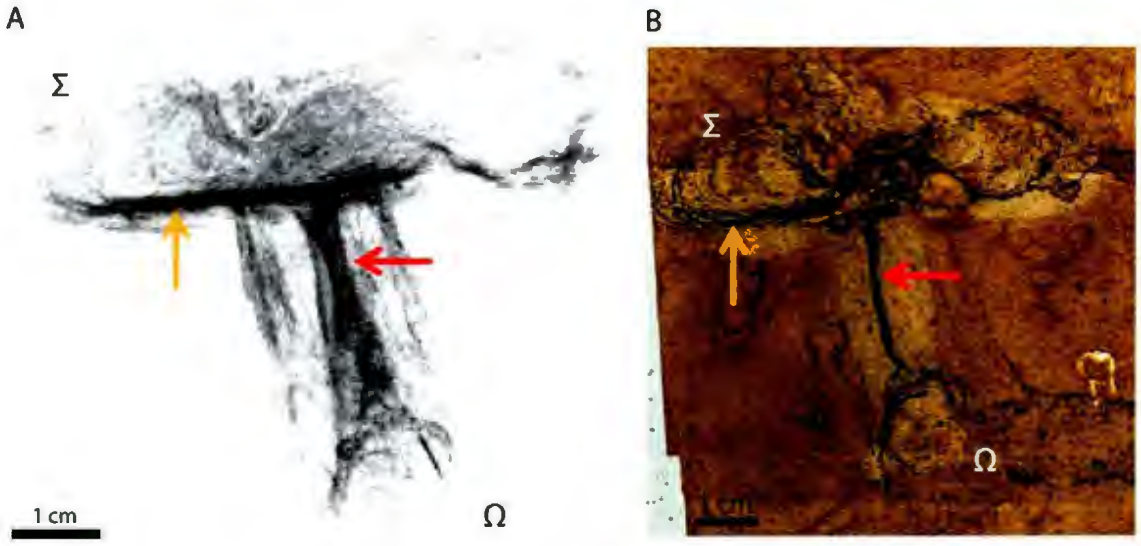

Fig. 4.4: *Diplocraterion* Morphological Element #2: Plan view of two *Diplocraterion*. *Diplocraterion* Ω was present first, and then Σ. Orange arrows point to an organic matter margin of *Diplocraterion* Σ. Red arrows highlight the thin accumulation of organic matter that is above *Diplocraterion* Ω. Same arrows are in Fig. 4.5. A: Three-dimensional model showing high densities of mud in dark grey/black. B: An image slice of the same two *Diplocraterion* model A is made from. Two sandy causative burrows are visible in *Diplocraterion* Σ, while only one is visible in Ω.

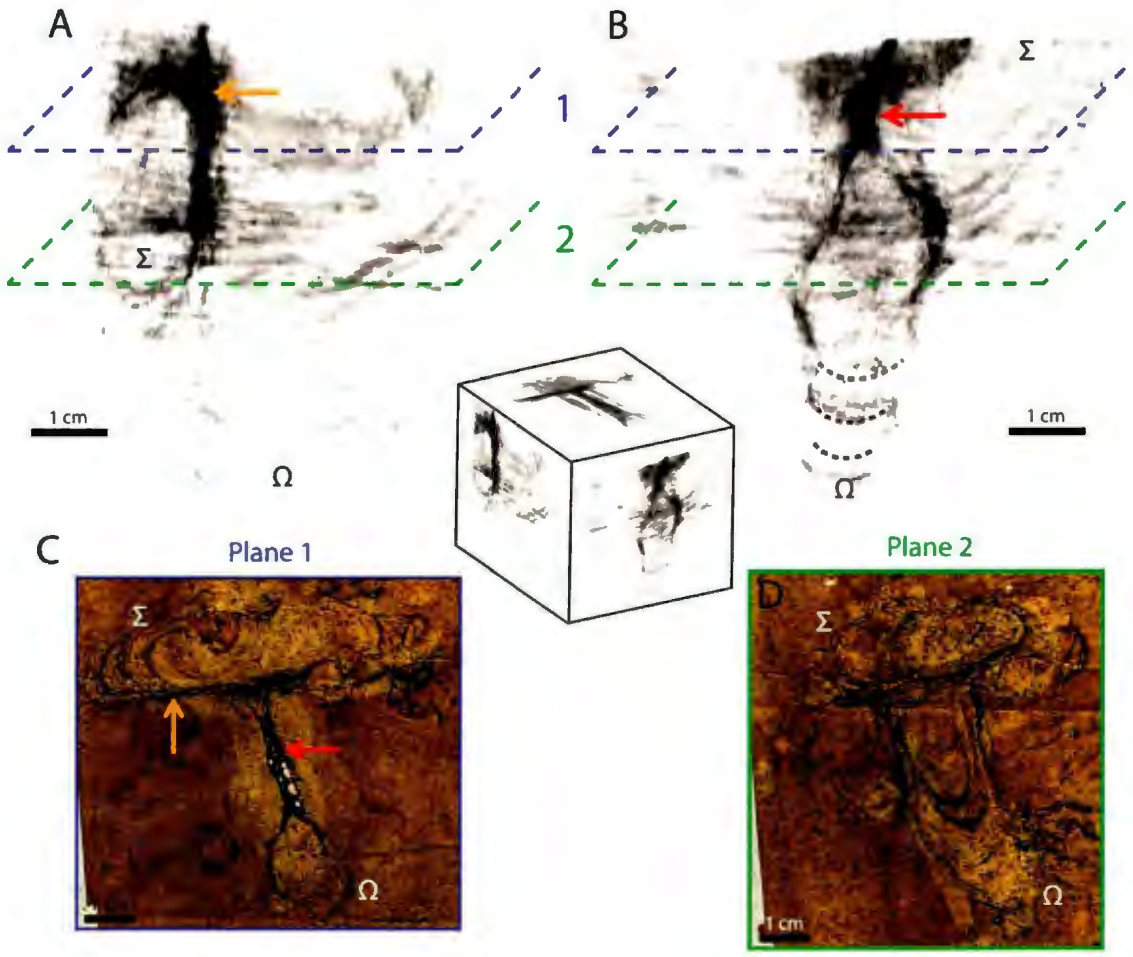

Fig. 4.5: *Diplocraterion* Morphological Element #2: View orientations are represented by the cube in the centre of the figure. Top of cube is Fig. 4.4A. A: Parallel down length of *Diplocraterion* Σ and perpendicular to *Diplocraterion* Ω. Organic matter (orange arrow, same arrow in Fig. 4.4) on burrow edge is visible on *Diplocraterion* Σ and vertical profile of *Diplocraterion* Ω is visible. Predominately retrusive spreite are visible in *Diplocraterion* Σ, however at the base of the burrow protrusive spreite cross-cut retrusive. B: Parallel down length of *Diplocraterion* Ω and perpendicular to *Diplocraterion* Σ. A vertical organic matter accumulation is observed above the retrusive spreite (black dashed lines) of *Diplocraterion* Ω (red arrow, same arrow in Fig. 4.4). C: Grind image slice from near the top of the burrow, representing the same location in A and B. Orange arrow highlights a portion of the organic matter margin cutting into *Diplocraterion* Ω. Red arrows highlights the organic matter accumulation that is above the retrusive spreite of *Diplocraterion* Ω. No sandy causative burrows are visible in *Diplocraterion* Σ. C and D are separated by only 0.95 mm. D: Grind image slice approximately half way down into the burrows, representing the same location in A and B. No large accumulation of organic matter is visible like in C.

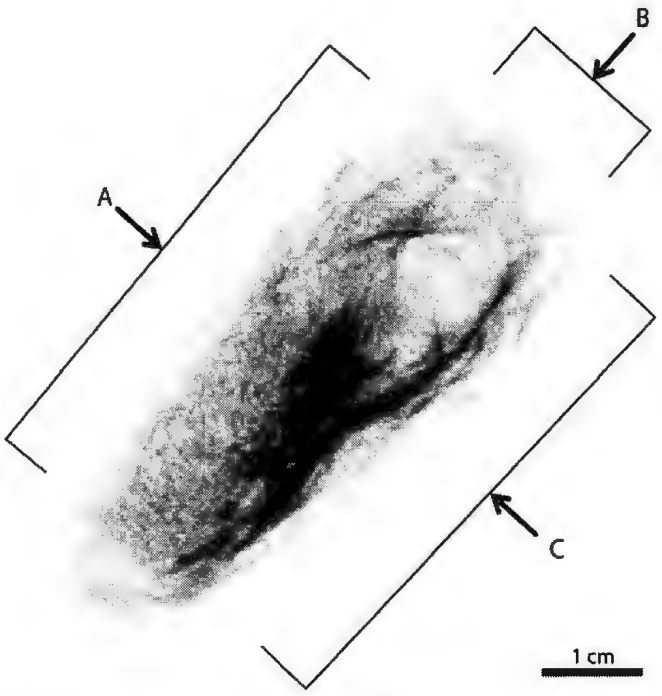

Fig. 4.6: *Diplocraterion* Morphological Element #3: Plan view of a unique *Diplocraterion* morphology. A sandy shaft opening is faintly visible (white) in the top right portion of the burrow. Lettered arrows indicate view orientations in Fig. 4.7.

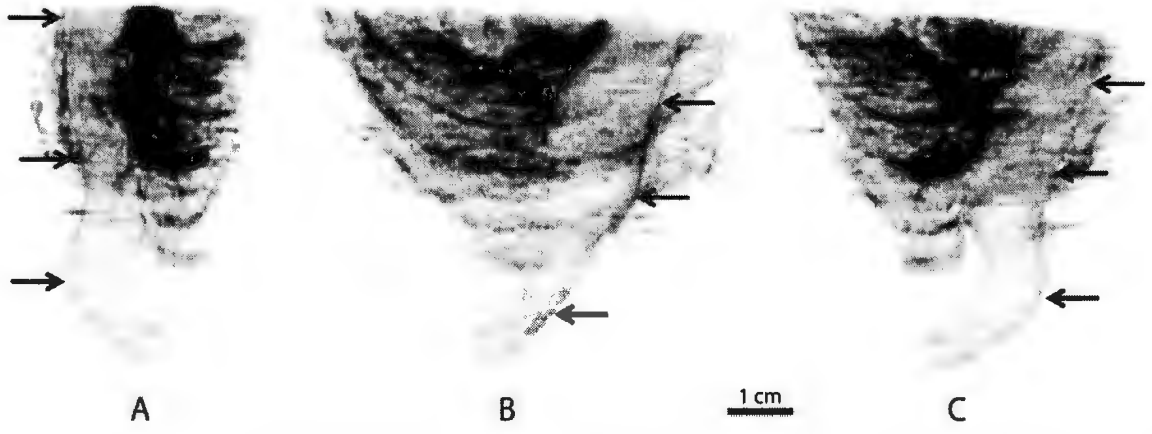

Fig. 4.7: *Diplocraterion* Morphological Element #3: Vertical cross sections of same burrow from Fig. 4.6. View orientations and letters correspond to arrows from Fig. 4.6. A through C depict the J-tube (arrows) cross-cutting the burrow and terminating just below the spreite in the matrix.

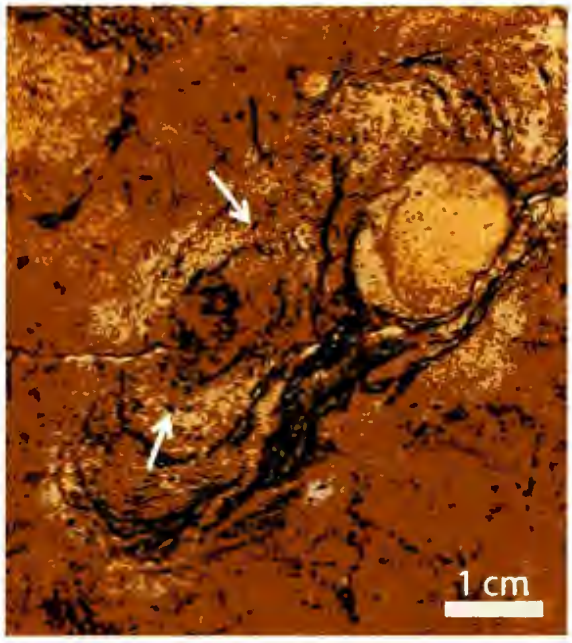

Fig. 4.8: Plan view of *Diplocraterion* morphological element #3 in the original rock image slice. White arrows highlight a few of many fecal pellets (black elongated cylinders) present near the base of the burrow. Fecal pellets are aligned parallel with the spreite.

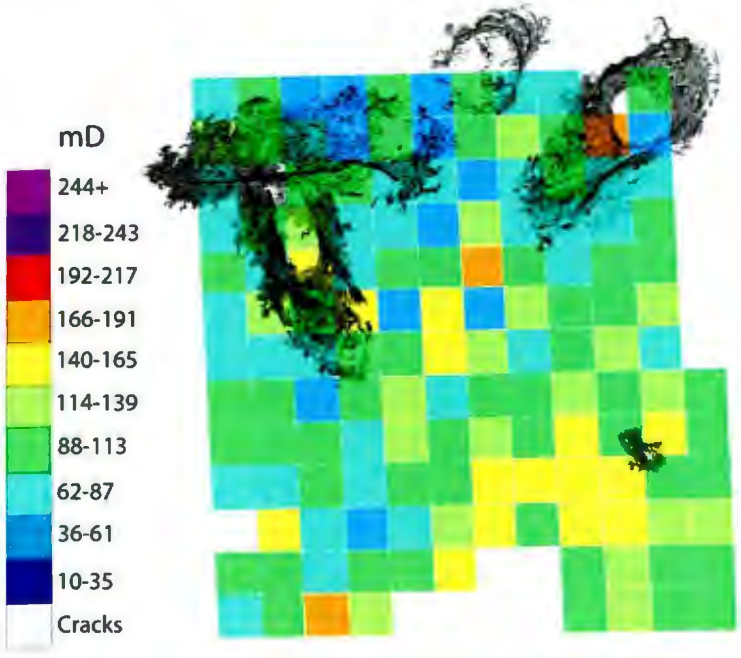

Fig. 4.9: Top permeameter surface read in the *Diplocraterion* sample block, 2 cm below the first grinding surface. Each square = one centimeter. *Diplocraterion* burrows present within the 20 grind surfaces overlie the permeameter grid. White squares represent cracks in the rock sample.

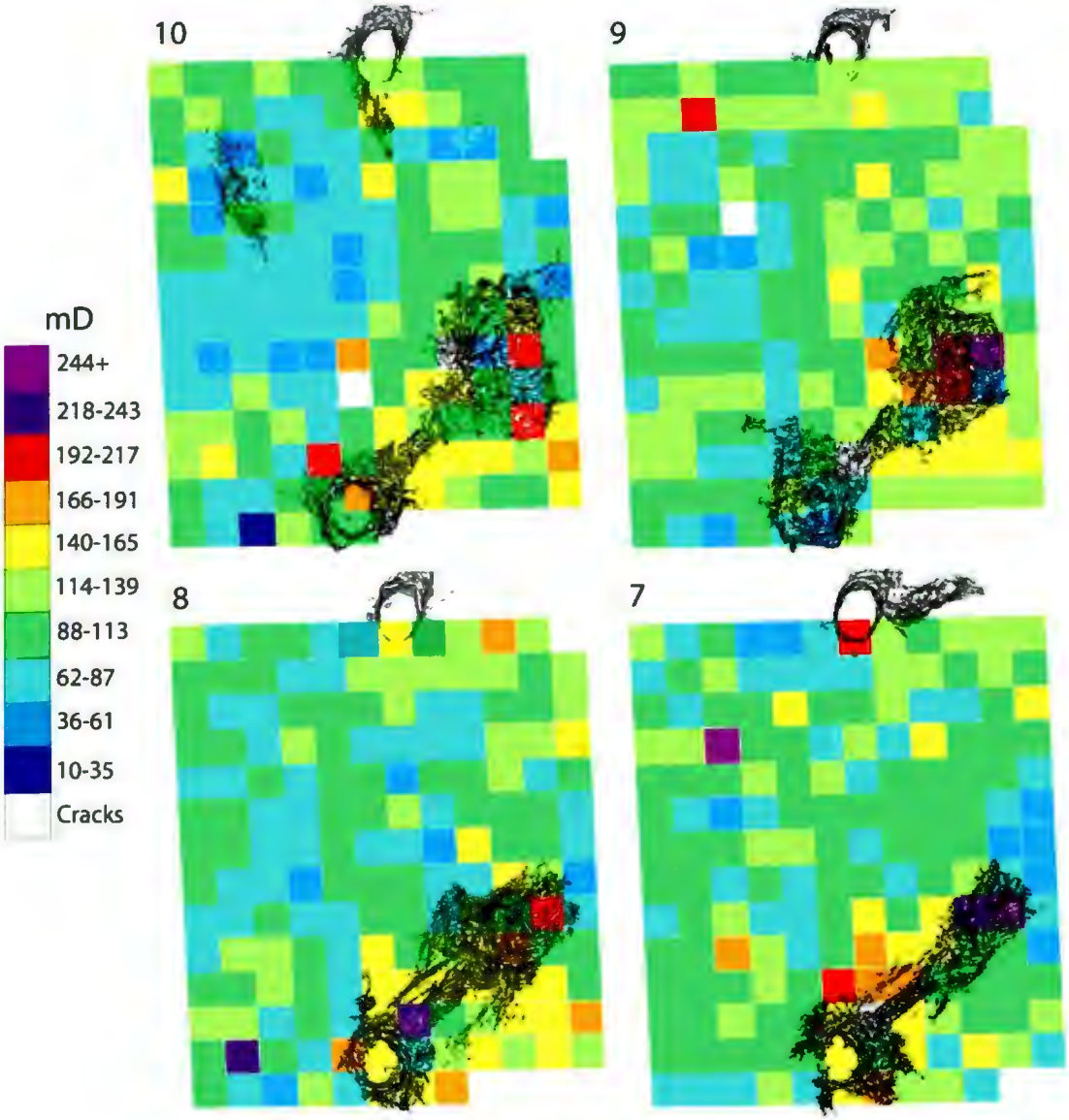

Fig. 4.10: Permeametry surfaces 10 (closest to the top) through 7 (closer to the base; see Appendix D) each reads 1 cm into the rock surface, also equal to 20 grind slices. Each square = one centimeter. These four surfaces are halfway through the sample. Notice the higher permeability (hot colours) measurements around the 'dumbbell' morphology of *Diplocraterion* morphological element #1.

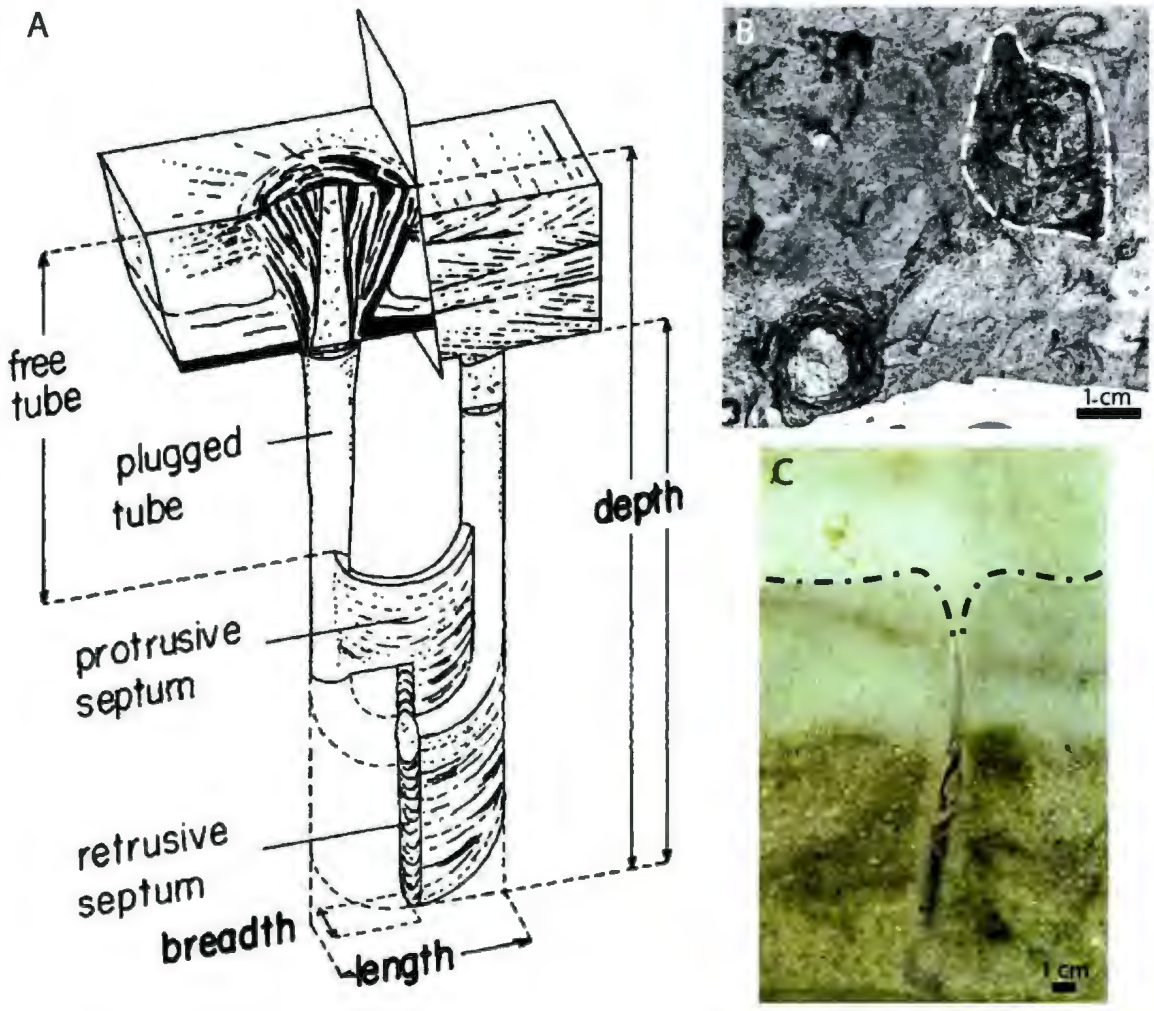

Fig. 4.11: A: Roland Goldring's sketch of *Diplocraterion yoyo* from the Devonian Baggy Beds of North Devonshire, England (Goldring, 1962). B: Plan view of *Diplocraterion* morphological element #1 in the original rock image slice (converted to black and white). White dashed line encompasses the messy muddy rings of shaft B. C: Vertical cross section (burrow formed against glass wall) of a *Neotrypaea californiensis* shrimp in a lab aquarium. The thalassinidean crustacean is feeding from below a collapsed cone feature (not at the sediment-water interface).

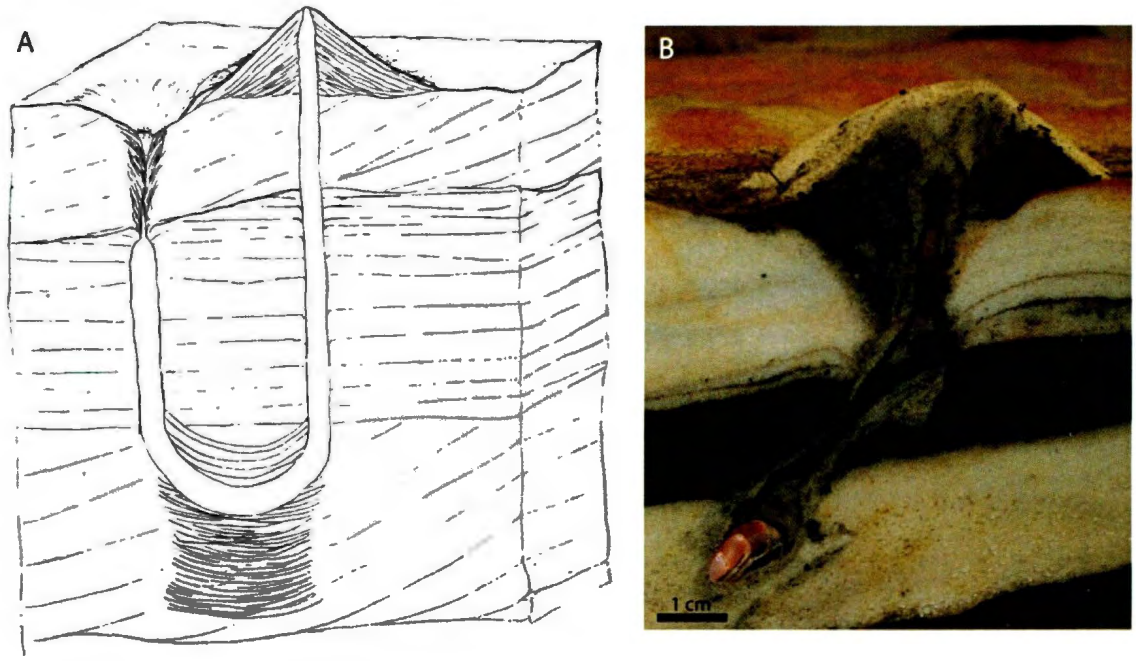

Fig. 4.12: *Diplocraterion* morphological element #1: A: Idealised sketch showing the behaviour of *Diplocraterion*. A funnel-feeding feature is connected to the sediment-water interface on the left-hand side of the U-burrow. The organism would sit below the funnel structure and feed from above. The other side of the U-burrow shows a volcano-like feature that is rarely preserved in the rock record. B: The same sediment volcano feature is visible in modern-day tank experiments with *Neotrypaea californiensis* shrimp.

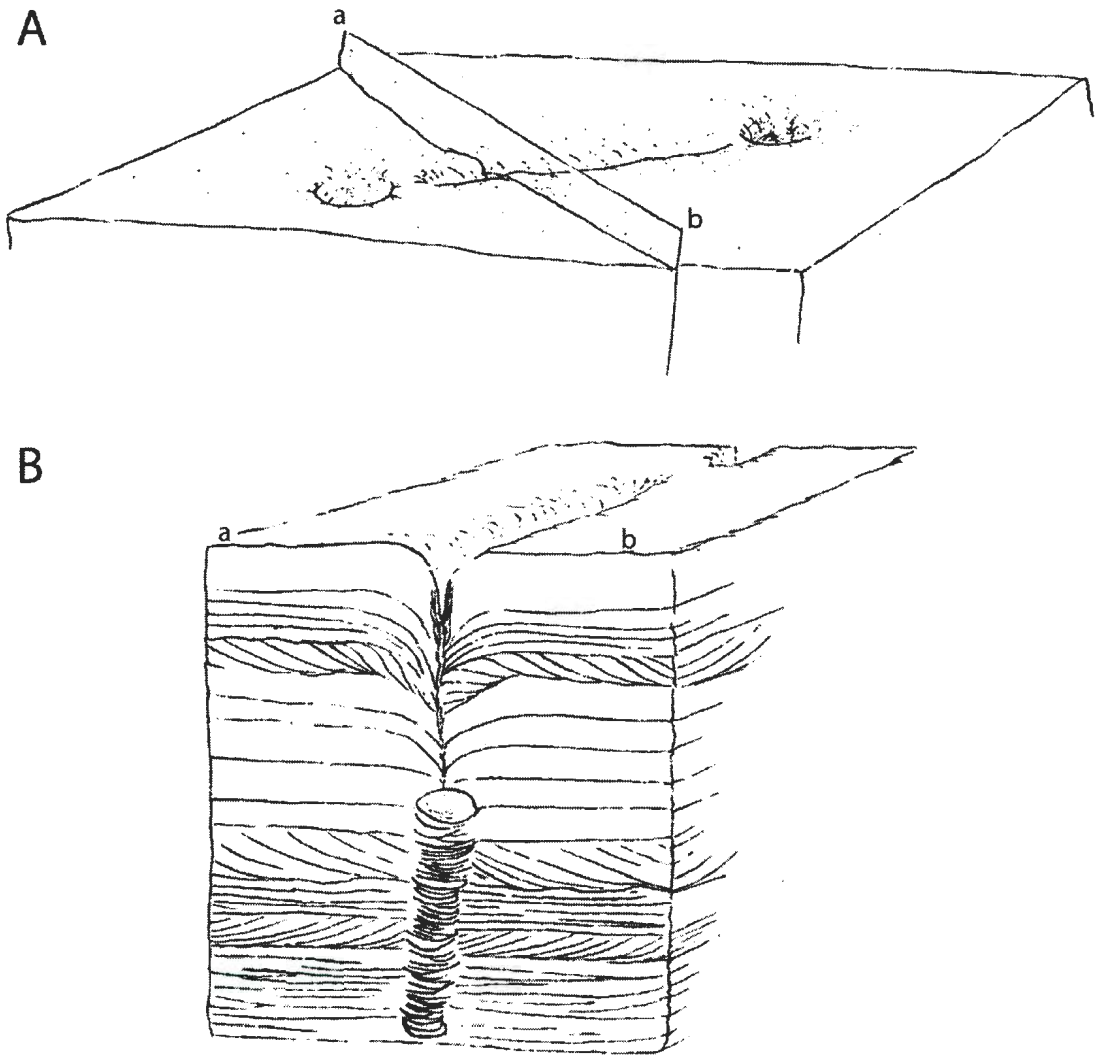

Fig. 4.13: *Diplocraterion* Morphological Element #2: A: At the sediment-water interface a slight depression is used by the trace-maker to collect fine-grained materials. B: Vertical cross section through A showing the trace-maker's location to feed from below the collapse cone. The thin depression in A is the typical 'dumbbell'-like morphology ichnologists use to identify *Diplocraterion*. It does not represent spreiten.

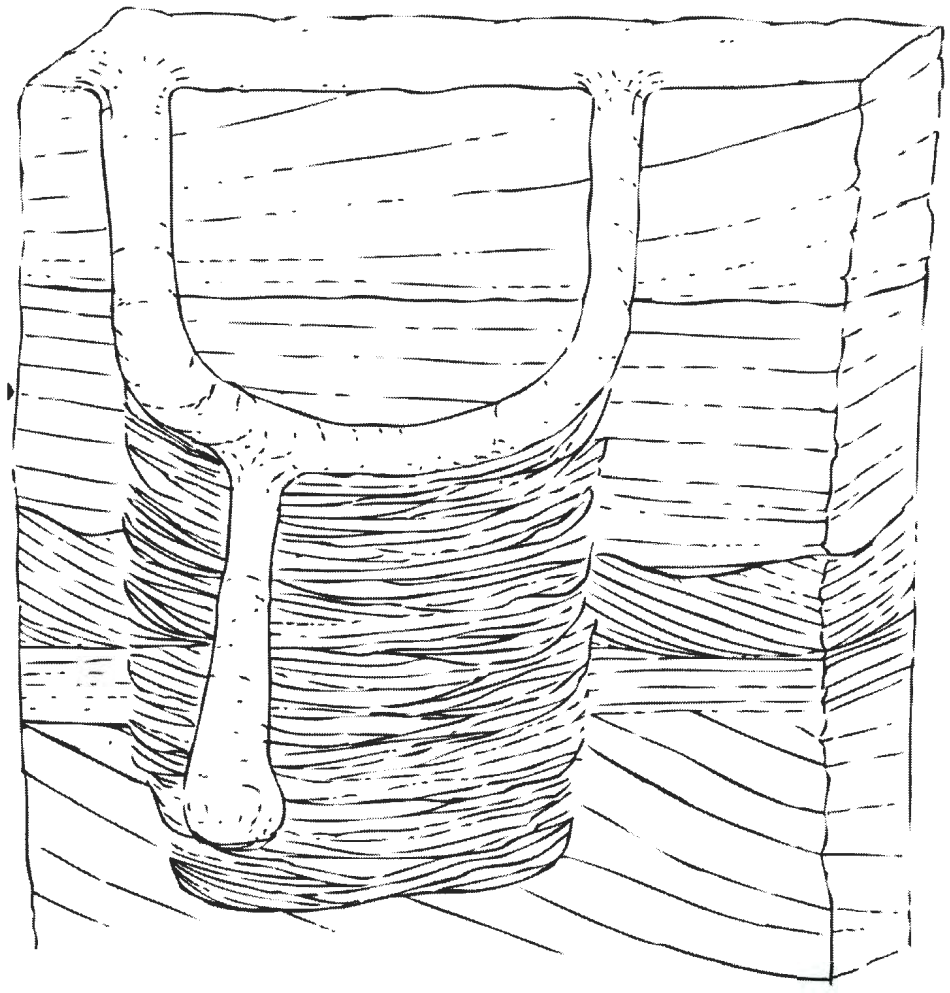

Fig. 4.14: *Diplocraterion* Morphological Element #3: Modification of a typical *Upogebia* Y-shaped burrow to include spreiten of a *Diplocraterion*. The trace-maker of *Diplocraterion* creates the U-burrow and later protrudes downwards (forming a J-burrow) from the base of the U through previous retrusive spreite to access microbial matter. The trace-maker could then resuspension feed from within this burrow.

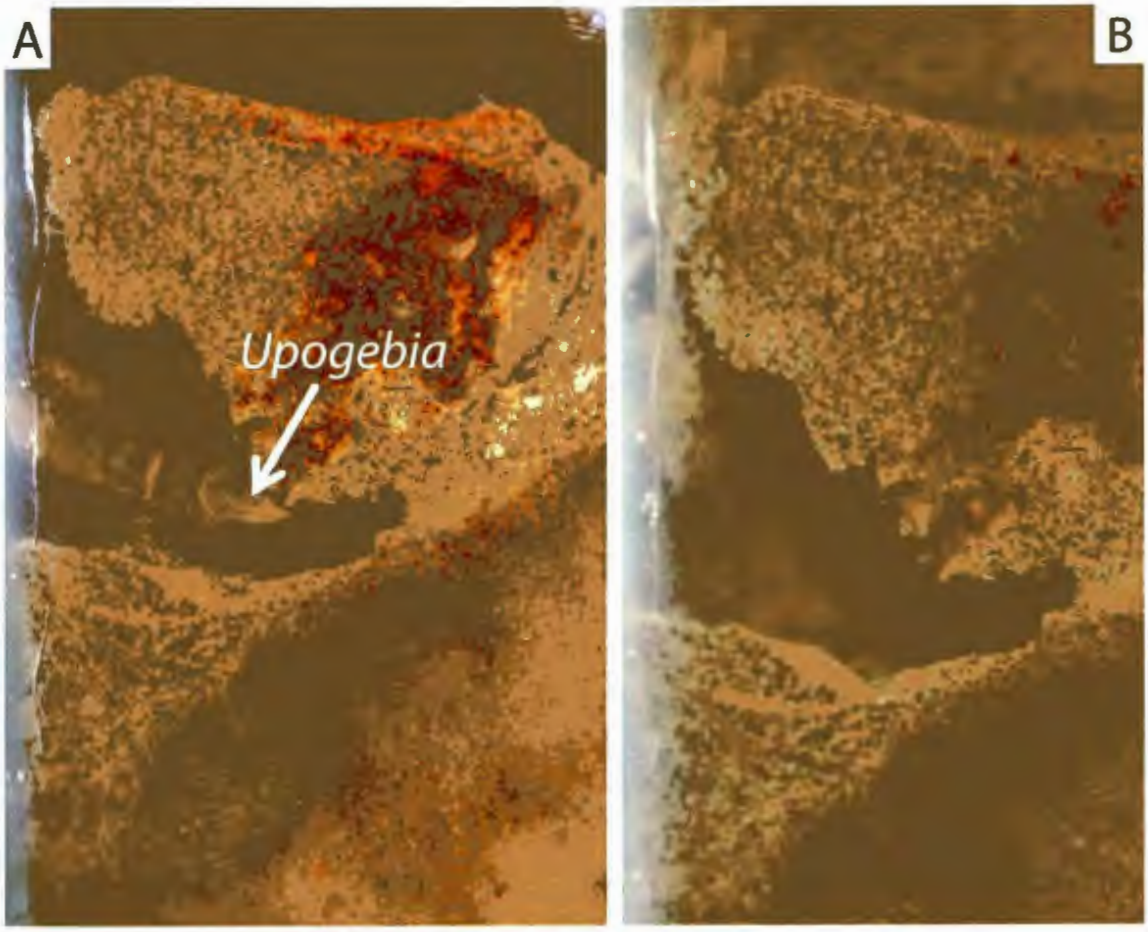

Fig. 4.15: ***Diplocraterion*** **Morphological Element #3: Lab aquarium containing** ***Upogebia*** **crustaceans. A: Shrimp is within the burrow tube shown beating its pleopods to disrupt the sediment and access any microbial nutrients. B: Burrow tube is murky with resuspended material the shrimp is now feeding on. Photos are taken through the aquarium glass wall. Modified after Herringshaw and McIlroy (in press).**

CHAPTER 5

Summary

Chapter 5 – Summary

5.1 Introduction

The main purpose of this thesis was to investigate the effects that bioturbation has on marine siliciclastic facies and augment the current understanding of trace fossil morphology. Such marine facies can be major hydrocarbon reservoirs, including the Ben Nevis reservoir offshore Newfoundland. Two common trace fossils, *Diplocraterion* and *Ophiomorpha*, were chosen to assess the influence that burrows may have on reservoir quality. *Ophiomorpha* and *Diplocraterion* are both abundant in marine siliciclastic systems and are commonly recognised by geologists and even non-specialists. Trace fossils were studied from outcrop and core hand samples (L-55 well) including samples of *Ophiomorpha irregulaire* from its type locality in the Book Cliffs, Utah. Study of type material allows realistic comparison with other material.

The outcomes of this research are relevant to bioturbated reservoirs worldwide. The characterisation of the sedimentological impact of *Diplocraterion* and *Ophiomorpha* on sedimentary fabric will improve the understanding of reservoir quality, which will improve production and recompletion in bioturbated reservoirs. Three-dimensional reconstructions of *Diplocraterion* and *Ophiomorpha* aid in field- and core-based identification of trace fossils, particularly based on the two-dimensional cross sections observed in core. The need for a better morphological understanding of *Ophiomorpha irregulaire* for taxonomic classification has previously been highlighted (McIlroy et al., 2009; Boyd et al., 2012). Understanding these trace fossils in greater detail is also of

paleoecological significance, providing new information on trace-maker behaviour. The impact of this stems from the fact that inferred behaviour is commonly incorporated into palaeoenvironmental analysis (MacEachern et al., 2007).

5.2 *Ophiomorpha*

5.2.1 Morphologies

A variety of pelletal morphologies and compositions have been identified from the three-dimensional models and core. The range of pellets for *Ophiomorpha irregulaire* includes flame-like (Fig. 2.7A); sand-filled and mud-lined (Fig. 2.7B and C); and conical froms (Fig. 2.7D). In the tank experiments (see section 5.2.2. below), sand-only pellets were observed lining *Neotrypaea californiensis* burrow walls (Fig. 2.12). Burrow morphology from the Californian sample showed a partial meander maze (Fig. 2.6 and Fig. 2.12). In core, the meander maze can be identified by two burrow openings adjacent to one another (turning points; Fig. 2.9). Core samples of *Ophiomorpha irregulaire* also showed protrusive pelleted-roof spreiten (Fig. 2.7 B and C), and collapsed sediment above burrows (collapse cones; Fig. 2.10), features not previously described from *O. irregulaire*.

The three-dimensional modeling technique has shown us that the pelletal morphology of *Ophiomorpha irregulaire* is not as straight forward as only "flame-like" pellets. The morphologies of the remaining ichnospecies of *Ophiomorpha* would benefit from a similar in-depth examination, ideally with the serial grinding and three-

dimensional reconstruction techniques. Preliminary studies suggest that it is possible that *O. puerilis* and *O. annulata* (Fig. 1.4) could be synonymised after more study.

5.2.2 Palaeobiology of *O. irregulaire*

From tank experiments *Neotrypaea californiensis* exhibit burrowing behaviours that result in extremely similar burrow morphologies to *Ophiomorpha irregulaire*. This includes pelletal morphology (Fig. 2.12), meander maze and turning points (Fig. 2.11), and collapse cones (Fig. 2.11C). *Ophiomorpha irregulaire* is inferred to have undertaken deposit feeding and suspension feeding behaviour.

5.2.3 Palaeoenvironmental Range and Distribution of *O. irregulaire*

Ophiomorpha irregulaire has been identified worldwide (Fig. 2.2) in rocks of a variety of ages (Table 2.2) based on findings in the literature and compared with our observations from the three-dimensional model and core samples. Based on the analogue studies of *N. californiensis* in aquaria and the fact that the shrimp are known to live in water depths of up to 2000 meters (Dworschak, 2000), we conclude that *O. irregulaire* are not restricted to shallow marine facies. The possible trace-makers of *O. irregulaire*, *N. californiensis*, are normal residents of deep water environments. The Juncal Formation sample supports this statement in that the burrow matches with all ichnospecific morphological criteria, including pellets and a portion of the meander maze, of the Utah type locality sample, but are from slope-channel facies.

5.3 *Diplocraterion*

5.3.1 Three-Dimensional Morphology

From the three-dimensional model, three new morphologies were identified from *Diplocraterion* leading to new interpretations of the trace-maker behaviour. The first morphology shows the classic *Diplocraterion* 'dumbbell' morphology, in which one of the shafts is stratigraphically higher and muddier than the other, with no evidence of differential erosion (Fig. 4.3); the second is another 'dumbbell' morphology burrow with a vertical thin accumulation of organic matter above the spreite (Fig. 4.4 and Fig. 4.5); the third morphology exhibits only one J-tube, which crosscuts spreite from the same burrow, and which terminates in the sediment below the spreite (Fig. 4.6 and Fig. 4.7). From the three listed morphologies three previously unreported possible trace-maker behaviours have been identified.

The first morphology shows some resemblance to Goldring's (1962) *Diplocraterion yoyo*, with the presence of a plugged muddy tube. The feeding behaviour, based on morphology, is deposit feeding from below funnel (Fig. 4.11).

The second morphology indicates collapse-feeding (deposit-feeding behaviour again; Fig. 4.13), revealing that the connecting material between the two shafts in plan view is not necessarily composed of spreite. The thin, connecting, organic-rich matter sheet between the spreite forms from a collapsed zone between the limbs of the U. The trace-maker uses the zone to collect fine-grained material from the sediment-water interface by collapsing the sediment into the base of the U. As such, if the connecting material between the two shafts is thinner than the causative burrow it is not a spreite.

Spreiten should be the same approximate thickness as the causative burrow, usually seen at the base of the U. The thin sheet of organic-rich sediment is inferred to represent the collapse feeding style.

Resuspending feeding behaviour is inferred from the presence of a J-burrow which crosscuts the retrusive spreite with abundant fecal pellets (Fig. 4.14 and Fig. 4.15).

The trace-maker of *Diplocraterion* is inferred to facultatively suspension- or deposit-feed depending on nutrient availability. Many of these behaviours correspond with behaviours of callianassid crustaceans, which employ similar feeding styles (e.g. collapse feeding and funnel feeding) to the proposed trace-maker of *Ophiomorpha irregulaire* observed in aquaria (as outlined in Chapter 2).

It is proposed that aspects of the morphology of *Ophiomorpha irregulaire* and *Diplocraterion* are comparable to features seen in studies of callianassid crustaceans. While there is no known analogue that creates a U-shaped burrow with spreite, this does not rule out the possibility of a similarly behaving organism.

5.3.2 Permeability

Three-dimensional permeability was conducted on a full *Diplocraterion* sample (15 cm tall) with the help of our developed serial grinding method (see Appendix A and B). At each one centimeter depth into the rock sample, there is a corresponding permeability surface (equal to 1 cm thick) and 20 grind images (at Z-depth 0.5 mm). Burrows are stacked on top of the permeability grids and any patterns or trends are visible (Fig. 4.9 and Appendix D, Fig. D.1 to Fig. D.3).

Enhanced permeability was observed in the coarse-grain-filled *Diplocraterion* shafts as well as surrounding the typical 'dumbbell' morphology (Fig. 4.10). This enhancement is observed for almost the full length of the vertical *Diplocraterion.* The surrounding matrix is completely burrow mottled with no original sedimentary structures preserved. This increase of permeability is inferred to have been caused by the trace-makers' behaviour while living in the burrow, e.g. sediment cleaning and selective feeding strategies could both cause cleaning of the sediment surrounding the burrow. The combination of these behaviours makes the studied *Diplocraterion* a reservoir-enhancing trace fossil.

5.4 Ben Nevis L-55 Core Permeability

Ophiomorpha irregulaire was found to variably decrease k_h by 70% (maximum; 28% average) but can also increase k_h by 82%; k_v can be decreased by 14%. The near-burrow sedimentary fabric must be taken into account when considering permeability influences. The overall bioturbation intensity must also be quantified to determine the volume of the burrows of *Ophiomorpha irregulaire* occupy within the sediment. A reduction or increase in permeability is explained by the behaviour of the trace-making organism, *Neotrypaea californiensis.* Understanding the burrow morphology and behaviour has provided insight on how fluid flows through burrows in a highly bioturbated reservoir. *Ophiomorpha* is one of the most recognizable trace fossils, and this research proves *Ophiomorpha irregulaire* has profound effects on reservoir volume.

APPENDICES

Appendix A – Precision serial grinding and volumetric 3D reconstruction of large ichnological specimens

Precision serial grinding and volumetric 3D reconstruction of large ichnological specimens

Małgorzata Bednarz[a], Liam G. Herringshaw[b], Christopher Boyd[a], Mary Leaman[a], Elisabeth Kahlmeyer[a] and Duncan McIlroy[a]

[a] Memorial University of Newfoundland, Department of Earth Sciences, 300 Prince Philip Drive, St. John's, Newfoundland, A1B 3X5, Canada
[b] Durham University, Department of Earth Sciences, Durham, DH1 3LE, UK.

KEYWORDS

Serial grinding, three dimensional, reconstruction, *Phycosiphon*, volume, ichnology, tortuosity, 3D models, ichnofabric, morphology

3D reconstruction in ichnology

Corresponding author: Małgorzata Bednarz, Memorial University of Newfoundland, Department of Earth Sciences, 300 Prince Philip Drive, St. John's, Newfoundland, A1B 3X5, Canada, m.bednarz@mun.ca; 0048 508 66 17 17

A.1 Abstract

We present herein a methodology for obtaining precise, deterministic, volumetric three-dimensional reconstructions of large or complex trace fossils. Two stages are outlined: a laboratory stage, involving precision serial grinding and high-resolution digital photography, and a computer analysis stage, where burrow volumes are visualized and analysed. It is shown that the techniques can be used successfully for bioturbated rocks that have little or no density contrast between the matrix and the burrows, upon which non-destructive techniques, such as CT scanning, are ineffective. The serial grinding method, employing automated, computer-controlled machinery, enables precise removal of extremely thin, parallel increments of sedimentary rock. After each grinding run, a high-resolution digital photograph of the specimen surface is taken. From this, computer analysis of the generated stack of images allows high-resolution, 3-D reconstruction of the trace fossils, and subsequent visualization of burrow morphology, volume, and sedimentological impact. To demonstrate the technique, several trace fossil samples (phycosiphoniform burrows, *Chondrites*, *Ophiomorpha*) were serially ground and digitally photographed. We show that the method enables volume calculations to be determined precisely for a single burrow, burrow networks and ichnofabrics.

A.2 Introduction

Serial grinding has been used to reconstruct the three-dimensional morphology of palaeontological specimens for over a century (e.g. Sollas 1903; Stensiø 1927; Ager 1965, Watters and Grotzinger 2001), but never widely, due to its limitations as a destructive, time-consuming process. With the advent of low-cost digital photography and fast, high quality image-processing software, however, the approach has become increasingly accessible, and the techniques developed by Sutton *et al.* (e.g. 2001a, 2001b, 2005, 2006) for studying the body fossils of the Herefordshire Lagerstätte have proved particularly influential. With the high resolution, easily manipulable images produced, and the wealth of morphological data that can be garnered, this approach has now been applied to a variety of fossil material (e.g. Rahman and Zamora 2009; Maloof *et al.* 2010).

Despite its potential value in elucidating morphology and sedimentological impact, serial grinding and 3D reconstruction has been little used in ichnology. Exceptions are the trace fossil studies of Naruse and Nifuku (2008) and Bednarz and McIlroy (2009, 2012), both of which applied the technique to the reconstruction of phycosiphoniform ichnotaxa. Other studies have used serial polishing to examine ichnofabrics, but without the creation of 3-D reconstructions (Wetzel and Uchman 1998, 2001).

Serial grinding and 3D reconstruction of trace fossils and ichnofabrics in large rock samples has never been attempted, but such work is critical to full morphological characterization of many ichnotaxa (cf. McIlroy et al. 2009). Since trace fossils can comprise volumetrically significant components of many sedimentary rocks—affecting sedimentological properties at a reservoir scale (Buatois et al. 2002; Gingras et al. 2004;

Burns et al. 2005; Gordon et al. 2010; Tonkin et al. 2010; Bednarz and McIlroy 2012)—it is vital to understand their three-dimensional morphology.

Volumetric 3D reconstruction of such trace fossils has the potential to provide new insights into reservoir characterization. Several techniques have been used previously to obtain spatial models of the burrowing activity of living animals, or to measure the volumes of trace fossils and ichnofabrics. These include computed axial tomographic (CT) scanning (e.g. Dufour et al. 2005; Herringshaw et al. 2010), magnetic resonance imaging (MRI) (e.g. Gingras et al. 2002), multi-stripe laser triangulation scanning (MLT) (Platt et al. 2010) and serial grinding (Naruse and Nifuku 2008; Bednarz and McIlroy 2009, 2012). All these methods have their limitations, depending upon the examined rock or sediment properties. The density contrast between matrix and burrow is commonly minimal, and it can be difficult to determine the true morphology of a trace fossil from two-dimensional cross sections. As such, only destructive serial grinding can be employed satisfactorily to obtain a volumetric 3D reconstruction of the burrow (cf. Gingras et al. 2002; Naruse and Nifuku 2008; Bednarz and McIlroy 2012). In most palaeontological and ichnological studies, the serial grinding has been carried out manually (e.g. Wetzel and Uchman 1998; Sutton et al. 2001; Bednarz and McIlroy 2009). While this is acceptable for small specimens, such an approach is not appropriate for larger ones, as it is too unwieldy and imprecise.

By using serial grinding to produce high resolution reconstructions, new information can also be obtained on the ecology of the tracemaker and the sedimentological impact of bioturbation. Furthermore, such studies can be used to resolve ichnotaxonomic issues by resolving trace fossil morphology within the host sediment. This approach to ichnological/ichnotaxonomic research is particularly relevant if applied to specimens from the type locality (Boyd et al., 2012).

A.3 Methodology

A.3.1 Sample preparation

Large trace fossil-bearing blocks can be trimmed in the field using a hand-held rock saw, if care is taken to leave sufficient matrix around the trace fossil. In our study, to create a regular shape for precise image alignment, each block was placed in a box and plaster of Paris poured around it (cf. Bednarz and McIlroy 2009, 2012). Once the plaster is set, the block can be removed from the box, and cut into a rectangular prism with a laboratory rock saw. The regular outline of the block is used as the basis for image registration (see below; Fig. 1A). For further accuracy of image alignment, vertical holes can be drilled into the block (cf. Sutton et al. 2001a). Prior to photography (see below), visual contrast between the ichnofabric and the rock matrix can be enhanced considerably by wetting the ground surface of the specimen with water or a light oil (cf. Bromley 1981). To prevent disintegration of the plaster of Paris from frequent moistening, non-fossil-bearing surfaces of the block can be coated with plain, transparent lacquer.

A.3.2 Serial grinding set-up

Serial grinding was carried out using a Haas VF3 VOP-C Vertical Machining Center (20hp vector dual drive, 1000 IPM), capable of grinding to a precision of 0.001 inches (0.0254 mm). Specimens were clamped in place (Fig. 1B), with the gantry raised by remote control to the start position, and then raised by the required increment after each grinding run. The most effective grinding element was found to be a diamond disc (diameter = 70 mm).

The increment of rock removed during each serial grinding run can be varied according to the dimensions and expected complexity of the material studied. For example, phycosiphoniform burrows with a diameter of 2–3 mm were serially ground at increments of 0.2 mm; whereas a block containing *Diplocraterion* with a width of ~60 mm and an estimated depth of over 100 mm, was serially ground at increments of 0.4 mm. The choice of serial grinding interval resolution depends also on the purpose of the reconstruction, with coarser increments used for gross-scale reconstructions, and finer increments used to provide highly detailed reconstructions and to enable volume measurements of small specimens.

A.3.3 Photography

Canon 30D and 50D digital SLR cameras were used to photograph the specimens after each grinding run. For accuracy in the subsequent registration process (see below), it is crucial to maintain the distance between the freshly exposed sample surface being photographed, and the objective (lens) of the camera being used. Owing to the fact that the sample decreases in thickness after each run of the grinding tool, the camera–specimen surface distance must be adjusted each time to ensure consistency. This can be achieved by: 1) successively changing the camera position (Fig. 2A); 2) successively changing the sample position (Fig. 2B); or 3) setting up a workspace where both the camera and sample surface can be placed a constant distance from one another (Fig. 2C). If the camera–sample distance is not adjusted during the serial grinding procedure, the images obtained will need to be scaled with computer graphic software. This will make the registering process more time-consuming and can introduce errors due to the distortion artificially imposed on the image.

The photographs should be taken under invariant lighting conditions that best illuminate the ichnofabrics. To test this, a series of photographs of the same sample surface should be taken under different conditions, after the first serial grinding run. Lighting conditions to consider include photography under ambient lighting, under flash lighting, and under controlled directional lighting. It is essential to avoid shadows across the sample, which might obscure important features or be confused subsequently as being of lithological origin.

If contrast is insufficient when the rock surface is dry, it may be necessary to wet the surface to enhance the contrast: this is particularly true of finer-grained rocks, or specimens where the trace fossil fill is of a similar colour to the matrix. If water is used to enhance contrast, however, surface glare can be a problem. This can be circumvented by the use of a softbox or light tent. Images from successively ground surfaces should be

consecutively numbered using a permanent marker or pencil, and photographed with a scale bar (Fig. 1A).

The images can be taken in camera RAW or JPEG format, but RAW image format is preferable as it captures substantially greater detail. Standard JPEG images are captured at 8-bit colour depth, with up to 256 levels of luminosity on each channel (Red, Green, Blue), allowing more than 16 million colours at each pixel site. Camera RAW format offers 12, 14, or 16-bit colour depth (12-bit for the Canon 30D), encompassing 4,096 levels of luminance and allowing for more than 68 billion colours at each pixel site. This increase in colour spectrum provides a much finer colour gradient and detail. RAW format also has a much higher tolerance of image manipulation, exposure or colour correction; enabling image processing without disruption of the whole image. The photograph stack can be subjected to bulk processing, including conversion of RAW images into smaller file formats such as TIFF, JPEG and PNG.

For sufficient depth of field in the image, photographs should be taken with an aperture of f/8 or greater. To ensure the photos are properly focussed, the camera should be mounted on a tripod or stand, and a fast shutter speed should be used (typically $1/30^{th}$ of a second or faster). To guarantee sharp images, it may be helpful to use a remote-controlled or timed shutter release, or the 'Mirror lock-up' or 'Live view' modes of the digital SLR. To keep barrel distortion to a minimum, use of an ultra-wide-angle (<15 mm) lens should be avoided.

A.3.4 Digital image-processing and interpretation

Images can be processed with a range of filters (e.g. brightness, contrast) in a 2D graphic software package such as Adobe Photoshop to enhance the contrast between the burrow and the matrix. Depending on the characteristics of the sample, the photographs may need to be changed to greyscale to do this effectively.

In the worked examples considered here, each photograph of the serially ground sample was stacked consecutively as layers in a single Photoshop (.PSD) document (if file sizes are large, more than one .PSD file may be necessary). The first photograph in the series can be used as a base layer, and all other layers registered (aligned) with this base layer by setting new layer opacity to ~50% and repositioning or rotating the new layer until the reference points (e.g. corners of block, drill holes) are aligned. Layer opacity can then be reset to 100%, and the process repeated for each successive image. Each successive layer should be named using the number of the serial grinding run captured in the photograph.

A.3.5 Burrow selection methods

Once all images are aligned, the image stack can be cropped to focus on the area of interest. Cutting out superfluous host rock may significantly reduce file size. The burrows can be selected, either by mouse or tablet pen, using one of the many tools in Photoshop (e.g. Magic Wand, Paint Bucket, Pen, Magnetic Lasso, Brush). The choice of tool depends upon the nature of the burrows (Figs. 3A and D). If the burrows are large and the contrast between them and the matrix is sufficient, the Magic Wand tool can be

used. If the burrows are small, however, and the contrast between the trace fossil and matrix minimal, the Magic Wand tool might select a range of pixels that do not belong to the burrow, introducing errors (cf. Figs. 3B and E) and overly complex 3D isosurfaces (see below). The most accurate – but time-consuming – method of burrow selection is to use the Brush and Magnetic Lasso tools with a tablet pen (Figs. 3C and F). These tools enable the most accurate selection of burrow shape and minimize spuriously accurate or complex burrow margins.

Once the burrows have been selected accurately, they can be saved on a separate layer using the Clipping Mask tool, attached to the layer representing the original photograph. The layer with the selected burrow shape can then be named accordingly. When the examined ichnotaxon is known to be composed of more than one element (e.g. Fig. 3A-C; cf. Bednarz and McIlroy 2009), all elements are selected separately, and saved on separate layers. In this case, the file names should include both the slice number and a letter prefix (e.g. c_099 might represent the burrow cores of the 99th slice through a *Phycosiphon* specimen, whilst h_099 would represent the halo surrounding the core). This makes it possible to reconstruct different elements of the same burrow separately in 3D. In addition, modelling different components of the burrow separately in the same 3D volume enables artificial colouring of the different components of the trace fossil, and can be used for volume measurements and comparisons.

The burrow selection layers are then saved as grey-scaled images, with white silhouettes on a black background. This is necessary because the volume visualization software used (VG Studio Max or VolView) interprets black pixels as transparent, white pixels as opaque, and all intermediate shades of grey accordingly, to visualize the spatial model from the image stack. The file extensions of saved images were either .JPG or .PNG, and these consecutive, two-dimensional raster images were stacked to form the basis of the three-dimensional modelling.

An alternative means of obtaining images suitable for importing into a 3D volume visualization software package has been described by Watters and Grotzinger (2001). Their technique was based on body fossil material. The sharp contrast between biomineral and the surrounding rock was such that 2D graphic software filters and grey-scale histogram manipulation could be used to select the fossil. This technique could probably be used successfully for reconstructing isolated trace fossils that have a marked colour contrast relative to the surrounding sediment.

For morphologically complex trace fossils and ichnofabrics, however, where a greater number of burrows are present and/or the contrast between the burrows and the matrix is subtle, each image needs to be treated individually. Unless the burrow fill is mono-minerallic, an automatic filter- or histogram-based selection of the shapes will not work precisely enough (Fig. 4). This will result in the generation of spuriously complex burrow margins that are difficult to "polygonize" and produce quantitative measurements of volume from (Fig. 4B).

A.3.6 Image spacing and 3D modeling

In our study, stacks of the images to be reconstructed were imported into the commercial edition of one of two 3D volume visualization software packages: VG Studio

Max 1.2, and VolView 2.0. Both programs can reconstruct spatial geometry from a sequence of 2D images representing the cross-sections of any object or structure, by the process of voxel (volume element) rendering. These programs are primarily used in the fields of medicine and engineering to produce spatially interactive models from .DICOM files(Digital Imaging and Communications in Medicine) during CAT (computed axial tomographic) scanning . DICOM image files incorporate volumetric data (voxel dimensions) that 3D software packages use to create three-dimensional reconstructions.

When importing raster image formats such as .JPG or .PNG into the programs, however, sample spacing values (x, y and z) must be provided manually. The data imported into the volume-visualizing software are sampled anisotropically (i.e. the distance between the parallel consecutive slices is different from the in-plane pixel size: Al-Shayeh and Al-Ani 2009). Voxel resolution is based on the in-plane pixel dimension (number of pixels per unit length in the image; x and y axes) and the increment at which the specimen was serially ground (z axis). With the photograph dimensions (in mm) set to the measured dimensions of the sample, spacing in the x and y axes was calculated according to the equation:

x = Width of image / Number of pixels in axis

In-axis pixel width = Width of field of view (mm) / width of image (pixels)

An image with a field of view 167.606 mm wide, composed of 2000 pixels, would therefore have an in-plane pixel width (x axis) of 0.0838 mm. In-plane pixel width is the same in the x and y axis, so if that same sample was serially ground in increments of 0.2 mm, the sample spacing would be: x=0.0838 mm, y=0.0838 mm, and z=0.2 mm (see Fig. 4).

1. Volume visualization and polygonal surface extraction

The burrow volumes are visualized as 3D objects by the software on the basis of the greyscale iso-values of the voxels in merged 2D slices. Volume generation is calculated by the connection of voxels with the same grey intensity in each consecutive image (iso-grey-value surface; Fig. 5B). Thus obtained, the 3D volumes of the trace fossils can be artificially coloured to better visualize different elements of the trace fossil (e.g. Fig. 5A and C).

Volumetric studies of trace fossils and ichnofabrics require that the external morphology of the reconstructed burrows be "polygonized". The polygonal models of reconstructed burrows are generated from the volumetric data sets through isosurface extraction in VG Studio or VolView (Fig. 6A). Polygonal surface extraction is based on the grey-scale or opacity iso-value that is chosen to be the most accurate representation of the object being reconstructed (Fig. 6B). The polygonal mesh created is exported at 1:1 scale into the .SLT file format (Stereo Lithography 3D object) that can be opened and edited by most 3D modelling programs(e.g. Autodesk 3ds MAX).

2. 3D modeling software and polygonal mesh optimization

The mesh of the generated polygonized objects reflects the three-dimensional morphology of the modelled trace fossil, modifying the surface to account for the limitations of the rectangular character of the voxels, and the deterministic data missing from between each serial grinding increment. The generated mesh is dense, composed of millions of triangle-shaped polygons, and usually contains duplicated vertices and faces as well as isolated fragments and open holes. As a result, the exported file is usually very large and needs considerable system and graphic card memory to be opened and edited. The mesh representing the reconstructed surface must therefore be optimized, simplified and/or re-meshed to reduce the number of polygons (decimation). The surface of the polygonized trace fossil must also be smoothed to account for the unknown distribution of the trace fossil surface between the known two dimensional planes, which have been averaged in the process of creating voxels (Fig. 7).

In this study, the first stage of simplification was achieved in the volume-visualizing software prior to exporting the mesh. Further simplification and optimization can be accomplished using most 3D modelling programs (e.g. MeshLab v1.2.2 or Autodesk 3ds MAX). The resultant 3D objects were further modified by: 1) the application of artificial colours to the specified volumes of distinct transparency (representing different density or porosity within the specimen); 2) the cropping of reconstructed volumes along specified planes; 3) the isolation of discrete burrows as detached objects; and 4) the rotation and animation of objects.

Volumetric binary data obtained through digital reconstruction can be exported to many file types that maintain the 3D structure. This enables further examination using commercial freeware software, such as Right Hemisphere Deep View, GLC_Player, and Cortona3D Viewer. Exporting burrow reconstructions to widely used, interactive file formats allows for further investigation of 3D morphology by the creation of artificial cross-sections, animations, visualization of connected high porosity zones in three dimensions, and the measurement of volumes of the different burrow components. The 3D reconstructions can then be converted into formats suitable for presentation as digital documents (e.g. .PDF, .DOC or .PPT files) or as movie formats and interactive 3D files for display on the Internet (e.g. .OBJ, .STL, .WRL files; see MUN Ichnology Research Group website [http://www.ichnology.ca/] for examples).

A.3.7 Volumetrics in ichnology

Once a polygonized surface is created, it is possible to apply a volumetric approach to the three-dimensional models produced. Volume measurements can be calculated correctly for closed meshes in 3D volume-visualizing software (such as VolView). However, if the polygonal mesh has open holes, the measurement will not be performed or will be erroneous, so it is essential to ensure the object is fully enclosed (such as by using a boundary or smoothing filter in VolView, or mesh optimization in the 3D modelling software). Once the polygonal surface has been generated, a great many measurements and calculations can be carried out to characterize the reconstructed burrow or ichnofabric. The volume or surface area of the polygonized ichnological model

can be measured directly by VolView, or by using a third-party program such as Autodesk 3ds Max.

Recent studies have revived volumetric approaches in ichnology (see Platt et al. 2010; Bednarz and McIlroy, 2012). The main measurements used to characterize a single burrow or burrow associations are presented in Table A.1; distances and angles can be measured in any 3D modelling or volume-visualizing software. From a volumetric perspective, the most valuable measurements are those of surface area and volumes of the examined burrow, which are either given in metric units or as relative magnitudes in percentages.

Surface area (SA, after Platt et al. 2010) is a measurement of the polygonal surface area generated by the volume-visualizing software. It is crucial to measure the optimized polygonal mesh to avoid flawed results, such as those caused by overlapping polygons (Platt 2010).

There are two main volumes that describe any burrow or ichnofabric. These are: 1) the volume of a prism bounding the burrow or ichnofabric, or *volume available* (VA, after Platt et al. 2010); and 2) the volume of the burrow or ichnofabric itself, or *volume utilized* (VU, after Platt et al. 2010). VA is the volume of the smallest rectangular prism (width = a, height = b and length = c) that encloses the burrow or burrow association (Fig. 8):

$$(1)\quad VA = a \cdot b \cdot c$$

The volume of the entire burrow or burrow association is the VU, calculated using the 3D reconstruction, and describes the amount of the sediment reworked by the trace maker.

On the basis of these volumes, further measurements can be made. These describe and quantify the characteristics of the measured burrow or ichnofabric in relation to the main volumes (VA and VU), as follows:

Volume exploited (VE) describes burrow density and the efficiency of space usage by the trace maker, reflecting the percentage of the volume of the sediment that was reworked by the trace maker. It is calculated using the following equation (after Platt et al. 2010):

$$(2)\quad VE = {}^{VU \cdot 100}/_{VA}$$

Volume component percentage (%Vcomp) represents the volumetric contribution of a particular component (Vcomp) of the burrow or ichnofabric, where reconstructed separately (e.g. the core or halo of *Phycosiphon*). %Vcomp is calculated as a percentage of the VA:

(3) $\%Vcomp = {}^{Vcomp \cdot 100}/_{VA}$

If the length of some component of the burrow (L) is known (by measurement using the 3D modelling software), the tortuosity index (T) and burrow length index (Li) can be calculated.

The tortuosity index is the ratio between the diagonal length (d) of a rectangular prism bounding the burrow, and the total length of the burrow (L):

(4) $T = {}^{d}/_{L}$

When calculated for a burrow that does not branch or intersect itself at any point (i.e. a string, as observed in ichnotaxa such as *Phycosiphon, Helminthoida, Nereites, Spiroraphe,* and *Cosmoraphe*), the T value can illustrate the degree of burrow sinuosity and how densely packed it is in three dimensions. In cases when the burrow is branched or intersects itself, the T value indicates how densely the burrow is packed within the burrow-bounding 3D prism, but not necessarily its curvature (e.g. *Chondrites, Thalassinoides, Ophiomorpha*). T values vary between 0 and 1, with straight burrows having a T value equal one or close to one (e.g. T=0.9 for an individual phycosiphoniform burrow; Fig. 8D), and highly tortuous/densely packed burrows having a T value that approaches zero (e.g. T=0.3 for a highly tortuous burrow in Fig. 8C).

The shortest distance between the two end-points of the burrow (from the centre of the cross-section of the burrow opening to the centre of the cross-section of the burrow termination) is termed the *marginal length* (L_M). Since L_M has to be a straight line, it can only be applied to a burrow that has no branches or intersections.

The ratio between L_M and the total burrow length (L) is the *length index* (L_i):

(5) $L_i = {}^{L_M}/_{L}$

As with the T value, Li indicates a straight burrow when the value is close to one, and a tortuous (or looped) burrow when close to zero, but this cannot be assumed without considering the tortuosity index also.

Measurements of lengths and angles can be made in the 3D modelling software while examining the polygonal mesh of the models. A variety of possible measurements can be applied to different trace fossils, such as examining the branching angles of *Chondrites*, or the inclination of a burrow relative to the bedding.

A.3.8 Popularization of 3D interactive models

To enable the most comprehensive use and investigation of 3D ichnological models, it is beneficial to generate file formats that can display any polygonal mesh in an interactive 3D environment, and which can be opened with a dedicated 3D viewer installed on the user's computer system (see Table A.2 for popular 3D software). The

best formats for this are .STL, .OBJ and .WRL files. WRL files also offer the possibility of publishing the interactive reconstructions on the internet, and it is therefore the most desirable file format in terms of rapid sharing and dissemination of 3D models and data (see e.g. www.ichnology.ca). All the file formats listed above can be generated in most forms of 3D modelling software, such as Autodesk 3ds Max.

For presentation purposes, 3D models can be converted into widely used file formats, such as .PDF, .DOC or .PPT. To include and display a spatial reconstruction in one of these file formats, however, a dedicated program must be used (e.g. the freeware application DeepView).

A.4 Applications and future work

Three-dimensional reconstructions of trace fossils and ichnofabrics give ichnologists the possibility to review or determine the true morphology and geometry of any ichnological specimen. Deterministic calculations of the true volumes and surface areas of trace fossils also provide new insights of significance to reservoir studies (Bednarz and McIlroy, 2012).When evaluating ichnological impact on reservoir quality, the volumetric assessment of the trace fossils or ichnofabrics is probably the most significant factor. Depending on the characteristics of the reconstructed trace fossils, their volumetric description can help determine reservoir quality. Phycosiphoniform burrows, for example, can significantly increase the reservoir quality of mudstones in unconventional shale-gas plays; their silt-rich burrow haloes can create porous and permeable zones within otherwise impermeable host rocks (Bednarz and McIlroy, 2012). Three-dimensional visualization of such biogenic pore networks is thus highly relevant to hydrocarbon reservoir characterization. Future work on 3D reconstructions is likely to enhance the availability/accessibility of 3D models and streamline their generation to make them a widely used tool for ichnologists and petroleum geologists.

Three-dimensional reconstructions of trace fossils and other ichnologically generated sedimentary fabrics have the potential to greatly inform ichnotaxonomic studies, as well as palaeobiological and palaeoecological models accounting for the processes of burrow formation and modification. At present, with few exceptions (*Macaronichnus*: Gingras et al. 2002; phycosiphoniforms: Nifuku and Naruse 2008; Bednarz and McIlroy 2009, 2012; Boyd et al., 2012), the true morphology of many common, ichnofabric-forming trace fossils is not known. It has been shown recently that there are at least three trace fossils that produce similar "frogspawn" ichnofabrics in vertical cross–section, while having considerably different three-dimensional geometries (Bednarz and McIlroy 2009, 2012).

A.5 Conclusion

Automated, computer-controlled, serial grinding allows for highly precise abrasive removal of extremely thin, parallel portions of examined rock samples. This method creates the possibility of obtaining – through digital photography – a large number of high-resolution images showing the three-dimensional structure of

ichnological specimens. The reconstruction process necessitates the careful, and time-consuming, manual selection of burrows within these photographic images using 2D software. This precision, however, plays a vital role in the subsequent reconstruction of the trace fossils with volume-visualizing software. After the volume has been reconstructed, it is possible to produce a polygonal mesh of the trace fossil surface that can be the basis for volumetric analysis. Quantification of many burrow or ichnofabric parameters can then be calculated once the polygonal mesh is produced, including: 1) burrow dimensions; 2) the volume of sediment that the trace-maker reworked; 3) the surface area of the burrow; and 4) burrow tortuosity.

When the 3D models are exported to popular file formats, they can be made widely accessible to researchers, giving the opportunity for further analytical work. This volumetric approach to ichnology is likely to have a particularly significant impact in petroleum geology, where the characterization of trace fossils has already proven to have a major effect on the permeability and fracturability characteristics of reservoir intervals (Buatois et al. 2002; Gingras et al. 2004; Burns et al. 2005; Gordon et al. 2010; Tonkin et al. 2010; Bednarz and McIlroy 2012).

A.6 Acknowledgements

This work is supported by a NSERC, RDC and by the award of a Canada Research Chair to Duncan McIlroy. Technical support from Jennifer Dunne of the Department of Technical Services, Memorial University, who assisted through many hours of rock grinding and problem solving, is gratefully appreciated.

A.7 References

Ager, D. V. 1965. Serial grinding techniques. In Kummel, B. and Raup, D. (eds.). Handbook of Paleontological Techniques. p. 212–224. W. H. Freeman, New York.

Al-Shayeh, K. K., and Al-Ani, M. S. 2009. Efficient 3D object visualization via 2D images. International Journal of Computer Science and Network Security, no.11 9: 234–239.

Bednarz, M. and McIlroy, D., 2009, Three-dimensional reconstruction of "phycosiphoniform" burrows: implications for identification of trace fossils in core: Palaeontologia Electronica, v. 12, no. 3; 13A: 15p; http://palaeo-electronica.org/2009_3/195/index.html.

Bednarz, M. and McIlroy, D. 2012. Effect of phycosiphoniform burrows on shale gas reservoir quality. AAPG Bulletin. 96, 1957-1980.

Boyd, C., McIlroy, D., Herringshaw, L., and Leaman, M., 2012. The recognition of *Ophiomorpha irregulaire* on the basis of pellet morphology: restudy of material from the type locality. Ichnos. 19, 185-189.

Bromley, R.G. 1981. Concepts in ichnotaxonomy illustrated by small round holes in shells. Acta Geologica Hispanica, 16: 55–64.

Buatois, L.A., Mángano, M.G., Alissa, A., and Carr, T.R. 2002. Sequence stratigraphic and sedimentologic significance of biogenic structures from a late Paleozoic reservoir, Morrow Sandstone, subsurface of southwest Kansas, USA. Sedimentary Geology, 152: 99–132.

Burns, F.E., Burley, S.D., Gawthorpe, R.L., and Pollard, J.E. 2005. Diagenetic signatures of stratal surfaces in the Upper Jurassic Fulmar Formation, central North Sea, UKCS. Sedimentology, 52: 1155–1185.

Dufour, S. C., Desrosiers, G., Long, B., Lajeunesse, P., Gagnoud, M., Labrie, J., Archambault, P., and Stora, G. 2005. A new method for three-dimensional visualisation and quantification of biogenic structures in aquatic sediments using axial tomodensitometry. Limnology and Oceanography: Methods, 3: 372–380.

Gingras, M. K., Macmillan, B., Balcom,B. J., Saunders, T., and Pemberton, S. G. 2002. Using Magnetic Resonance Imaging and petrographic techniques to understand the textural attributes and porosity distribution in Macaronichnus-burrowed sandstone. Journal of Sedimentary Research, no. 4 72: 552–558.

Gingras, M. K., Mendoza, C. A., and Pemberton, S. G. 2004. Fossilized worm burrows influence the resource quality of porous media. AAPG Bulletin, no. 7 88: 875-883.

Gordon, J.B., Pemberton, S.G., Gingras, M.K., and Kornhauser, K.O. 2010. Biogenetically enhanced permeability: A petrographic analysis of Macaronichnus segregatus in the Lower Cretaceous Bluesky Formation, Alberta, Canada. AAPG Bulletin, 94: 1779–1795

Herringshaw, L.G., Sherwood, O.A., and McIlroy, D. 2010. Ecosystem engineering by bioturbating polychaetes in event bed microcosms. Palaios, 25: 46–58.

Maloof, A. C., Rose, C. V., Beach, R., Samuels, B. M., Calmet, C. C., Erwin, D. H., Poirier, G. R., Yao, N., and Simons, F. J. 2010. Possible animal-body fossils in pre-Marinoan limestones from South Australia. Nature Geoscience, 3: 653–659.

Naruse, H., and Nifuku, K., 2008, Three-dimensional morphology of the ichnofossil Phycosiphon incertum and its implication for paleoslope inclination. Palaios, no. 5 23: 270–279.

Platt, B. F., Hasiotis, S. T., and Hirmas, D. R. 2010. Use of low-cost multistripe laser triangulation (MLT) scanning technology for three-dimensional, quantitative paleoichnological and neoichnological studies. Journal of Sedimentary Research, no. 7 80 : 590–610.

Rahman, I.A. and Zamora, S. 2009. The oldest cinctan carpoid (stem-group Echinodermata), and the evolution of the water vascular system. Zoological Journal of the Linnean Society, 157: 420–432.

Sollas, W. J. 1903. A method for the investigation of fossils by serial sections. Proceedings of the Royal Society of London, 72: 98.

Stensiø E. A. 1927. The Downtonian and Devonian vertebrates of Spitzbergen. Skrift, Svalbard Nordishavet. 12: 1–31.

Sutton, M. D., Siveter, David J., Briggs, D. E. G., and Siveter, Derek J. 2001a. Methodologies for the visualization and reconstruction of three-dimensional fossils from the Silurian Herefordshire Lagerstätte. Palaeontologia Electronica, no. 1 4: 17.

Sutton, M. D., Briggs, D. E. G., Siveter, David J., and Siveter, Derek J. 2001b. An exceptionally preserved vermiform mollusc from the Silurian of England. Nature, 410: 461–463.

Sutton, M. D., Briggs, D. E. G., Siveter, David J., Siveter, Derek J. 2005. Silurian brachiopods with soft-tissue preservation. Nature, 436: 1013–1015.

Sutton,M. D., Briggs, D. E. G., Siveter, David J., and Siveter, Derek J. 2006. Fossilized soft tissues in a Silurian platyceratid gastropod. Proceedings of the Royal Society B, 273: 1039–1044.

Tonkin, N.S., McIlroy, D., Meyer,R., and Moore-Turpin, A. 2010. Bioturbation influence on reservoir quality; a case study from the Cretaceous Ben Nevis Formation, Jeanne d'Arc Basin, offshore Newfoundland, Canada. AAPG Bulletin, no. 7 94: 1059–1078.

Watters, W. A. and Grotzinger, J. P. 2001. Digital reconstruction of calcified early metazoans, terminal Proterozoic Nama Group, Namibia. Paleobiology, 27: 159–171.

Wetzel, A. and Uchman, A. 1998. Deep-sea benthic food content recorded by ichnofabrics: A conceptual model based on observations from Paleogene flysch, Carpathians, Poland. Palaios, no. 6 13: 533–546.

Wetzel, A. and Uchman, A. 2001. Sequential colonization of muddy turbidites in the Eocene Beloveza Formation, Carpathians, Poland. Palaeogeography, Palaeoclimatology, Palaeoecology, no. 1-2 168: 171–186.

A.8 Figures

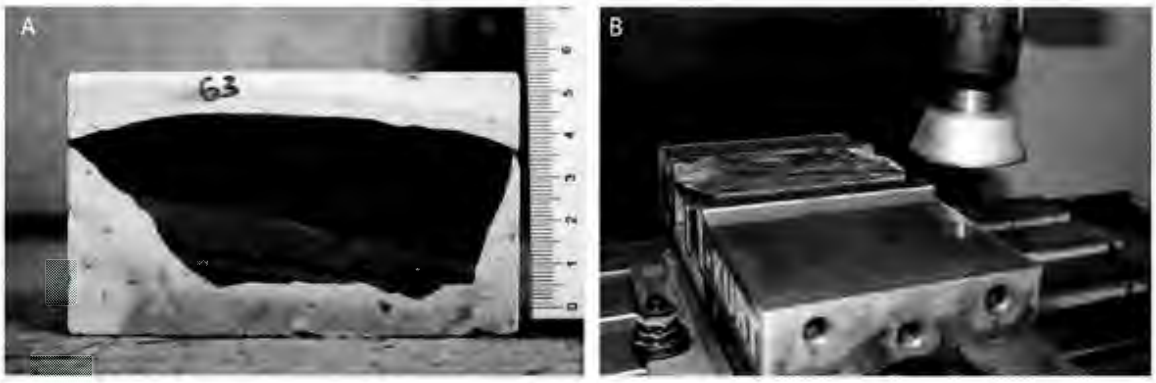

Figure 1: Set-up and procedure for precise, computer-controlled, serial grinding of ichnological samples. A. Freshly exposed surface of sample embedded in plaster of Paris, ready for photography. B. HAAS VF-3 CNC Vertical Machining Center, showing diamond-tipped rotating blade with sample clamped in place prior to grinding.

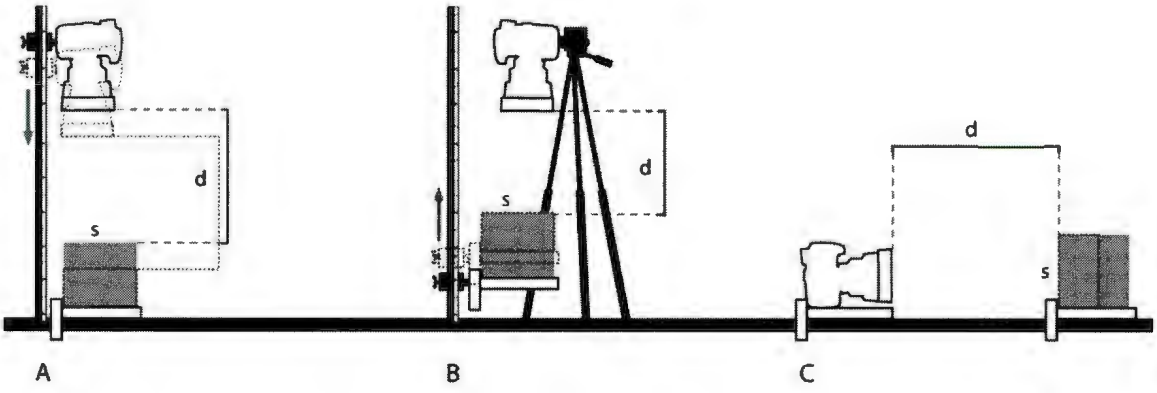

Figure 2: Photographic procedures for maintenance of consistent distance between camera objective (d) and freshly exposed sample surface (s). A. Camera attached to photographic stand with height-controlling screw feed; cuboid sample in fixed position. After each serial grinding run, camera height adjusted (moved down) by same distance as serial grinding interval. B. Cuboid sample located on shelf attached to stand with height-controlling screw feed, camera mounted on tripod. After each serial grinding run, position of shelf with sample adjusted (moved up) by same distance as serial grinding interval. C. Camera positioned or mounted on table in specified place; cuboid sample positioned on table facing camera objective. After each serial grinding run, distance between camera objective and freshly ground sample surface adjusted parallel to line drawn on table or mount.

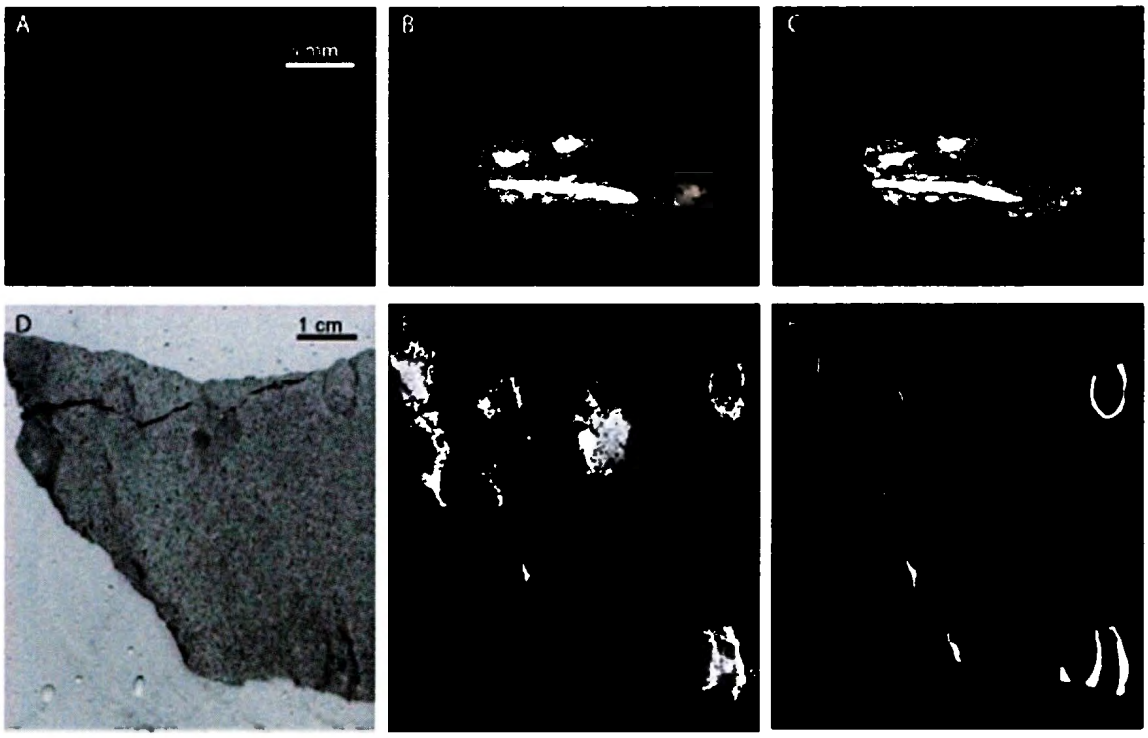

Figure 3: Selection of features in two samples of serially ground trace fossil: phycosiphoniform burrows (A, B, C; composed of two elements: core and halo) and Ophiomorpha burrows (D, E, F). Phycosiphoniform burrow core shown in white in images B and C; burrow halo in grey. A, D. Images showing polished surface of ichnological samples, prior to burrow selection. A, black shapes represent burrow cores surrounded by haloes of lighter-coloured material in low contrast to matrix material. D, dark grey areas represent muddy lining/fill of Ophiomorpha burrows. B, E. Shapes of burrows obtained using Magic Wand selection tool. Pixelization of burrows visible, resulting from imprecise nature of tool. C, F. Burrow shapes obtained using Magnetic Lasso and Brush tools. Smooth outlines represent real burrow margins and are most suitable for subsequent interpretation by 3D rendering software.

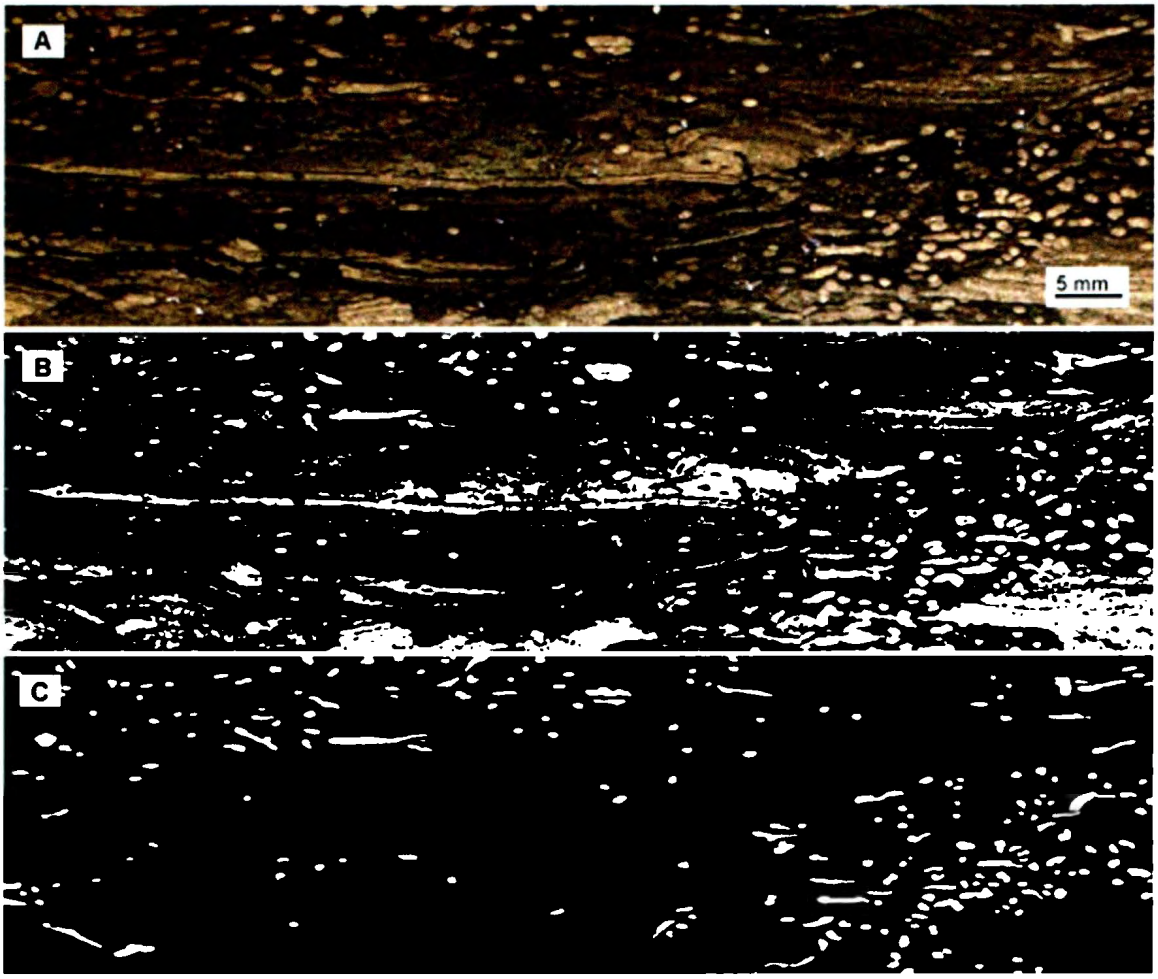

Figure 4: Illustration of differences between images obtained via application of fast, automatic software (native filters) and via time-consuming manual selection. A. Original photograph of polished surface of sample bioturbated with *Chondrites*. B. Image resulting from application of filters (e.g. level histogram) offered in 2D graphic programs to obtain grey-scaled illustration of ichnofabric. Fast method results in generation of noisy and imprecise delineation of burrow shapes, plus all accompanying structures composed of same material as burrows. C. Image obtained using manual, time-consuming methods of burrow selection (see text for details), reflecting *Chondrites* ichnofabric much more precisely.

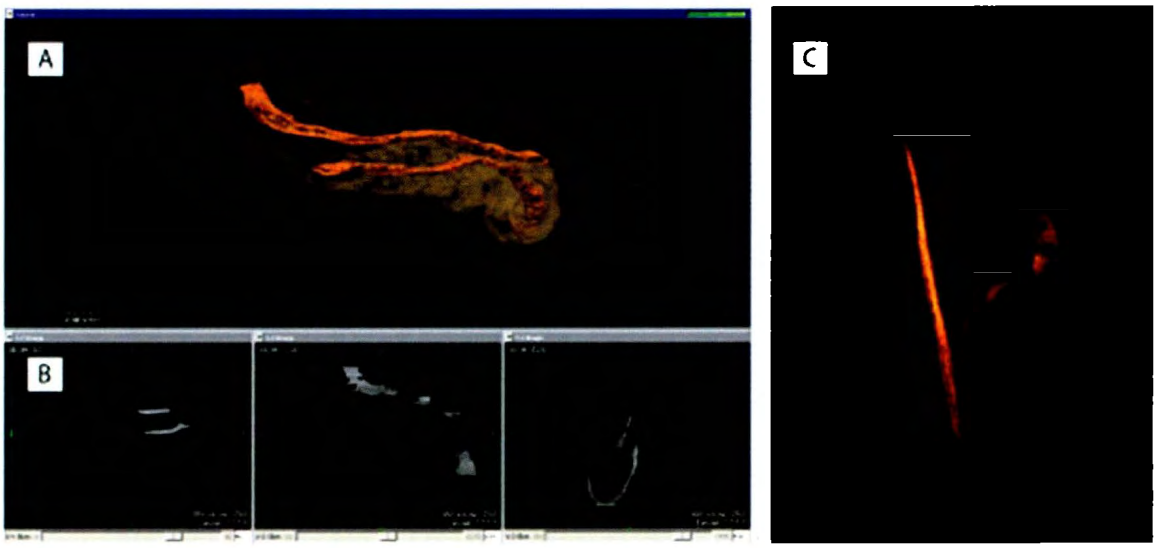

Figure 5: Application of artificial colors for visual enhancement of burrow structures. A. Reconstruction of phycosiphoniform burrow in 3D: core shown in orange; halo in grey; B. Series of 2D slices showing phycosiphoniform burrow elements (core and halo) in greys of dual intensity (iso-grey-values); screenshot of reconstructed specimens from Rosario Formation, Mexico, generated in VolView software. C. Reconstruction of *Ophiomorpha* from Blackhawk Formation, Utah; screenshot generated in VG Studio.

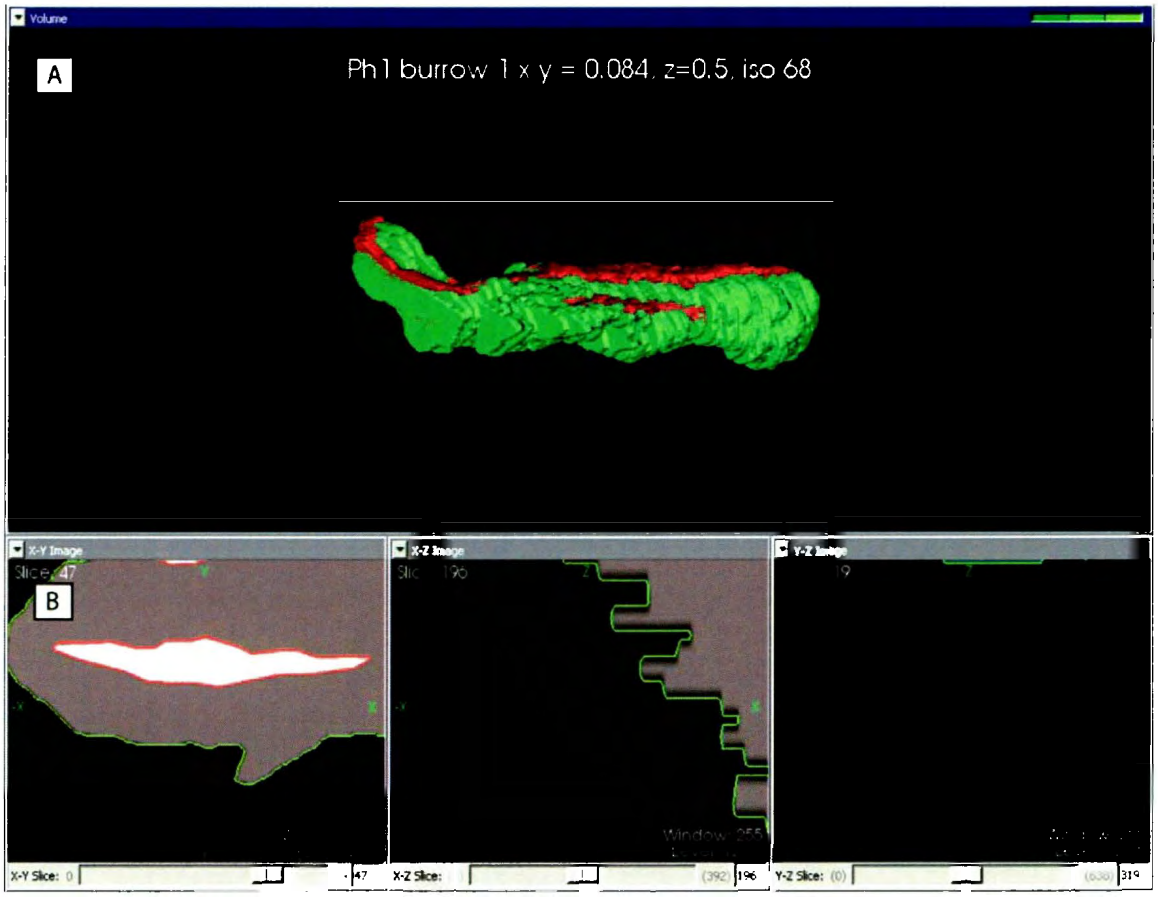

Figure 6: Polygonal surface extraction of reconstructed phycosiphoniform burrow from Rosario Formation, Mexico, based on grey isovalues; screenshots generated in VolView software. A. Resultant polygonal surface showing core (red) and halo (green); B. Surface component lines applied to iso-grey-values of distinct burrow elements (core and halo) in each of 2D slices.

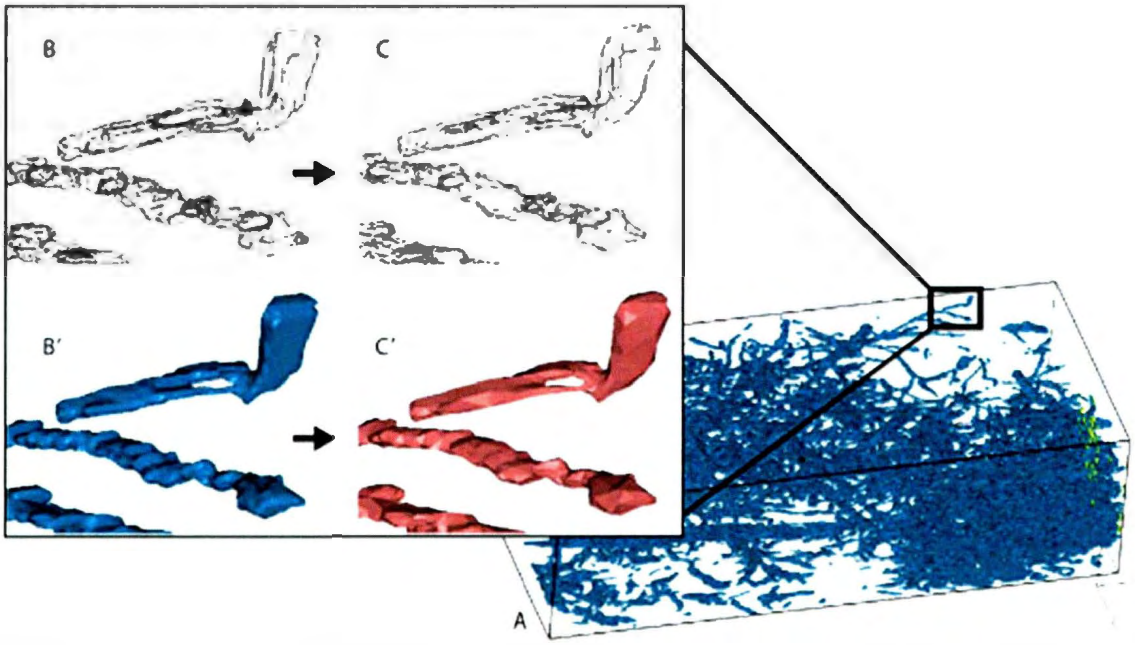

Figure 7: Mesh simplification of reconstructed trace fossils. A. Polygonized 3D model of *Chondrites* ichnofabric. Mesh was exported as .STL file from VolView software and was 314 MB in non-simplified mesh format. B, B'. Zoomed-in selection of non-simplified polygonized mesh; C, C' Zoomed-in selection of simplified polygonized mesh (decimated, optimized, smoothed). Resultant simplified mesh file size reduced to 68 MB.

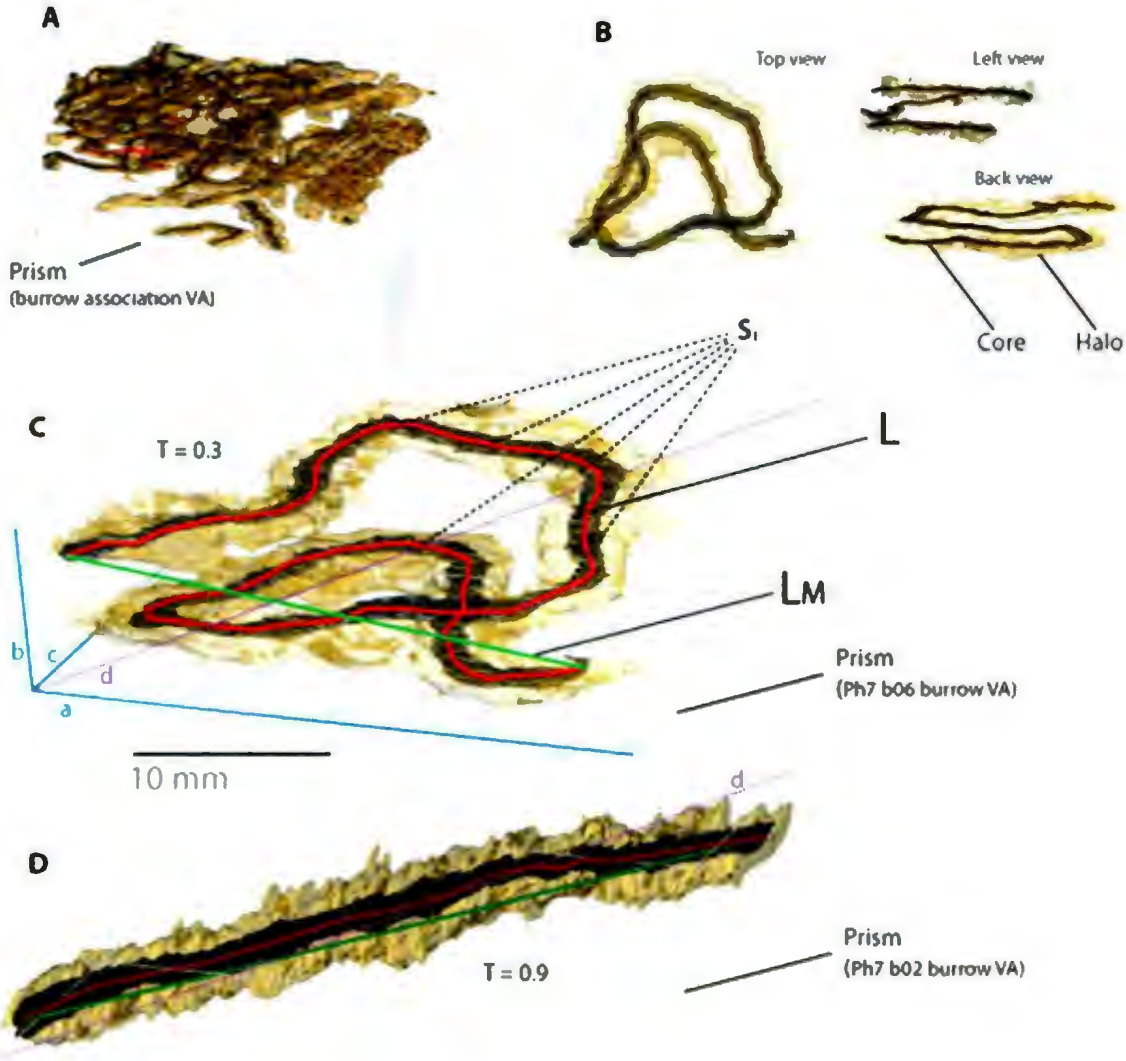

Figure 8: 3D model of reconstructed ichnofabric composed of phycosiphoniform burrows (Lower Carboniferous Yoredale Sandstone Formation, Northumberland, UK). A. Reconstruction of burrow network; B. Individual burrow (Ph7 b06) isolated from reconstructed burrow network, shown in top, lateral, and back views; C. Reconstruction of burrow Ph7 b06, showing tortuosity value (T) = 0.3; D. Reconstruction of burrow Ph7 b02 from same sample network, showing tortuosity value (T) = 0.9. Symbols: VA – Volume Available; Si – straight elements composing core length line; L – core length ; LM – marginal length; T – Tortuosity index; a, b, c – prism dimensions; d –diagonal space within prism.

Table A.1: Measurement terms used in characterizing spatial models of individual burrows or ichnofabric.

Abbreviation	Full name	Equation
VA	Volume available (the prism bounding the burrow/s)	$VA = a \cdot b \cdot c$ Measured by 3D software
d	Space diagonal (of the prism)	$d = \sqrt{a^2 + b^2 + c^2}$
VU	Volume utilized	Measured by 3D software
VE	Volume exploited	$VE = {}^{VU \cdot 100}/_{VA}$
Vcomp	Component volume	Measured by 3D software
%Vcomp	% Component volume	$\%Vcomp = {}^{Vcomp \cdot 100}/_{VA}$
SA	Surface Area	Measured by 3D software
L	Core length	$L = \sum_{i=n}^{s} = s_1 + s_2 + s_3 + \ldots + s_n$ Measured by 3D software
T	Tortuosity index	$T = {}^{d}/_{L}$
L_M	Marginal length	Measured by 3D software
Li	Burrow length index	$L_i = {}^{L_M}/_{L}$

Table A.2: List of chosen 3D software used for visualizing, modeling and viewing 3D models.

Software	Type	Website	License
VGStudio Max	3D volume visualizing (reconstruction)	www.volumegraphics.com	commercial
VolView	3D volume visualizing (reconstruction)	www.kitware.com	commercial
Autodesk 3ds Max	3D modeling software	www.autodesk.com	commercial
MeshLab	3D modeling software	meshlab.sourceforge.net	freeware
DeepView	3D viewer	www.righthemisphere.com	freeware
GLC_Player	3D viewer	www.glc-player.net	freeware
Cortona3D Viewer	3D viewer	www.cortona3d.com	freeware

Appendix B – The recognition of *Ophiomorpha irregulaire* on the basis of pellet morphology: restudy of material from the type locality

The recognition of *Ophiomorpha irregulaire* on the basis of pellet morphology: restudy of material from the type locality

Christopher Boyd[a], Duncan McIlroy[a], Liam G. Herringshaw[b], and Mary Leaman[a].

[a] Memorial University of Newfoundland, Department of Earth Sciences, 300 Prince Philip Drive, St. John's, Newfoundland,A1B 3X5, Canada
[b] Durham University, Department of Earth Sciences, Durham, DH1 3LE, UK.

KEYWORDS

Ophiomorpha irregulaire; Serial grinding; three dimensional; reconstruction; ichnology; pellet morphology; Spring Canyon Member, Utah

Recognition of *O. irregulaire*

Corresponding author: Christopher Boyd, Memorial University of Newfoundland, Department of Earth Sciences, 300 Prince Philip Drive, St. John's, Newfoundland, A1B 3X5, Canada, c.boyd@mun.ca; 709 864 6762; 709 864-7437 (fax)

B.1 Abstract

Serial grinding of a specimen of *Ophiomorpha irregulaire* collected from Coal Creek Canyon in the Book Cliffs of Utah, USA—the type locality of the ichnospecies—allows us to assess the validity of pellet morphology as an ichnotaxobase for species-level identification. The importance of *O. irregulaire* stems from its abundance in petroliferous shallow marine strata of post-Paleozoic age. Our three-dimensional reconstruction of the burrow wall of *O. irregulaire* demonstrates for the first time that it is composed of sand-cored pellets. The typically spiky nature of the pellets in cross-section is inferred to result from differential compaction of the sand core and pelletal lining. Rupturing of the thin outer clay coating of the sand pellets is considered to produce the distinctively attenuated, spiky outer surface to the burrow wall of this ichnospecies. This study demonstrates the utility of pellet morphology in species-level classification of *Ophiomorpha,* and lends support to *O. irregulaire* being a cosmopolitan ichnospecies present in post-Paleozoic strata. It demonstrates also the need to ensure that ichnotaxonomic identifications are based on three-dimensional knowledge of the trace fossil in question.

B.2 Introduction

Recently published studies of *Ophiomorpha irregulaire* have highlighted the need for thoughtful and cautious use of ichnospecific names for trace fossils seen in core (Bromley and Pedersen, 2008; McIlroy et al., 2009). From the time of its original description (Howard, 1966; Frey et al., 1978; Bromley and Ekdale, 1998), the criteria primarily used for identification of *O. irregulaire* have been the presence of a meander maze (when studied in the field), and a spiky outer surface to the burrow wall (both in the field and in core-based material). With the increased recognition of the importance of trace fossils to paleoenvironmental analysis, ichnospecies of *Ophiomorpha—especially O. nodosa* and *O. irregulaire*—have been routinely identified in core based on their pelletal-wall morphology (McIlroy, 2004a; Bromley and Pedersen, 2008; McIlroy et al., 2009).

One of the most distinctive species of *Ophiomorpha, O. irregulaire,* has recently been the focus of some contention regarding the relative importance of its ichnotaxobases. The first description of this taxon was as "horizontal trails" from the Panther Sandstone Tongue of the Star Point Formation, in the Book Cliffs of Utah (Howard, 1966). *Ophiomorpha irregulaire* was subsequently described formally from the Star Point and Blackhawk formations (Frey et al., 1978; Bromley and Ekdale, 1998), with Bromley and Ekdale (1998) designating Unit 19 of the Spring Canyon Member (Blackhawk Formation) at Coal Creek Canyon, Carbon County, Utah, to be the type locality. The ichnotaxobases used in the ichnospecific diagnosis of *O. irregulaire* were:

1) The gross form of the bedding-parallel galleries being a meander maze;
2) Galleries commonly having lined roofs and unlined floors;
3) Vertical shafts being rare;
4) The mud-rich wall pellets being sparse and irregularly distributed;

5) Pellets in the wall-lining being variously ovoid to mastoid, sometimes in the form of pelletal masses.

One of the most commonly used distinguishing features of *O. irregulaire* is that the pellets and pelletal masses are "drawn-out like flame structures" (Pedersen and Bromley, 2006, p. 964). These flame-like projections of clay-grade material are most abundant along the sides of *O. irregulaire* burrows, and it has been hypothesized that they may result from compression of originally much less elongated clay-rich pellets (Frey et al., 1978; Bromley and Ekdale, 1998). The distinctive morphology and distribution of the pellets has enabled ichnospecific identification of *O. irregulaire* in the vertically cut surfaces of core-based material. In subsequent years, the ichnospecies has been recognised from Mesozoic and younger strata from around the world, particularly in core from petroliferous strata (Martin and Pollard, 1996; MacEachern and Hobbs, 2004; McIlroy, 2004b). *O. irregulaire* has become an important paleoenvironmental indicator owing to it having only been recorded from marine palaeoenvironments.

The three-dimensional nature of *Ophiomorpha irregulaire* is not fully understood, however, and has led to recent contention regarding its identification. This was stimulated by Bromley and Pedersen (2008), who considered ichnospecific diagnosis based exclusively upon pellet morphology to be insufficient. They asserted that many previous studies that relied upon pellet morphology as a species-diagnostic tool were erroneous (specifically core-based studies of *Ophiomorpha;* e.g. McIlroy, 2004a; MacEachern and Gingras, 2007), and that true examples of *O. irregulaire* occurred solely in the Cretaceous Western Interior Seaway (Bromley and Pedersen, 2008). A published response (McIlroy et al., 2009) highlighted the need to collect material from the type locality, with which the pellet morphology could be characterized. It is noteworthy that the only published image of a type specimen is a line drawing of the neotype (cf. Bromley and Ekdale, 1998, fig. 3.4), and that pellet morphology in vertically cut faces was not a component of the ichnospecific diagnosis (Howard, 1966; Frey and Howard, 1970, 1982, 1990; Frey et al., 1978; Bromley and Ekdale, 1998; Bromley and Pedersen, 2008; McIlroy et al., 2009).

To characterize the pellet morphology of *Ophiomorpha irregulaire* and to enable comparison with material identified as *O. irregulaire* in core, specimens were collected in 2009 from the type locality, and investigated using the serial grinding methodology of Bednarz and McIlroy (2009). Emphasis was placed on the reconstruction of pellet morphology, since other ichnotaxobases, such as the presence of a meander-maze (Howard, 1966; Frey and Howard, 1970, 1982, 1990; Frey et al., 1978; Bromley and Ekdale, 1998; Bromley and Pedersen, 2008) are difficult to assess in core (but see McIlroy et al., 2009).

B.3 Method

The methodology used in this study followed the methods discussed by Bednarz and McIlroy (2009). The samples were encased in plaster and using a computer-guided milling machine, serially ground in increments of 0.305 mm. Each successively ground surface was labelled and photographed under identical conditions. The resulting images

were imported into Adobe Photoshop, stacked and aligned. Areas of interest, (burrows, specific pellets, etc.), were then selected and exported as monochromatic images over a white background. These images were imported into VG Studio MAX 1.2.1 and modelled with voxel dimensions of x/y = 0.041167 mm and z = 0.0305 mm. Various image-enhancing filters were used to better view the specimen.

B.4 Results

Compiling the 200 serially ground surfaces cut through *Ophiomorpha irregulaire* into a single, three-dimensional model allows detailed analysis of the structure of the burrow wall. When visualized using an opaque outermost layer, the external morphology of *O. irregulaire* is shown to be a somewhat irregular surface without systematic variability. By rotation of the reconstruction in 3D space, the flame-like projections that have been used to characterize the ichnospecies previously can be visualized fully (Figs. 1A-D). This demonstrates that the extension of the pellets into laterally attenuated, flame-like projections is indeed a feature of *O. irregulaire* from its type locality (Figs. 2A and B).

The distribution of pellets within the roof of *O. irregulaire* from the type locality was discussed by McIlroy et al. (2009), who suggested that their apparently irregular distribution might have resulted from partial erosion. Field photographs from the type locality (Bromley and Ekdale, 1998) appear to show erosion of the upper surface to the centre of the horizontal galleries. The completeness of the type material is therefore questionable. The 3.66 cm (grinding depth) of *O. irregulaire* studied in the course of this work show complete pelletal lining of the burrow roof (Figs. 1A-D). While this is not conclusive, in all cases where the pelletal lining was absent, there was found to be demonstrable modern erosion cutting into the burrow fill, with the upper parts of the burrow having been eroded away. Additionally, our field investigations at the type locality did not reveal any *Thalassinoides-like,* pellet-free, burrow morphologies.

With the 3D reconstructions it is possible to make modelled components (in this case, the mudstone in the burrow lining) semi-transparent using the sum-along-ray feature of VG Studio Max, which creates images comparable to X-radiographs. This enables the investigation of the internal structure of the trace fossil. In doing so, it is evident that some pellets of the burrow wall of *O. irregulaire* (cf. Frey et al., 1978; Fig. 3A) are formed of sand-grade material that is encased by a clay-grade rind. The outer surface view of the pelleted burrow roof shows the typical mastoid morphology of *O. irregulaire* pellets. Cross-sections of the pellets on the roof of the specimen were created by digitally transecting the pellets. These cross-sections reveal the presence of flame-like projections of clay grade material (Figs. 3B and C). While these spiky projections have been the primary feature used to recognise *O. irregulaire* in vertical cross section, it is apparent that the clay-rich, tapering projections encase sand-pellets, and are not themselves pellets (Fig. 4). The projections are wider at their base, where they amalgamate to produce a continuous internal lining to the burrow (Fig. 4). The distal thinning of the clay lining to the pellets is such that they are thinnest at the point where they encapsulate the outer margin of the sand-pellet (Fig. 4). Sand-grade material has

been previously noted by one of us (DMc) in earlier studies (Fig. 5), though it was considered at the time to be a novelty rather than the norm. That *O. irregulaire* pellets are often cored with sand-grade material is completely unexpected. With this model in mind, it is clear that sand-filled pellets have been inadvertently figured several times (e.g. MacEachern et al., 1992, fig. 14F; Pemberton et al., 1992a, fig. 16D; Pemberton et al., 1992b, fig. 17D; Raychaudhuri et al., 1992, fig. 7H; MacEachern et al., 2007a, figs. 7C and 8C; MacEachern et al., 2007b, fig. 6F; McIlroy et al., 2009, fig. 2F). In the burrow roof, pellets tend to maintain their original sand-filled morphology (Fig. 3A). However, perhaps due to differential compaction of the relatively uncompressible sand-fill as opposed to the highly compressible clay-rich coating, the morphology of the pellet lining is likely to be compromised upon burial. We consider that burial compaction of the sand-filled pellets produces the characteristic, extended flame-like structures (Fig. 6) described by many authors. In core material cross-sections, many ichnospecies-level identifications of *Ophiomorpha irregulaire* are based upon this distinctive morphological feature (Raychaudhuri and Pemberton, 1992; MacEachern and Pemberton, 1994; McIlroy, 2004a; MacEachern and Gingras, 2007).

B.5 Conclusion

Re-examination of material from its type locality, employing a serial grinding method to make three-dimensional reconstructions of the burrow-wall, provides a more complete understanding of the burrow morphology of *Ophiomorpha irregulaire.* Discoveries arising from of our reconstructions are:

1) Pellets on the burrow roof are ovoid to mastoid and sand-filled.

2) The flame-like spiky projections from the outer burrow wall are the burrow-proximal portion of an outer clay-rich pellet lining.

One of the objections to using the flame-like projections as an ichnotaxobase has been that they could result from purely mechanical compression during burial, rather than representing a primary burrow feature (Pedersen and Bromley, 2008). Our work suggests that the characteristic flame-like projections result from differential compaction of clay-grade material around the sand core of a pellet. Since the flame-like features derive from a primary morphological characteristic of the burrow wall, we are confident in assigning taxonomic importance to them. No other *Ophiomorpha* ichnospecies is known to have pellets with sandy centres; as such, we consider that recognition of *O. irregulaire* on the basis of pellet morphology is valid and relevant. Re- examination of the photographic record of reports of *O. irregulaire* (e.g. McIlroy, 2004a; MacEachern and Gingras, 2007; and many others) allows us to confirm that the taxon occurs in non-Cretaceous rocks from beyond the Western Interior Seaway. It was not an endemic, short-lived ichnospecies (contra Bromley and Pedersen, 2008), and its value as one of the most easily recognised and paleoenvironmentally useful ichnospecies is reaffirmed (cf. McIlroy et al., 2009).

Ophiomorpha irregulaire is perhaps the most distinctive ichnospecies within the genus. Study of material from the type locality was necessary to augment the ichnospecific diagnosis with an understanding of pellet morphology. This approach of

three-dimensional reconstruction has the potential to bridge the gap in understanding of trace fossil morphology between classical studies of full relief material, and the study of trace fossils in core, which is becoming an increasingly important aspect of both ichnology and sedimentology (McIlroy, 2004a, b, 2008; Bednarz and McIlroy, 2009).

While many trace fossils are routinely identified to ichnospecific level from 2D cross sections in core, it is seldom possible to recognise all the requisite ichnotaxobases. Degrees of uncertainty are common when studying paleontological materials; this is particularly common in ichnological studies, and even more so when studying core or slabbed material. In most cases, open nomenclature is preferable to emphasise the degree of uncertainty inherent in inferring the morphology of a three-dimensional structure from a two-dimensional cross-section. Few ichnotaxa are sufficiently distinctive that they can be reliably identified to ichnospecific level in core material. We consider that species of *Ophiomorpha,* particularly *O. irregulaire,* are an exception to this rule. The potential of using 3D pellet morphology to characterize fully the other ichnospecies of *Ophiomorpha* (O. *annulata, O. borneensis O. nodosa, O. puerilis,* and *O. rudis)* is therefore great, and such investigations should be undertaken.

B.6 Acknowledgements

This work was supported by an NSERC Discovery Grant, and an NSERC/PRAC CRD grant to D. McIlroy. Małgorzata Bednarz is thanked for her field assistance and technical advice.

B.7 References

Bednarz, M. and McIlroy, D. 2009. Three-dimensional reconstruction of "phycosiphoniform" burrows: Implications for identification of trace fossils in core. *Palaeontologica Electronica,* 12: 15pp.

Bromley, R.G. and Ekdale, A.A. 1998. *Ophiomorpha irregulaire* (Trace Fossil): Redescription from the Cretaceous of the Book Cliffs and Wasatch Plateau, Utah. *Journal of Paleontology,* 72: 773-778.

Bromley, R.G. and Pedersen, G.K. 2008. *Ophiomorpha irregulaire,* Mesozoic trace fossil that is either well understood but rare in outcrop or poorly understood but common in core. *Palaeogeography, Palaeoclimatology, Palaeoecology,* 270: 295-298.

Frey, R.W. and Howard, J.D. 1970. Comparison of Upper Cretaceous ichnofaunas from siliceous sandstones and chalk, Western Interior Region, U.S.A. *Geological Journal Special Issues,* 3: 141-166.

Frey, R.W. and Howard, J.D. 1982. Trace fossils from the Upper Cretaceous of the Western Interior: Potential criteria for facies models. *The Mountain Geologist,* 19: 1-10.

Frey, R.W. and Howard, J.D. 1990. Trace Fossils and Depositional Sequences in a Clastic Shelf Setting, Upper Cretaceous of Utah. *Journal of Paleontology,* 64: 803-820.

Frey, R.W., Howard, J.D., and Pryor, W.A. 1978. *Ophiomorpha:* Its morphologic, taxonomic, and environmental significance. *Palaeogeography, Palaeoclimatology, Palaeoecology,* 23: 199-229.

Howard, J.D. 1966. Characteristic trace fossils in Upper Cretaceous sandstones of the Book Cliffs and Wasach Plateau: *Utah Geological and Mineralogical Survey Bulletin,* 8: 35- 53.

MacEachern, J.A. and Gingras, M.K. 2007. Recognition of brackish-water trace fossil suites in the Cretaceous Western Interior Seaway of Alberta. *In* Bromley, R.G., Buatois, L.A., Mángano, M.G., Genise, J.F., Melchor, R.N. (eds.), Sediment-Organism Interactions: A Multifaceted Ichnology: *Society of Economic Paleontologists and Mineralogists, Special Publication,* 88: 149-193.

MacEachern, J.A. and Hobbs, T.W. 2004. The ichnological expression of marine and marginal marine conglomerates and conglomeratic intervals, Cretaceous Western Interior Seaway, Alberta and northeastern British Colombia. *In* Moslow, T. and Zonneveld, J.-P. (eds.), Marine Conglomerates: *Bulletin of Canadian Society of Petroleum Geology,* 52: 77-104.

MacEachern J.A. and Pemberton, S.G.1994. Ichnological aspects of incised valley fill systems from the Viking Formation of the Western Canada Sedimentary Basin, Alberta, Canada, *In* Boyd, R. Dalrymple, R. and Zaitlin, B. (eds.), Incised valley systems: origin and sedimentary sequences: *Society of Economic Paleontologists and Mineralogists, Special Publication* 51, p. 129-157.

MacEachern, J.A., Pemberton, S.G., Bann, K.L., and Gingras, M.K. 2007a. Departures from the archetypal ichnofacies: effective recognition of environmental stress in

the rock record. *In* MacEachern, J.A., Bann, K.L., Gingras, M.K. and Pemberton, S.G. (eds.), Applied Ichnology: *Society of Economic Paleontologists and Mineralogists, Short Course Notes,* 52: 65-93.

MacEachern, J.A., Bann, K.L., Pemberton, S.G., and Gingras, M.K. 2007b. The ichnofacies paradigm: high resolution paleoenvironmental interpretation of the rock record. *In* MacEachern, J.A., Bann, K.L., Gingras, M.K. and Pemberton, S.G. (eds.), Applied Ichnology: *Society of Economic Paleontologists and Mineralogists, Short Course Notes,* 52: 27-65.

MacEachern, J.A., Raychaudhuri, I., and Pemberton, S.G. 1992. Stratigraphic applications of the Glossifungites Ichnofacies: Delineating discontinuities in the rock record. *In* Pemberton, S.G. (ed.), Applications of Ichnology to Petroleum Exploration: A Core Workshop: *Society of Economic Paleontologists and Mineralogists, Core Workshop,* 17: 169-198.

Martin, M.A. and Pollard, J.E. 1996. The role of trace fossil (ichnofabric) analysis in the development of depositional models for the Upper Jurassic Fulmar Formation of the Kittiwake Field (Quadrant 21 UKCS). *In* Hurst, A. (ed.), Geology of the Humber Group: Central Graben and Moray Firth UKCS. *Geological Society, London, Special Publications,* 114: 163-183.

McIlroy, D. 2004a. Ichnofabrics and sedimentary facies of a tide-dominated delta: Jurassic Ile Formation of Kristin Field, Haltenbanken, Offshore Mid-Norway. *In* McIlroy, D. (ed.), The Application of Ichnology to Palaeoenvironmental and Stratigraphic Analysis: *Geological Society, London, Special Publications,* 228: 237-272.

McIlroy, D. 2004b. Some ichnological concepts, methodologies, applications and frontiers. *In* McIlroy, D. (ed.), The Application of Ichnology to Palaeoenvironmental and Stratigraphic Analysis: *Geological Society, London, Special Publications,* 228: 3-29.

McIlroy, D. 2008. Ichnological analysis: The common ground between ichnofacies workers and ichnofabric analysts: *Palaeogeography, Palaeoclimatology, Palaeoecology,* 270: 332- 338.

McIlroy, D., Tonkin, N.S., Phillips, C., and Herringshaw, L.G. 2009. Comment on "Ophiomorpha *irregulaire,* Mesozoic trace fossil that is either well understood but rare in outcrop or poorly understood but common in core" by R.G. Bromley and G.K. Pedersen: [Palaeogeography, *Palaeoclimatology, Palaeoecology* 270 (2008) 295-298]: *Palaeogeography, Palaeoclimatology, Palaeoecology,* 284: 392-395.

Pedersen, G.K. and Bromley, R.G. 2006. *Ophiomorpha irregulaire,* rare trace fossil in shallow marine sandstones, Cretaceous Atane Formation, West Greenland. *Cretaceous Research,* 27: 964-972.

Pemberton, S.G., Reinson, G.E., and MacEachern, J.A. 1992a. Comparative ichnological Analysis of Late Albian estuarine valley-fill and shelf-shoreface deposits, Crystal Viking, Field, Alberta. *In* Pemberton, S.G. (ed.), Applications of Ichnology to Petroleum Exploration: A Core Workshop: Society of Economic Paleontologists and Mineralogists, Core Workshop, 17: 291-318.

Pemberton, S.G., Van Wagner, J.C., and Wach, G.D. 1992b. Ichnofacies of a wave-dominated shoreline. *In* Pemberton, S.G. (ed.), Applications of Ichnology to Petroleum Exploration: A Core Workshop: *Society of Economic Paleontologists and Mineralogists, Core Workshop,* 17: 339-382.

Raychaudhuri, I. and Pemberton, S.G. 1992. Ichnologic and sedimentologic characteristics of open marine to storm dominated restricted marine settings within the Viking/Bow Island Formations, South-Central, Alberta. *In* Pemberton, S.G. (ed.), Applications of Ichnology to Petroleum Exploration: A Core Workshop: *Society of Economic Paleontologists and Mineralogists, Core Workshop,* 17: 119-139.

B.8 Figures

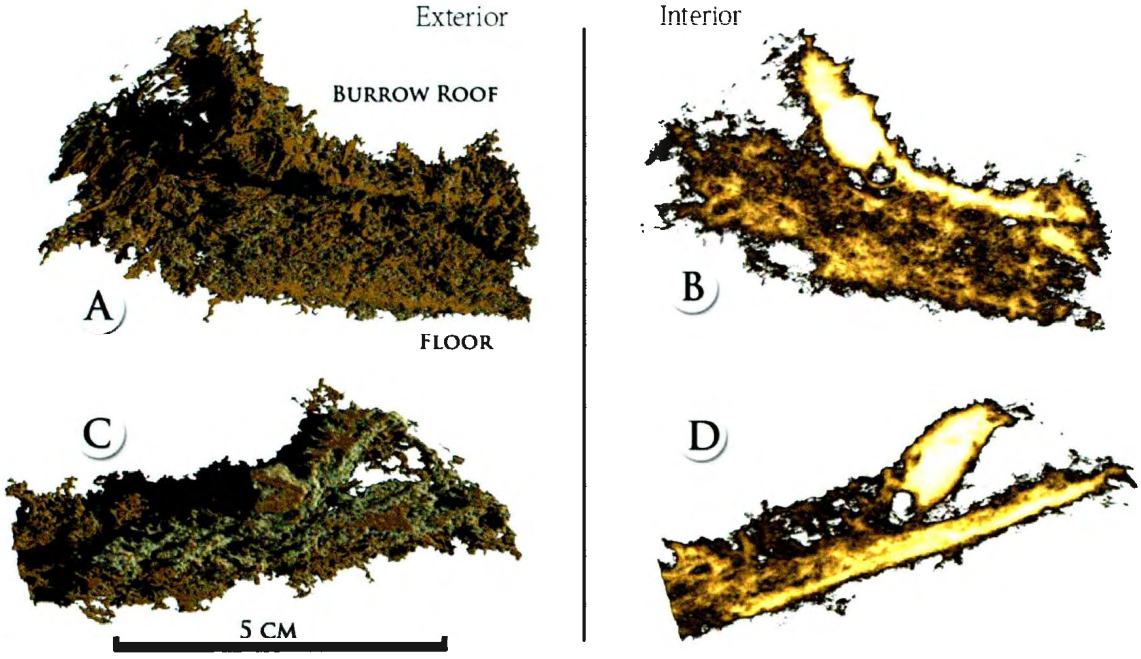

Figure 1: Three dimensional model of *Ophiomorpha irregulaire* from Unit 19 of Spring Canyon Member of the Upper Cretaceous Blackhawk Formation at Coal Creek Canyon, Book Cliffs, Carbon County, Utah, USA. Burrow exterior viewed with Scatter + gradients (A and C) and Sum Along Ray, showing the smooth burrow interior (B and D) rendered in VG Studio Max 1.2.1.

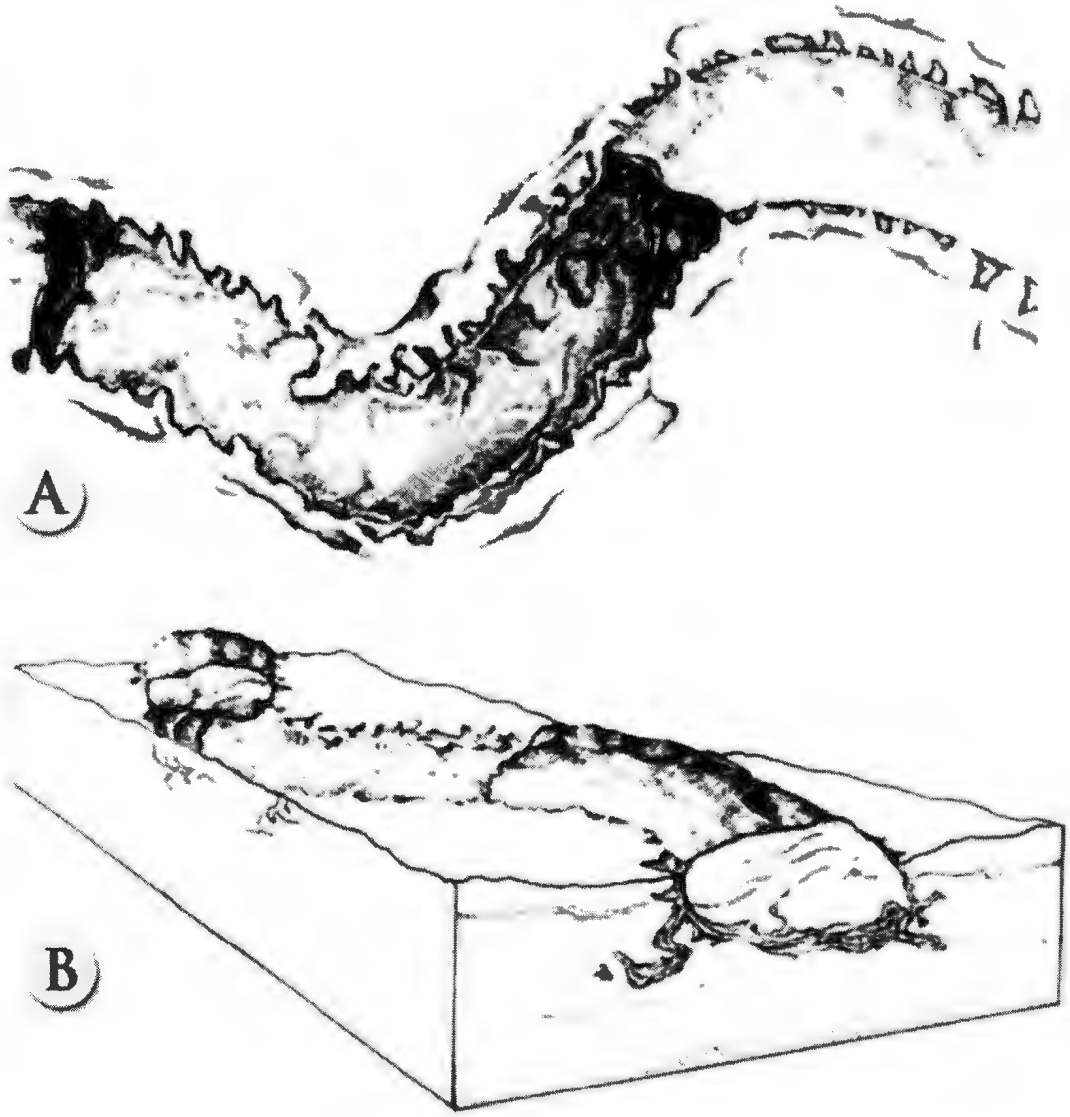

Figure 2: ***Ophiomorpha irregulaire*** **as figured in plan view (A) and perspective view (B) from Frey et al., 1978, fig. 14, showing the irregular and mastoid pellets. Sketched from Spring Canyon Member, Blackhawk Formation (Upper Cretaceous), Utah.**

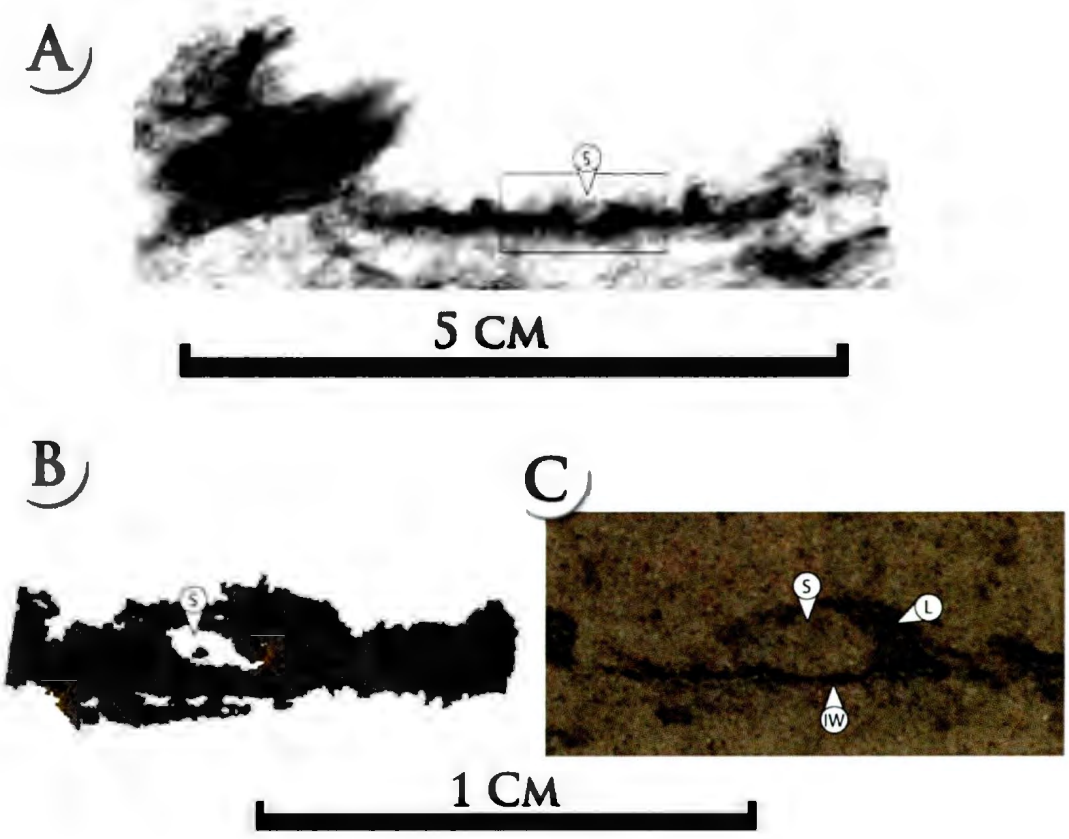

Figure 3: Models are from Unit 19 of Spring Canyon Member of the Upper Cretaceous Blackhawk Formation at Coal Creek Canyon, Book Cliffs, Carbon County, Utah, USA. Arrow labels: S = sand pellet; L = lining; IW = inner wall. A. Burrow roof viewed using Sum Along Ray showing internal structure of sand grade material encased by a clay-grade rind. Box highlights Figures 3 B and C. B. Enlarged pellet model, viewed with Scatter plus gradients showing mud surrounding a pocket of sand grade material. C. Enlarged photo showing the pellet modelled in Fig. 3B.

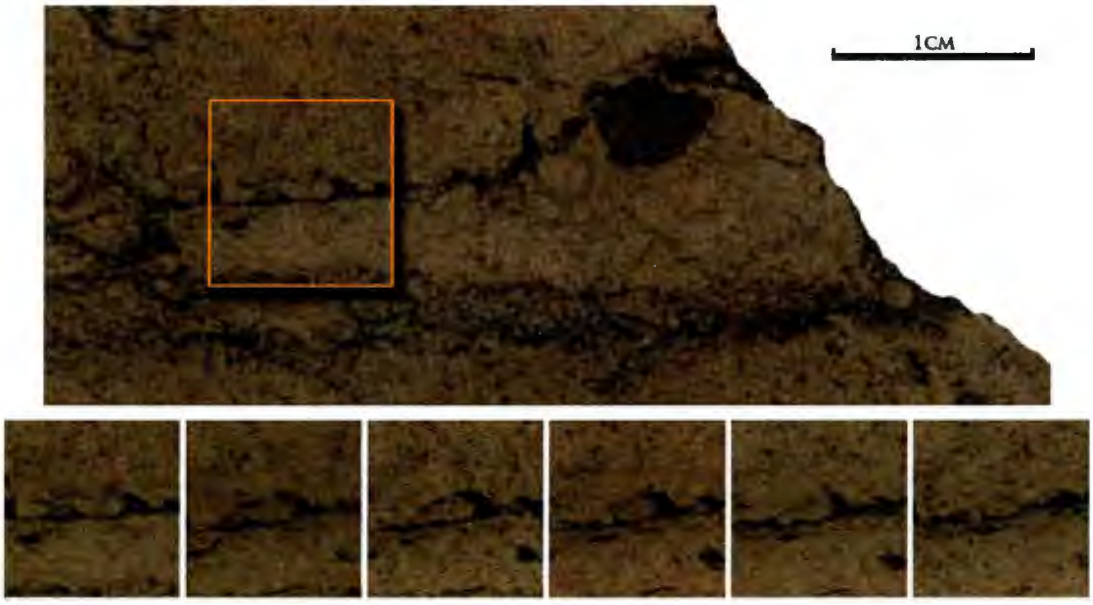

Figure 4: Photograph of burrow (top) at a depth of 2.1655 cm into the sample. The sequence below shows a progression through the pellet modelled in Figure 3B in 0.0305cm increments to a depth of 2.318 cm. Sample is from unit 19 of Spring Canyon Member of the Upper Cretaceous Blackhawk Formation at Coal Creek Canyon, Book Cliffs, Carbon County, Utah, USA.

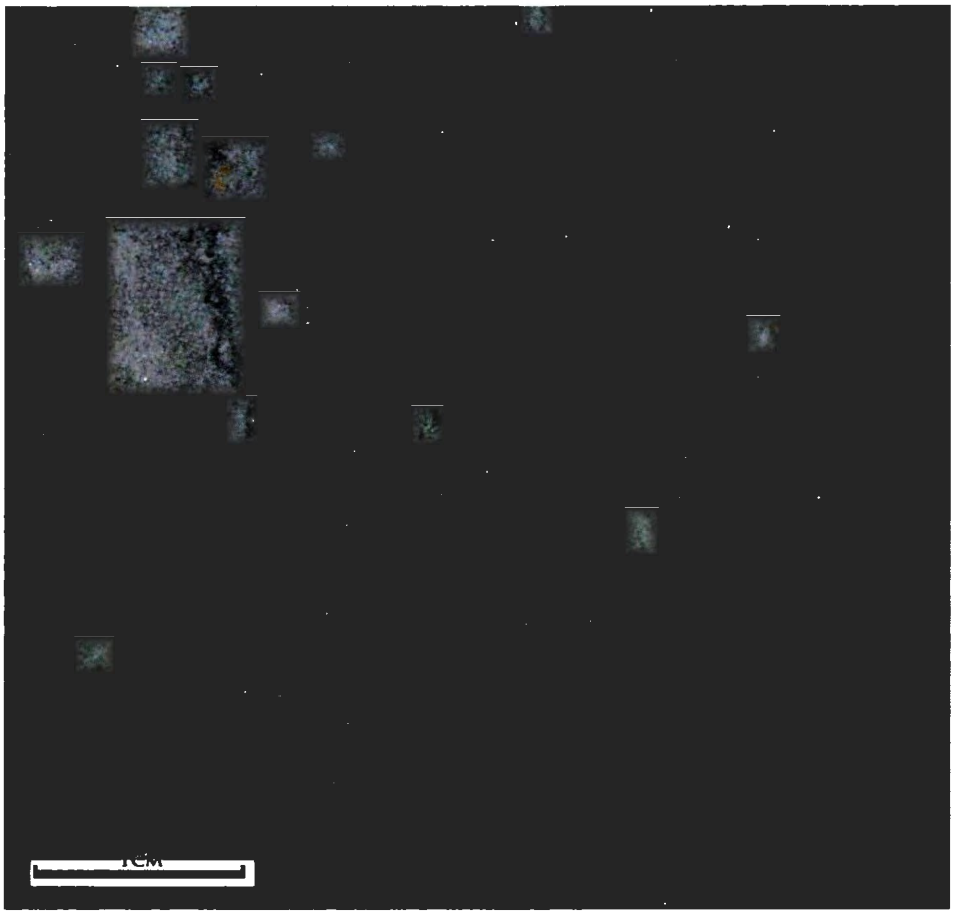

Figure 5: Vertical cross section through *Ophiomorpha irregulaire*, note sand filled pellets. Originally figured in McIlroy et al., 2009. Sample is from the Ben Nevis Formation of the Hebron Field, offshore Newfoundland.

Figure 6: Possible degradation of the clay grade rind surrounding the sand pellet as a result of differential compaction over time (indicated by arrows).

Appendix C – Ben Nevis L-55 Core Data

C.1 Raw Permeability Data

Each value is an average of three readings of the same location on the slabbed core face. Values are expressed in milliDarcies. Tables below correspond to the complied images in Figures 3.1 and 3.2.

Table C.1: *Ophiomorpha-Palaeophycus* Ichnofabric, Core C1 3/15, (see Fig. 3.1B)

	D	E	A	B	C	F	G
11	6.51	3.59	2.10	2.47	6.40	6.67	9.20
10	5.68	6.54	2.17	2.46	9.50	8.61	15.56
9	13.79	3.13	2.76	2.36	9.68	15.95	16.48
8	8.65	3.76	2.19	2.46	8.76	16.23	17.76
7	6.39	3.07	2.33	2.81	12.57	14.54	14.80
6	4.69	1.78	2.77	3.59	10.48	21.48	16.78
5	7.33	2.60	2.09	2.97	16.36	20.18	21.71
4	11.24	2.64	2.40	4.14	18.12	20.52	22.17
3	13.71	6.53	2.51	5.29	16.58	19.95	19.27
2	19.32	6.87	2.52	7.05	16.01	23.21	25.86
1	9.48	11.84	2.71	9.44	19.49	26.49	32.91
12	29.80	18.05	17.32	11.94	19.35	23.26	29.67

Table C.2: *Ophiomorpha*-Burrow Mottled Ichnofabric, Core C5 50/52, (see Fig. 3.1D)

	A	B	C	D	E	F
9	3.79	7.09	4.28	5.58	6.60	5.28
8	3.48	5.26	3.59	4.32	4.43	5.35
7	7.78	6.20	8.61	4.20	6.65	6.38
6	4.29	5.39	4.76	3.33	4.02	8.06
5	6.30	5.77	6.56	3.09	4.66	14.67
4	6.02	3.80	10.17	3.49	3.37	5.04
3	3.22	3.69	3.33	3.44	2.95	2.73
2	4.11	6.64	3.49	3.65	2.96	4.31
1	7.52	5.05	4.89	2.62	2.88	

Table C.3: *Ophiomorpha-Asterosoma* Ichnofabric, Core C5 38/52, (see Fig. 3.2B)

	F	G	A	B	C	D	E
5	23.50	27.59	34.40	29.86	15.96	23.22	9.01
4	6.94	8.03	16.68	18.16	24.41	19.16	3.54
3	38.38	29.96	45.60	41.06	34.46	5.06	41.66
2	44.38	34.26	81.45	16.22	5.43	46.82	48.03
1	39.14	44.14	20.19	34.84	50.01	54.73	82.27
6	12.66	9.40	16.30	15.55	18.39	13.35	28.26
7	33.55	26.43	37.07	21.73	26.02	23.93	22.15
8	14.33	15.32	18.02	17.99	15.22	20.43	16.79

Table C.4: *Ophiomorpha-Thalassinoides* Ichnofabric, Core C5 46/52, (see Fig. 3.2D)

	A	B	C	D	E	F
13		9.30	7.37	11.07	9.82	10.67
12	11.15	9.09	13.32	6.72	9.42	5.77
11	10.68	20.57	10.13	6.18	6.27	5.91
10	8.86	12.57	5.73	4.53	4.17	37.67
9	13.25	12.34	8.53	9.51	10.33	14.01
8	11.37	9.08	9.45	6.17	4.93	53.87
7	19.12	9.50	7.20	7.92	12.29	5.00
6	19.27	9.22	7.94	7.01	17.22	12.24
5	25.41	16.93	10.09	16.17	12.59	49.73
4	12.98	22.06	4.71	47.56	15.14	28.02
3	24.87	35.24	10.43	15.39	26.24	36.36
2	163.29	148.13	54.02	6.53	77.07	100.80

C.2 Thin Section Data

Table C.5: Four thin sections taken from two L-55 cores. All observations are recorded below.

TS Name	Top	Base	3a			3b
Ichnofabric	1	1	4	4	4	4
Description	*Oph* burrowed	Non-*Oph* burrowed	Passive burrow fill	near-burrow sediment	Host sediment	burrow mottled
% Quartz	65	65	60	70	similar	65
% Lithics	5	10	5	10	to	5
% Clay	15	0	0	10	core	10
% Porosity	15	25	35	10		20
Minor	Shell debris, OM/HC	OM/HC	OM/HC	OM/HC	Shell debris	Shell debris, OM/HC
Roundness	sub angular to sub rounded	sub angular to rounded (few)	sub angular to rounded (few)	sub angular to sub rounded	sub angular to sub rounded	sub angular to sub rounded
Size: Quartz (µm)	min 25; max 100; avg 50	min 25; max 120; avg 40	min 30; max 300; avg 100	min 20; max 150; avg 75-100	min 25; max 100; avg 50	min 25; max 175; avg 75
Size: Lithics (µm)	avg 50	avg 50-75	min 40; max 75 - 100; avg 75	min 25; max 125; avg 50	-	avg 75
Size: Pores (µm)	min 10; max 100; avg 30	avg 50 (hard to measure)	min 40; max 700 x 100; avg 75	max 100, avg 40	min 25; max 500 x 100; avg 75	min 25; max 250; avg ~50
Sorting	within patches, well sorted	well sorted	very/poorly sorted	moderately sorted	poorly to moderately sorted	moderately sorted
Cement Comp	quartz overgrowth	quartz overgrowth	quartz overgrowth	quartz overgrowth	quartz overgrowth	quartz overgrowth
Contact	grain-to-grain & grain-to-pore	grain-to-pore, some grain-to-grain	grain-to-pore, some grain-to-grain	grain-to-grain & grain-to-pore	grain-to-grain & grain-to-pore	grain-to-grain & grain-to-pore
Porosity Types	inter-granular, connected	inter-granular, connected	inter-granular, sub-euhedral dissolution	inter-granular, no dissolution, clay-filled	inter-granular, connected, more euhedral dissolution	inter-granular, some shell dissolution; euhedral

C.3 Large Thin Slice Images

Large thin slices were created by cutting a thin slice from the face of slabbed core. The slice was epoxied to glass, and was subsequently ground (the technique has been improved by using the C&C milling machine) to a thickness whereby they become translucent under intense transmitted light (Garton and McIlroy, 2006).

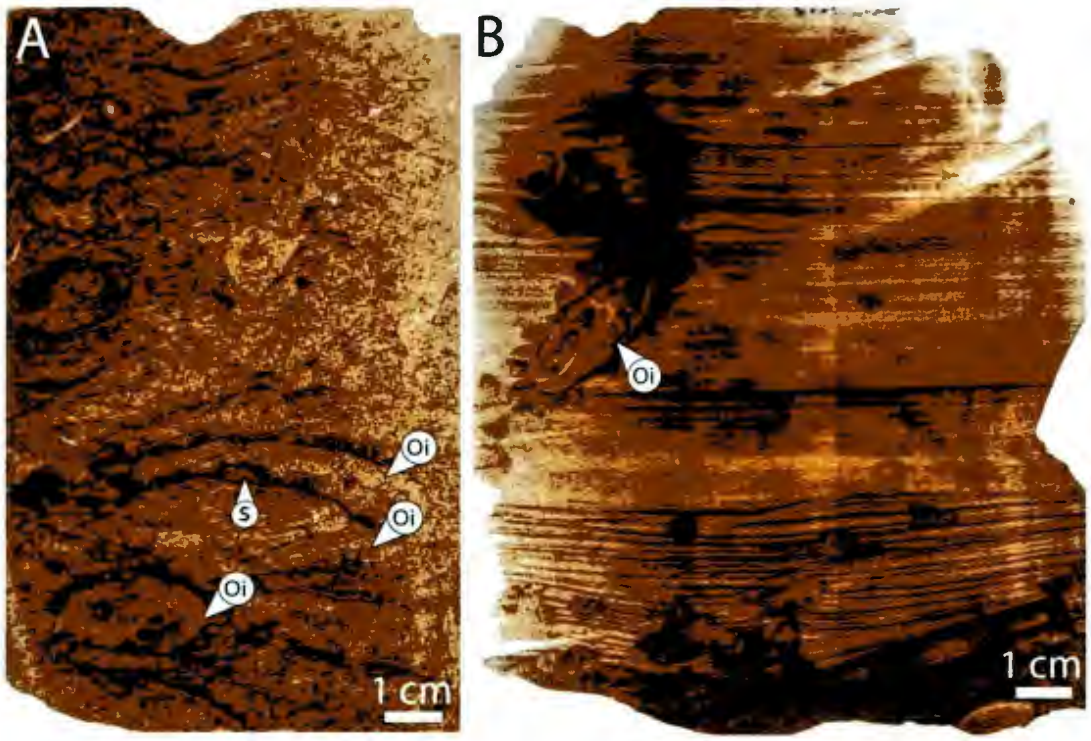

Fig. C. 1: Large thin slices of L-55 cores. A: Same core slab as in Fig. 2.7B. Double-roofed *Ophiomorpha irregulaire* burrow is visible (Oi), including a sand-filled pellet (s). Above the double-roofed *O. irregulaire* is a highly bioturbated and burrow mottled fabric, made visible by the large thin slice technique. B: Planar lamination is very pronounced surrounding the *Ophiomorpha irregulaire* (Oi). The burrow has many well-defined pellets and an internal structure within the burrow core.

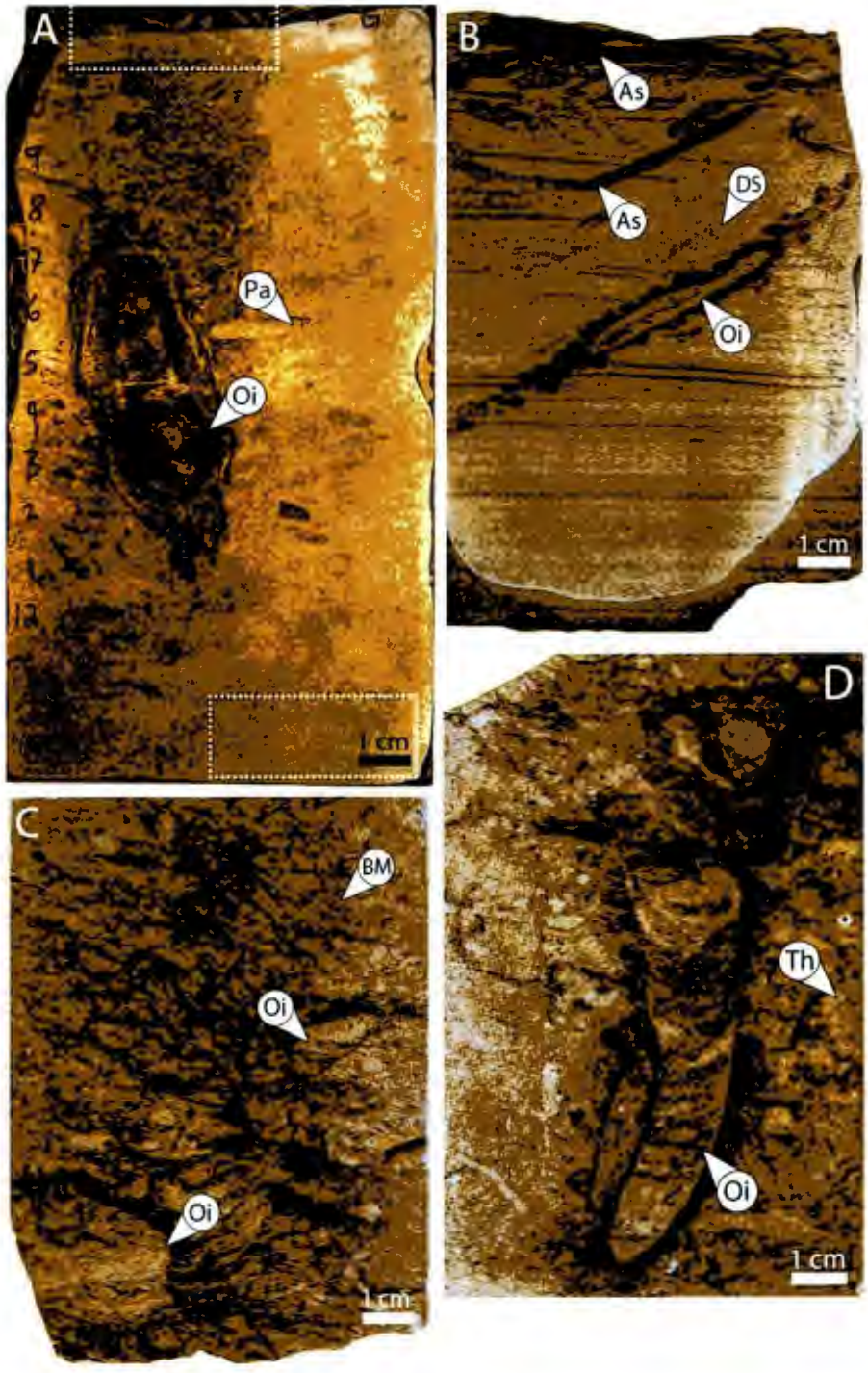

Fig. C.2: Large thin slices of L-55 cores, used within Chapter 3 for mini-permeametry. As = *Asterosoma*; BM = Burrow mottling; DS = diffuse sediment; Oi = *Ophiomorpha irregulaire*; Pa = *Palaeophycos*; and Th = *Thalassinoides*. Dashed boxes on A represent thin section locations (see Fig. 3.3). Thin sections taken from D are not visible on this cropped image (see Figs. 3.2C, 3.4 and 3.5). For more information refer to Chapter 3.

Appendix D – *Diplocraterion* Permeability Data

D.1 Raw Permeability Data

Each value is an average of three readings of the same location on the slabbed core face. Values are expressed in milliDarcies. Blank spaces in the tables represent cracks in the sandstone that resulted in the mini-permeameter not reading the rock; grid squares too close to the rock edge; or human error.

The rock sample was accidentally ground upside-down. Therefore, Surface 1 is the base of the rock/burrows, not the top. Depth readings (in centimeters) and rock slice values (e.g., 1-20) have not been changed to account for the up-side-down grinding.

Table D.1: Permeability Surface 1 (0.0 - 1.0 cm depth), mini-permeameter is reading rock slices 1-20.

	A	B	C	D	E	F	G	H	I	J	K	L
1	60.56	34.84	29.53	31.46	21.83	18.17	18.13	21.45	31.16	48.28	54.79	43.79
2	31.28	24.26	32.96	20.88	27.11	35.24	32.47	38.12	48.56	39.11	48.84	81.58
3	92.18	35.37	50.10	18.06	58.32	32.41	32.15	36.54	106.72	65.62	50.78	63.97
4	33.40	37.70	70.64		74.08	60.75	97.36	79.72	67.22	46.38	34.75	39.23
5	47.77	53.13	21.91	44.37	51.16	75.23	87.84	67.59	52.75	37.62	84.20	43.41
6	78.40	60.87	63.29	42.39	28.38	59.48	88.16	78.50	43.04	48.71	67.11	51.66
7	61.59	59.68	19.86	30.04	15.46	63.29	54.75	40.70	52.45	42.82	60.14	43.08
8	31.67	36.25	26.61	26.66	62.09	88.03	96.19	64.83	60.90	26.67	77.05	27.91
9	16.46	25.25	27.89	30.17	71.24	85.68	91.83	89.16	78.09			56.45
10	21.47	32.31	18.32	27.34	27.22	65.68	68.25	38.95	71.73		66.29	44.95
11			46.07	65.19	20.35	81.14	73.16	68.45	82.17	44.59	44.71	35.41
12	32.77	29.56	18.20	18.87	34.69	50.56		56.82	33.23	37.82	48.81	46.87
13	61.08	48.02	35.30	48.39		84.88	41.02	32.37	32.91	28.71	25.77	44.26
14	91.78	59.15	41.49	44.64	29.71	32.85	34.80	42.82	48.48	41.42	58.41	56.33

Table D.2: Permeability Surface 2 (1.0 - 2.0 cm depth), mini-permeameter is reading rock slices 21-40.

	A	B	C	D	E	F	G	H	I	J	K	L
1	70.27	64.85	80.42	207.20	86.22	81.86	98.60	96.57	137.30	97.02	94.20	98.41
2	169.13	58.06	104.66	86.54	66.63	91.94	79.12	105.81	119.60	94.48	97.98	108.92
3	113.65	68.89	110.90	103.02	122.61	126.06	100.99	99.62	132.70	107.22	90.34	87.25
4	82.99	84.57	149.33	118.00	127.16	141.08	114.47	78.95	92.08	90.22	64.95	92.01
5	102.06	67.07	40.61	96.53	130.64	118.10	125.06	92.37	69.59	64.62	66.94	84.66
6	87.48	107.39	80.84		123.38	117.15	89.85	106.23	73.20	55.69	88.99	59.04
7	120.06	82.95	89.67	81.84	96.56	91.46	89.47	93.82	71.52	79.21	74.42	70.08
8	66.94	84.84	74.02	95.23	79.20	62.37	118.01	106.28	109.47	75.85	189.49	49.49
9	99.65	94.60	106.36	125.45	77.25	127.96	107.31	82.10	84.85		266.08	78.22
10	99.44	91.12			157.15	126.80	91.07	115.26	46.18	208.98	88.50	70.33
11			94.01		108.89	94.68	155.39	95.30	95.80	93.12	93.17	83.73
12	93.51	93.33	109.00	184.92	100.98	96.33	31.79	72.52	123.89	86.15	115.56	87.83
13	108.72	106.28	106.59	89.82	106.61	230.87	84.16	49.43	112.77	83.66	84.92	78.00
14	92.86	94.41	86.56	103.30	69.62	57.18	99.66	91.67	104.06	95.50	93.05	80.11

Table D.3: Permeability Surface 3 (2.0 – 3.0 cm depth), mini-permeameter is reading rock slices 41-60.

	A	B	C	D	E	F	G	H	I	J	K	L
1	74.73	87.55	110.26		131.26	96.75		138.40	143.02	118.58	127.92	149.96
2	213.71	103.97	109.26	179.56	130.03	79.98	83.41	135.17	104.87	113.83	124.62	182.59
3	103.98	58.59	174.21	107.43	200.52	118.46	133.30	133.68	94.56	101.40	132.39	136.57
4	101.28	98.98	110.70	138.01	141.31	108.78	120.49	89.77	113.89	142.71	135.46	142.57
5	92.17	139.18	66.28	126.68	147.73	197.94	139.31	94.11	101.30	88.14	87.99	95.54
6	99.10	95.51	99.08	156.57	82.23	74.22	81.23	99.86	113.49	94.17	76.49	95.54
7	112.46	117.01	79.81	63.04	133.20	129.70	120.28	110.89	94.95	89.16	85.28	74.89
8	93.48	92.21	74.47	106.48	96.54	141.85	203.21	103.37	80.49	78.67	178.05	80.11
9	109.63	98.47	147.51	89.78	93.36	126.30	107.56	161.37	109.38			100.80
10	89.73	91.18	137.21	165.03	106.15	104.72	127.34	131.59	54.43	49.62	113.40	88.85
11	86.54	118.79	121.87		140.69	116.42	127.01		111.08	123.24	158.37	108.54
12	106.99	92.83	142.82	114.04	75.24	139.05	32.29	99.90	101.49	103.96	155.00	120.76
13	132.03	90.98	148.29	94.33	233.01	239.54	82.80	115.78	104.90	116.16	114.45	109.23
14	113.93	109.15	87.08	116.05		149.24	139.53	114.09	155.89	70.90	111.70	91.06

Table D.4: Permeability Surface 4 (3.0 – 4.0 cm depth), mini-permeamter is reading rock slices 61-80.

	A	B	C	D	E	F	G	H	I	J	K	L
1	108.18	78.89	83.57	93.40	122.86	95.97	113.47	103.39	114.26	140.13	101.08	100.22
2	116.32	101.65	104.40	87.10	77.75	84.18	73.18	97.29	113.11	107.84	77.43	85.24
3	117.94	46.44	145.65	109.83	99.48	96.60	100.29	108.42	109.30	107.00	99.39	104.78
4	132.56	159.07	97.73	131.98	105.10	127.80	103.10	90.31	102.45	75.53	103.99	109.03
5	155.95	147.72	105.54	181.44	65.54	58.06	79.30	114.77	61.96	79.43	92.60	83.92
6	89.16	146.30	68.72		104.59	98.00	97.15	87.15	79.71	74.36	62.13	57.80
7	100.10	106.39	89.69	65.48	97.41	114.34	99.57	97.62	82.09	67.61	65.24	64.10
8	107.59	106.16	68.17	81.02	79.73	146.45	90.40	71.63	93.25	116.59	138.33	58.27
9	117.77	110.33	163.53	90.20	94.18	116.19	100.10	102.43	85.91	147.08	176.15	87.32
10	129.82	98.79	130.95	95.23	97.68	89.54	83.07	146.20	102.11	68.35	103.61	69.17
11	106.30			121.81	151.14	103.91	109.38	106.04	85.60	55.60	105.63	82.98
12	105.76	121.29	124.87	87.63	73.12	90.89	98.39	190.25	76.55	84.67	114.92	100.50
13	83.80	134.33	113.48	110.05	157.94	169.89	55.03	92.79	94.56	77.93	105.94	88.29
14	114.14	118.40	118.51	136.56	111.74	96.75	41.05	72.23	98.83	87.63	55.00	86.65

Table D.5: Permeability Surface 5 (4.0 – 5.0 cm depth), mini-permeameter is reading rock slices 81-100.

	A	B	C	D	E	F	G	H	I	J	K	L
1	96.32	119.93	138.53	133.51		75.42	121.51	99.75	128.51	119.43	111.00	125.37
2	89.05	103.11	113.08	117.88	123.99	76.25	69.43	94.05	117.99	127.51	95.39	114.04
3	107.60	73.61	119.73	91.69	140.98	72.05	136.57	110.42	125.68	85.92	93.69	115.31
4	97.89	162.68	80.24	119.61	100.67	92.27	89.12	89.60	85.10	87.28	103.56	114.81
5	196.51	186.69	120.51	120.34	109.53	78.69	94.05	46.01	110.55	90.60	115.45	97.46
6	122.93	126.64	70.70	143.66	104.09	56.51	69.36	44.28	69.84	84.88	67.57	65.96
7	99.85	118.17	63.52	67.28	109.14	69.05	43.38	54.81	73.45	88.80	75.51	61.33
8	74.48	61.19	72.01	82.47	77.74	79.14	68.77	56.84	80.85	101.73	132.94	68.89
9	91.99	80.31	99.87	108.11	74.31	102.36	124.94	107.29	113.96	77.41	186.66	40.55
10	94.66	101.47	141.10	105.27	106.61	95.43	53.57	146.24	114.70	68.08	100.71	82.94
11	80.34	95.41	189.52	59.08		94.25	134.68	150.13		110.31	99.14	95.18
12	82.06	88.56	90.52	95.08	65.72	59.04		138.39	129.30	85.94	76.71	79.64
13	99.99	95.91	117.37	98.73	78.12	198.65	98.63	173.36	64.99	111.65	86.19	91.65
14	101.93	99.76	77.02	85.35	78.06	74.52	169.14	63.06	55.08	76.83	69.78	75.36

Table D.6: Permeability Surface 6 (5.0 – 6.0 cm depth), mini-permeameter is reading rock slices 101-120. Column J values were omitted in error.

	A	B	C	D	E	F	G	H	I	J	K	L
1	104.41	93.75	82.12	88.68	95.14	66.38		111.38	116.02	152.08	95.98	123.80
2	65.41	79.51	81.57	110.72	77.79	85.80	94.61	100.80	133.61	97.01	76.71	125.28
3	76.65	87.44	106.23	90.99	80.10	89.60	102.54	111.16	117.64	110.50	93.28	66.77
4	111.07	181.26	149.79	116.84	85.38	92.60	91.26	109.54	120.66	101.33	108.26	63.29
5	189.44	175.08	109.49	69.89	86.33	85.62	87.70	90.62	97.91		90.58	82.05
6	113.68	119.15	96.03	106.24	108.51	112.41	80.44	106.30	110.49		59.60	60.26
7	144.05	85.13	88.04	73.30	78.35	84.01	68.13	67.52	96.04		73.42	68.97
8	73.18	90.44	84.08	101.63	96.15	98.90	73.91	98.10	104.76		140.46	44.72
9	66.60	88.55	88.96	97.62	85.06	112.51	100.72	130.52	150.50		187.65	50.29
10	106.28	100.46	59.64	96.93	97.96	103.45	109.40	144.40	151.20		125.36	64.75
11	63.04	88.66	156.25	92.48	98.65	103.71	105.19	162.58			162.54	80.86
12	154.58	133.53	129.26	76.77	71.54	108.06	188.85	131.89	111.81		124.31	114.88
13	104.17	105.95	106.85	100.49	113.82	120.83	141.85	181.10	135.18		112.67	101.17
14	71.39	78.77	81.17	55.04	85.69	120.13	169.69	91.49	109.21		91.61	

Table D.7: Permeability Surface 7 (6.0 – 7.0 cm depth), mini-permeameter is reading rock slices 121-140.

	A	B	C	D	E	F	G	H	I	J	K	L
1	120.83	82.50	109.25	60.50	59.00	70.16	200.96	119.41	110.48	123.90	118.01	135.75
2	73.00	101.88	136.14	66.59	85.11	85.10	72.47	121.08	131.24	113.93	114.38	105.93
3	110.10	70.12	99.49	102.43	140.14	89.48	112.92	120.11	71.06	78.37	95.30	140.25
4	121.56	131.12	265.26	99.89	91.11	80.98	118.26	71.53	151.16	92.69	94.12	89.93
5	100.42	96.47	90.75	119.18	94.46	119.65	76.15	94.67	113.12	99.02	101.85	80.25
6	98.88	74.38	51.49	65.46	113.56	100.59	111.78	93.63	107.17	95.43	83.73	59.34
7	100.29	95.41	103.09	116.48	118.76	109.30	77.20	102.65	100.86	100.94	57.56	49.00
8	113.00	95.14	84.86	96.33	81.62	93.64	95.63	79.69	107.61	129.50	86.58	50.02
9	75.27	99.91	115.71	72.21	81.98	99.87	146.56	112.60	157.35	222.89	394.92	81.54
10	107.98	109.42	179.93	134.26	81.91	112.17	171.46	156.16	156.30	111.16	110.66	59.86
11	101.13	101.01	99.12	120.36	97.46	195.44	170.30	173.76	103.28	98.08	111.09	104.96
12	102.63	108.21	130.57	103.11	90.43	144.76		147.64	128.11	113.48	101.79	116.24
13	93.22	91.77	102.32	93.48	92.99	159.59	88.44	148.49	84.22	147.50	114.47	80.35
14	75.02	71.07	86.35	114.73	78.03	145.86	174.40	122.20	126.60	79.84		

Table D.8: Permeability Surface 8 (7.0 – 8.0 cm depth), mini-permeameter is reading rock slices 141-160.

	A	B	C	D	E	F	G	H	I	J	K	L
1	122.98	74.11	88.53	98.98	72.88	77.91	153.62	107.17	119.93	170.82	131.12	
2	113.06	89.69	104.17	77.88	77.52	126.13	116.30	131.88	122.88	119.37	105.82	123.21
3	95.62	78.27	65.48	101.89	98.09	92.57	129.63	73.43	85.29	96.39	96.54	114.58
4	94.92	111.65	81.57	137.59	97.12	75.59	77.36	68.43	82.78	119.04	132.96	147.45
5	85.86	86.26	86.25	83.72	99.58	106.37	54.73	95.43	98.38	120.06	86.77	112.63
6	104.75	90.49	81.68	81.02	93.24	96.06	118.00	76.48	91.82	88.54	111.37	76.07
7	90.41	92.36	79.45	74.47	113.20	86.70	74.83	43.24	151.64	112.18	110.62	68.64
8	88.00	76.03	81.78	61.75	104.33	99.48	90.16	70.72	73.51	141.12	117.90	61.57
9	86.62	84.32	91.75	64.35	72.48	101.76	106.56	82.40	136.23	110.09	193.42	77.32
10	87.84	136.01	134.08	95.77	64.90	143.98	110.39	121.07	152.45	169.15	94.50	93.31
11	104.85	96.31	127.53	93.51	72.96	141.31	157.36	141.43	147.83	150.60	140.20	109.28
12	122.43	119.57	86.31	91.49	72.51	159.14	224.41	100.75	138.81	145.30	156.41	186.72
13	101.06	228.91	103.22	83.39	189.30	149.58	80.66	119.52	148.93	119.21	161.32	126.87
14	88.14	73.53	59.34	128.38	64.46	142.83	159.13	179.04				

Table D.9: Permeability Surface 9 (8.0 – 9.0 cm depth), mini-permeameter is reading rock slices 161-180.

	A	B	C	D	E	F	G	H	I	J	K	L
1	92.33	98.80	120.08	101.55	93.25	91.10	138.58	121.13	115.99	128.74	129.79	
2	130.67	119.08	205.51	127.33	151.29	116.97	122.02	153.04	115.51	119.42	84.65	
3	139.96	78.49	69.67	92.32	68.19	104.46	93.02	89.20	101.30	99.22	138.88	121.37
4	123.23	67.66	65.43	124.68	105.05	93.60	105.48	156.00	93.92	132.12	127.21	120.60
5	87.64	103.93	100.26		80.25	91.20	117.24	109.97	117.64	83.75	127.95	97.53
6	103.04	117.18	45.85	61.16	82.07	113.72	129.78	127.98	99.73	121.02	105.22	82.49
7	81.66	113.09	65.56	150.31	111.20	109.75	142.88	103.98	89.29	105.89	151.85	84.31
8	103.62	80.12	78.18	70.45	99.54	103.23	122.40	78.32	116.59	133.21	125.27	88.85
9	89.02	90.64	112.96	94.92	75.60	94.78	112.47	174.96	129.10	206.45	318.68	133.85
10	80.09	122.61	130.91	124.81	69.73	131.47	106.98	158.10	180.19	199.44	55.51	114.78
11	124.85	132.95	111.03	111.70	74.83	92.33	135.80	139.85	66.15	159.96	143.11	118.47
12	122.95	135.39	63.51	86.42	84.38	100.47		160.31	161.95	157.75	142.07	148.79
13	88.60	96.65	99.26	88.99	114.15	73.68	78.02	131.75	120.08	135.97	121.90	135.11
14	97.62	86.62	56.95	113.40	84.68	54.58	134.60					

Table D.10: Permeability Surface 10 (9.0 – 10.0 cm depth), mini-permeameter is reading rock slices 181-200.

	A	B	C	D	E	F	G	H	I	J	K	L
1	115.14	102.00	110.15	128.44	107.12	89.69	123.19	118.90	101.18	109.54	108.98	
2	113.23	136.58	110.74	64.09	84.43	112.52	143.20	148.41	135.36	89.57	97.53	
3	96.23	75.24	59.73	96.23	87.78	78.17	88.27	64.38	61.53	54.22	90.82	
4	142.56	59.27	78.13	76.48	49.90	79.03	143.57	99.33	127.35	122.89	93.17	99.81
5	110.30	54.51	111.60	98.34	70.82	70.60	82.50	113.07	117.02	124.36	79.67	61.11
6	101.59	95.09	77.46	82.95	87.68	60.29	77.97	90.36	107.71	102.25	67.70	95.12
7	78.74	67.62	75.72	72.58	81.37	58.52	79.62	92.96	100.12	119.01	76.15	59.17
8	68.00	70.29	64.39	66.79	84.80	74.05	135.91	101.35	130.40	88.01	162.79	113.12
9	83.08	56.42	65.27	54.74	59.36	171.06	88.70	113.98		52.11	197.48	93.10
10	85.68	70.49	119.21	86.76	65.72		97.93	165.28	147.74	110.30	65.96	97.09
11	124.45	114.65	92.89	129.21	65.17	102.33	149.62	133.25	103.21	107.50	197.73	143.22
12	127.02	148.57	100.66	87.32	197.23	107.49	141.52	160.09	146.15	159.24	122.61	168.53
13	100.03	81.28	77.77	113.26	95.73	173.95	146.17	163.23	124.44	110.99	94.64	140.23
14	106.04	76.29	11.23	127.03	103.88	102.68						

Table D.11: Permeability Surface 11 (10.0 – 11.0 cm depth), mini-permeameter is reading rock slices 201-220.

	A	B	C	D	E	F	G	H	I	J	K	L
1	91.72	66.29	78.86	60.59	144.30	79.52	88.81	139.73	122.87	154.98	126.18	
2	106.92	117.14	83.78	206.94	47.59	88.21	135.21	146.18	109.41	120.79	76.77	
3	44.32	62.80	152.90	138.63	128.16	105.30	112.42	121.73	64.54	60.17	90.74	
4	60.19	54.47	141.77	110.92	67.99	104.70	110.35	83.95	115.24	124.95	139.12	
5	86.75	96.88	101.22	107.18	111.81	98.34	147.46	121.26	86.48	137.09	132.61	125.41
6	131.73	132.97	121.44	73.90	116.96	100.38	120.85	134.69	97.96	99.90	63.28	87.57
7	117.06	113.95	75.68	75.13	87.86	97.84	126.31	99.61	64.33	80.70	109.61	50.35
8	90.36	74.52	62.22	63.45	87.16	73.87		100.26	114.39	147.45	154.70	129.82
9	98.35	72.12	55.88	56.58	115.25		61.11	101.91	101.26	69.25	201.00	79.86
10	74.02	66.67	58.47	64.60	76.95	94.22	106.89	70.11	51.37	119.13	89.74	
11	110.80	100.78	112.83	75.87	108.71	166.90	128.29	53.18	77.84	128.30	144.92	81.00
12	99.87	120.94	144.52	82.86	121.27	59.61	102.90	117.35	151.78	109.06	135.87	103.53
13	105.76	98.32	116.84	71.66	276.88	103.84	58.74	100.55	85.80	115.15	112.75	75.05
14	82.06	76.00	110.07	109.13	113.87							

Table D.12: Permeability Surface 12 (11.0 – 12.0 cm depth), mini-permeameter is reading rock slices 221-240.

	A	B	C	D	E	F	G	H	I	J	K	L
1	94.93	53.45	61.68	66.67	49.05	78.09	132.48	156.53	143.55	132.67	164.19	
2	59.76	127.78	111.35		94.95	51.86	130.81	149.37	92.87	85.76	64.98	
3	66.72	72.02	178.36	160.86	89.65	52.96	148.79	106.40	97.66	57.80	77.43	
4	62.85	80.61	113.98	132.59	113.46	102.92	128.12	92.03	82.59	108.39	77.92	
5	93.88	102.34	105.93	119.99	90.40	95.47	78.52	92.49	84.68	82.04	111.91	
6	73.79	104.49	108.61	72.79	81.75	78.46	87.88	73.33	107.14	104.66	83.29	
7	107.03	179.20	69.81	57.23	86.47	103.86	106.19	72.38	79.13	81.46	141.59	73.86
8	110.93	64.76	75.08	61.89			130.56	115.90	111.79	84.57	135.92	105.45
9	99.07	93.18	109.82	67.61	172.99	107.54	85.31	99.24	108.48	70.96		92.60
10	102.24	78.71	75.88	64.74	125.57	97.81	138.72	98.17	161.48	107.82	116.76	130.80
11	134.76	81.94	67.51	74.40	96.49	116.00	92.50	102.28	174.37	162.52	123.27	80.05
12	114.34	143.36	94.95	111.41	108.41	67.98	97.43	34.41	48.62	119.25	101.44	109.54
13	111.09	110.00	178.63	115.31	127.65	147.99			31.23	86.24	107.39	116.28
14	100.29											

Table D.13: Permeability Surface 13 (12.0 – 13.0 cm depth), mini-permeameter is reading rock slices 241-260.

	A	B	C	D	E	F	G	H	I	J	K	L
1	65.19	90.86	58.43	61.44	97.22	59.87	91.58	87.53	83.13		90.65	
2	139.01	103.17	64.72	59.24	88.43	51.14	93.45	128.44	106.37	166.34	56.21	
3	86.12		110.58	113.67	79.87	81.93	61.16	74.52	99.43	64.24	87.81	
4	83.75	106.19	117.68	83.95	73.90	50.98	137.34	85.79	79.35	73.43	106.54	
5	102.12	77.33	159.86	78.88	94.66	101.63	181.63	110.99	64.74	88.59	89.48	
6	82.33	114.69	97.28	162.79	42.80	152.75	56.74	118.89	109.84	96.22	123.53	
7	85.08	81.27	70.33	111.83	110.49	146.94	134.26	81.69	91.02	115.57	85.98	
8	94.20	88.20	57.28	92.35	131.68	76.90	92.84	93.41	128.27	106.81	137.29	100.54
9	97.79	96.24	102.23	70.87	127.50	96.02	115.95	89.03	142.88	115.71	148.10	89.68
10	73.12	76.66	110.17	77.94	110.59	89.67	156.37	154.19	148.13	163.07	89.72	112.55
11		156.88	66.10	56.59	65.28	115.37	147.27	104.66	141.57	161.89	133.51	134.09
12	98.22	91.24	86.61	101.37	106.95	146.81			97.93	116.27	100.44	108.43
13	71.49	95.24	168.71	115.54					101.39	121.57	108.35	96.66
14												

D.2 Permeability Surface Figures

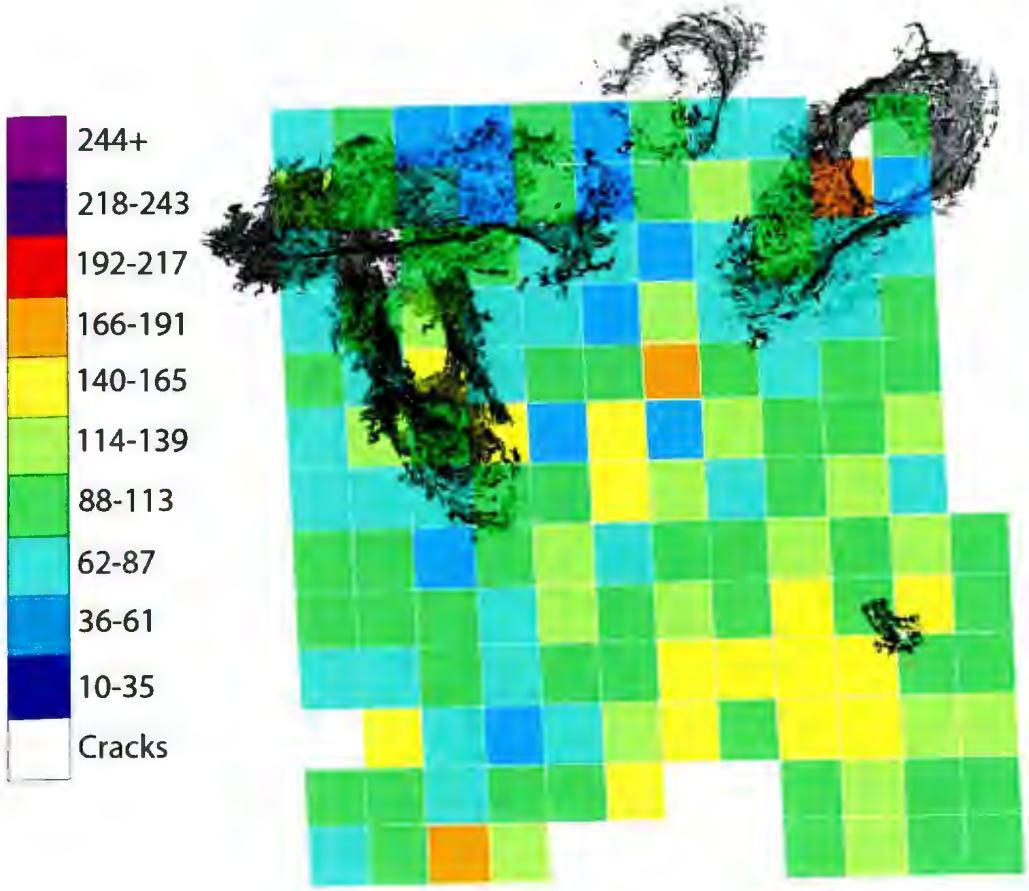

Fig. D.1: Surface 13 (actual top of rock sample).

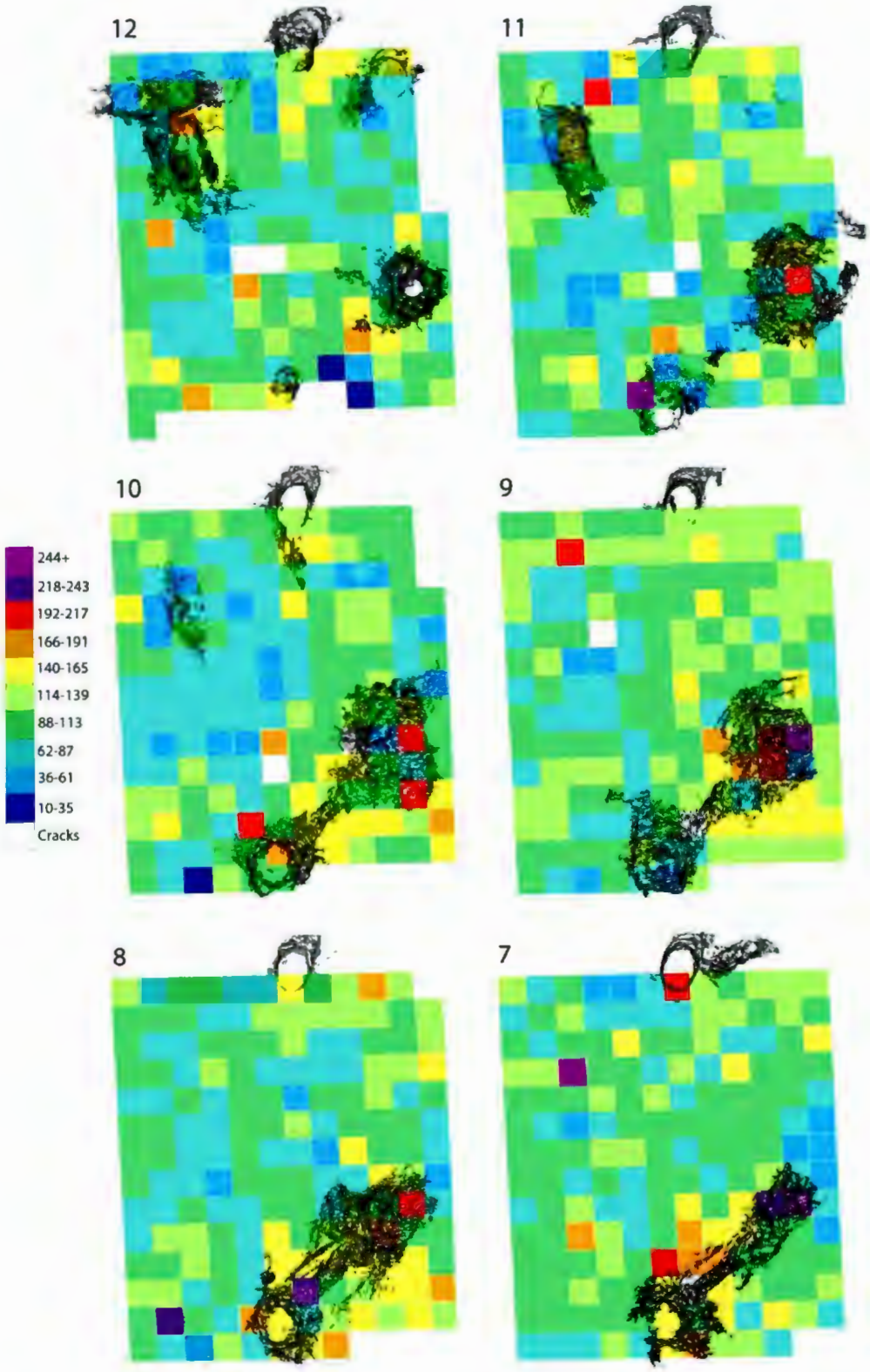

Fig. D.2: Surfaces 12 to 7, top half of rock sample.

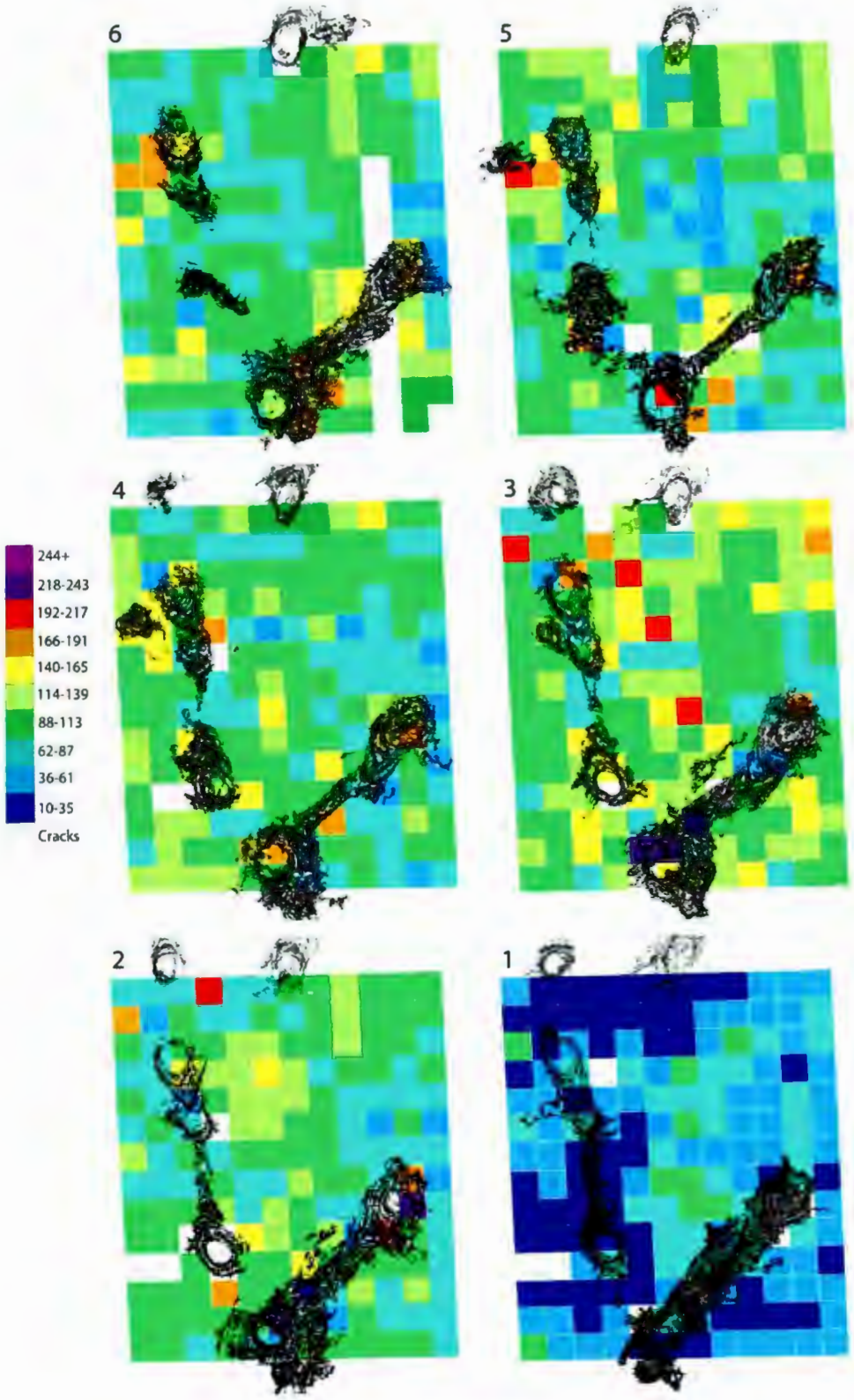

Fig. D.3: Surfaces 6 to 1, bottom half of rock sample.